International Scientific-Technical and Production Journal

The Paton WELDING JOURNAL

May
2006
5

English translation of the monthly «Avtomaticheskaya Svarka» (Automatic Welding) journal published in Russian since 1948

Founders: *E.O. Paton Electric Welding Institute of the NAS of Ukraine*
International Association «Welding»

Publisher: *International Association «Welding»*

Address:
E.O. Paton Electric Welding Institute,
International Association «Welding»,
11, Bozhenko str., 03680, Kyiv, Ukraine
Tel.: (38044) 287 67 57
Fax: (38044) 528 04 86
E-mail: journal@paton.kiev.ua
http://www.nas.gov.ua/pwj

State Registration Certificate
KV 4790 of 09.01.2001

Subscriptions:
$324, 12 issues per year,
postage and packaging included.
Back issues available.

CONTENTS

WELDABILITY OF SHAPE-MEMORY ALLOYS OF Ni–Ti SYSTEM

B.E. PATON[1], D.M. KALEKO[1], V.P. SHEVCHENKO[1], Yu.N. KOVAL[2], V.N. SLIPCHENKO[2], L.M. NEGANOV[2] and R.Ya. MUSIENKO[2]

[1]E.O. Paton Electric Welding Institute, NASU, Kiev, Ukraine
[2]G.V. Kurdyumov Institute of Metal Physics, NASU, Kiev, Ukraine

Welding processes with pulsed heating are the most promising for joining small cross-section alloys of Ni–Ti system. We studied the characteristics of wire and foil joints produced by spot welding by a capacitor discharge and alternating current, shock capacitor-type welding and laser welding. Methods of optical and X-ray microcsopy, X-ray microprobe analysis, resistance measurement and three-point bending were used to show that the capacitor-type and laser welding processes do not change the material composition and its thermomechanical properties near the welding site, and may be recommended for application in manufacture of nithinol products.

Keywords: spot capacitor-type welding, shock capacitor-type welding, laser welding, thermoelastic alloys, nithinol, microstructure, mechanical properties, thermomechanical properties

Over the last decades the designers are more and more often turning to the so-called shape-memory alloys (SMA). These alloys have two main features, which are the most attractive for developers of new products, instruments and apparatuses: possibility of restoring the specified shape at heating a pre-deformed item to a certain temperature (shape memory) and manifestation of considerable elastic deformation greater than in the majority of other metals and alloys (superelasticity).

The shape-memory effect has now been found and studied in many alloys: Ni–Ti, Fe–Ni, Cu–Al, Cu–Mn, Cu–Al–Ni, Co–Ni, Ni–Al, Cu–Zn–Al, etc. [1, 2]. We have selected from this sequence the Ni–Ti system (nithinols), which have found application both in engineering and in medicine, due to a high corrosion resistance in the living organism, as well as biological compatibility, which is confirmed by numerous cases of implantation of prosthesis, fastening parts (staples, fasteners, clips, etc.) and drive mechanisms [1, 3–5].

Welding of nithinol to nithinol and to other structural materials may greatly facilitate the solution of design problems in development of complex products of diverse, also medical purposes. However, at welding heating decomposition of intermetallics of equiatomic composition with formation of Ti_2Ni and $TiNi_3$ [3] and appearance of inner thermal stresses may occur, which may lead to a variation of the temperature interval of martensite transformation and degree of shape restoration. There is still insufficient data about it, which restrains development of the technology of treatment of thermoelastic alloys, and products from them, and their application, respectively.

Alloys of Ni–Ti system were earlier joined using such fusion welding processes as inert gas tungsten electrode, laser and electron beam welding. Fusion welding runs into several problems, leading to dissolution of oxygen, hydrogen and nitrogen, loss of superelasticity and shape-memory effect in the HAZ metal, formation of the above intermetallics compounds, brittle and having no shape memory [6–10]. As a result of that, even with preservation of the latter in welding of a 3 mm nithinol sheet with a 10 kW laser, the rupture strength of the joint turned out to be low because of the coarse grains in the fusion zone. On the other hand, surface heating of nithinol with ultrashort pulses [11] does not impair its structure.

The above disadvantages of fusion welding necessitated a search for acceptable solutions among the solid-phase joining processes, such as friction or explosion welding, resistance, diffusion or shock capacitor-type welding.

In keeping with the data of Edison Welding Institute [12], in resistance welding nithinol demonstrates a sufficient superelasticity even without any additional heat treatment of the welded sample (the work does not give any data on preservation of critical temperatures of martensite transformation in this process).

Friction welding [7] is a promising process for joining SMA, but there are geometrical limitations on the shape of the parts being welded, making problematic a broad application of this process.

Thermodeformational cycle of shock capacitor-type welding [13] led to embrittlement of the welded joint of nithinol wire of 1.8 mm diameter. Application of shielding gas and additional heat treatment of welded joints [14] allowed producing samples with the characteristics good enough for practical application.

A good result was obtained in explosion welding of nithinol to AMg6 alloy [15]. Reference samples of the joints had a minimum number of defects of the type of intermetallic interlayers, shrinkage cavities, pores, etc., preserved the shape-memory effect of nithinol and condition of the welded part surface.

The above indicates that welding of nithinol of a small cross-section (foil, wire), having predominant application in medicine and automatics, is not described in publications.

During selection of the welding processes, research was based on the assumption that changes in the structure and composition of the metal in the welding zone will be minimum only in the case, if the latter stays at a high temperature for a minimum time. We have selected a capacitor discharge (passage of a high cur-

Table 1. Modes of spot two-pulse AC welding of foil and nithinol

Sample #	Foil thickness, μm	Current value on the scale of RKS801 current regulator	Heating time (1st pulse), μs	Cooling time, μs	Heating time (2nd pulse), μs	Compressive force, N	Transformer stage
1-1	85	0	3	9	3	10	1
2-1	85	0	3	9	3	10	1
3-1	85	4	3	9	3	10	1
4-1	50	0	1	0	0	10	1
5-1	85	1	1	0	0	36	2
6-1	50	1	1	0	0	36	3
7-1	52	1	1	0	0	36	3
8-1	52	1	1	0	0	36	2

rent over a short time), alternating current pulses and laser beam as the heat source. Spot and butt joints of foil and wires from nithinol were studied.

Experiments on spot, shock capacitor-type, as well as laser welding, were conducted in MTK-2201 unit and special laboratory units UDK-1 and Alpha Laser ALV 100 (with the required upgrading).

Proceeding from the anticipated changes in the welded metal structure, spot welded joints were studied using metallographic analysis, comparative phase X-ray structure analysis of the welding area and removed sample ends, scanning electron microscopy and microprobe analysis. In addition, shape restoration in the resistance welding area was monitored.

Surfaces of samples welded by different processes were studied using metallographic microscope «Neophot-32» with different magnifications. To remove the oxide layer and reveal the structural microinhomogeneties, all the samples were processed in a solution of 47 % HNO_3 + 17 % HF + 36 % H_2O at room temperature for 10 s.

The main parameters of the mode of **spot welding** (Table 1 and 2) were determined experimentally. Both types of sample heating were used, namely by alternating (50 Hz) current of various values and duration* and capacitor-discharge current. In the latter case, the duration of current passage was adjusted by changing the capacitor capacitance. Amplitude value of current, which determines the coefficient of transformation (capacitor charging voltage remained constant at 600 V), was unchanged (see Table 2).

Table 2. Modes of spot capacitor-type welding

Sample #	Foil thickness, μm	Capacitor capacitance, μF	Transformation coefficient	Compression force, N
1-2	50	20	240	45
2-2	50	10	240	45
3-2	52	20	240	45
4-2	52	10	240	45
5-2	85	20	240	45
6-2	85	10	240	45
7-2	180	20	240	45
8-2	180	10	240	45

Investigation of the sample surface showed a considerable heating in the zone of foil surface contact with the electrodes, due to a high transient resistance between the electrodes and the foil, which is related to the presence of a titanium oxide layer on the sample surface and considerable hardness of nithinol, which increases at heating. An earlier unrecorded presence of concentric circles (Figure 1) on the thin foil surface (Table 2, sample # 2-2) is also observed. This phenomenon may be related to appearance of considerable tensile stresses, directed to the circle center, which are due to more difficult solidification of the molten metal of the weld spot.

Methods of scanning electron microscopy and microprobe analysis showed that in alternating current welding element distribution over the sample surface in the welding area corresponds to that in the base metal. No other elements than nickel and titanium were detected. In capacitor-type welding, tungsten particles which have moved over from the electrode metal, were detected in the area of electrode imprint.

Alongside microprobe analysis, also phase X-ray structure analysis of welding areas and ends of samples # 3-1, 4-1, 5-1, 6-1, 2-2, 4-2, 5-2, 6-2 was conducted. Filming was conducted in URS 2.0 unit in Cu–K_α-radiation in RKV-86 chamber. The radiographs show

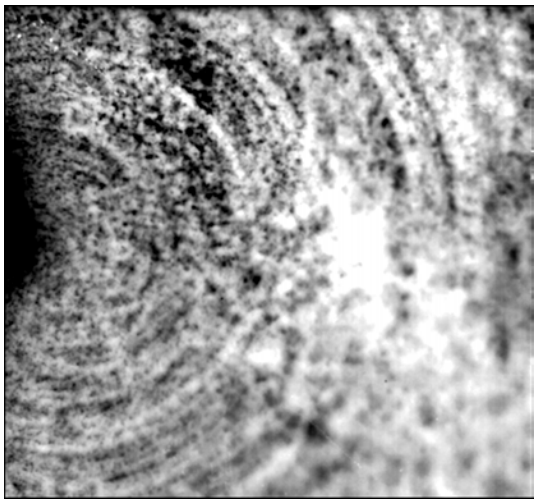

Figure 1. Concentric circles on the surface of sample # 2-2 (spot welding of foil 50 μm thick, Table 2) (×200)

*Welding was performed by Eng. V.N. Zaichko.

Table 3. Modes of spot capacitor-type welding of foil from nithinol of equiatomic composition

Sample #	Capacitor capacitance, μF	Charging voltage, V	Transformation coefficient
À-1	1100	200	100
À-2	1100	260	100
À-3	1100	200	150
À-4	1100	260	150
À-5	500	260	150

two line systems, which pertain to the initial (BCC-structure) and martensite (monoclinic structure) phase. Redistribution of intensities between the lines of these phases in the radiographs taken in different locations of the sample was not observed. This leads to the conclusion that the phase composition of the samples did not change as a result of welding. However, in samples # 6-1 and 2-2 the intensity of martensite phase lines is much weaker than in the other studied samples, but does not change at transition from the welding area to sample ends. This leads to the conclusion that the temperature interval of direct martensite transformation in these two samples shifts towards a region of lower temperatures, compared to other samples. Since measurements were performed on the sample surface, this leads to the conclusion that despite the softest welding mode, a sufficiently high energy evolves in the electrode–part resistance due to a small thickness of the foil and the associated relative increase of mechanical rigidity, this leading to surface heating above the temperature of decomposition of Ti_2Ni type intermetallics and lowering of the martensite transformation temperature.

The second experimental series was run to determine the dependencies of the characteristics of spot welded joints on the welding modes. Samples of $Ni_{50}Ti_{50}$ alloy in the form of strips 0.2 mm thick and about 3 mm wide (Table 3) and plates 0.25–0.28 mm thick of the area of 10×14 mm^2 (Table 4) were studied.

A characteristic feature of the studied processes of spot welding at different heating levels was manifested in the degree of welded metal deformation (Figure 2). The joint made by alternating current spot welding is produced in the solid phase (Figure 2, *b* and *c*), and in capacitor-type welding — with formation of a cast nugget (Figure 2, *a*).

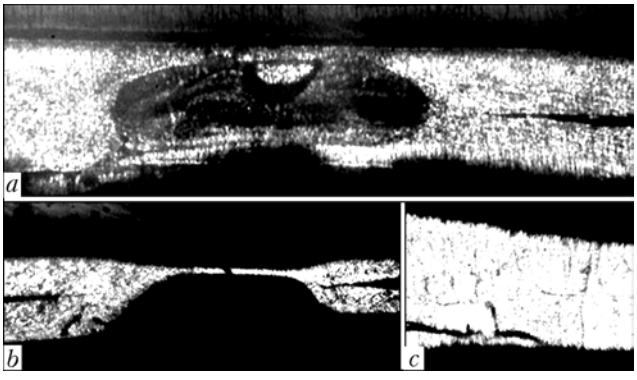

Figure 2. Transverse microsections of samples made by spot welding by capacitor-discharge (*a* — ×100) and AC pulses of industrial frequency (*b* — ×100; *c* — ×400)

Table 4. Modes of AC spot welding of nithinol foil of equiatomic composition

Sample #	Duration (number) of pulses, s	Pause duration, s
Â-1	0.06 (4) + 0.02 (1)	0.18
Â-2	0.06 (3) + 0.02 (1)	0.18
Â-3	0.12 (1) + 0.04 (1)	0.36
Â-4	0.24 (1) + 0.02 (2)	0.36

Metallographic analysis at a great magnification (Figure 3) showed that the dendrites forming at the cast nugget boundary (Figure 3, *a*) do not have enough time to grow into the central part of the spot nugget, where the structure is of a granular nature (Figure 3, *b*), which is related to a high cooling rate in capacitor-type welding.

Determination of the possible change in the composition of the nugget metal and boundary of the spot capacitor-type joint was conducted by scanning of the section surface in X-ray nickel and titanium radiation. It turned out that the imprint surface has a stable blackening density in both the cases, which is indicative of the absence of phase compositions of the intermetallics.

At mechanical testing by bending, samples of the greatest thickness (of about 180 μm) failed by the brittle mode under loading after capacitor-type welding. Analysis showed that such a fracture is characteristic of the base metal rather than being caused by thermal changes.

Samples deformed in the two-phase condition (initial β-phase + martensite phase), were heated up to the temperature of about 120 °C. Most of them (# 1-1, 2-1, 4-1, 5-1, 7-1, 8-1, 1-2, 3-2, 4-2, 5-2, 6-2, except for # 6-1 and 2-2, in which the martensite phase is absent at room temperature, as was noted above) showed a practically complete shape restoration. To restore the shape, samples # 6-1 and 2-2 were deformed at zero temperature (water with ice). As the samples had miniature dimensions, it did not seem possible to determine the exact temperature interval of martensite transformations.

Model samples in the form of $30 \times 30 \times 0.2$ mm plates were prepared by capacitor-type welding in the second experimental series, to determine the influence of the welding process on characteristic temperature of martensite transformation and degree of shape restoration. The welding zone on samples # A-1 and A-3 (see Table 3) was formed by two methods, namely a group of nine points adjacent to each other on a length of 9 mm in the plate center, and nine points at equal distance from each other. Characteristic points of martensite transformation M_f, M_s, A_s, A_f (Figure 4 and Table 5) were measured on these samples by strain gauge method.

Quantitative measurement of the degree of shape restoration was conducted in a special unit, in which the sample in the initial phase condition was deformed by the three-point bending method. Here the external load was selected so that the maximum stresses were significantly smaller than the material yield point. At temperature lowering before the start of martensite transformation, the sample developed plastic deformation (deflection is observed) under the impact of the applied stress, as a result of transformation plasticity. Deflection increases with increase of the amount of the martensite phase, this going on during the entire interval of martensite transformation. At heating (due to revers-

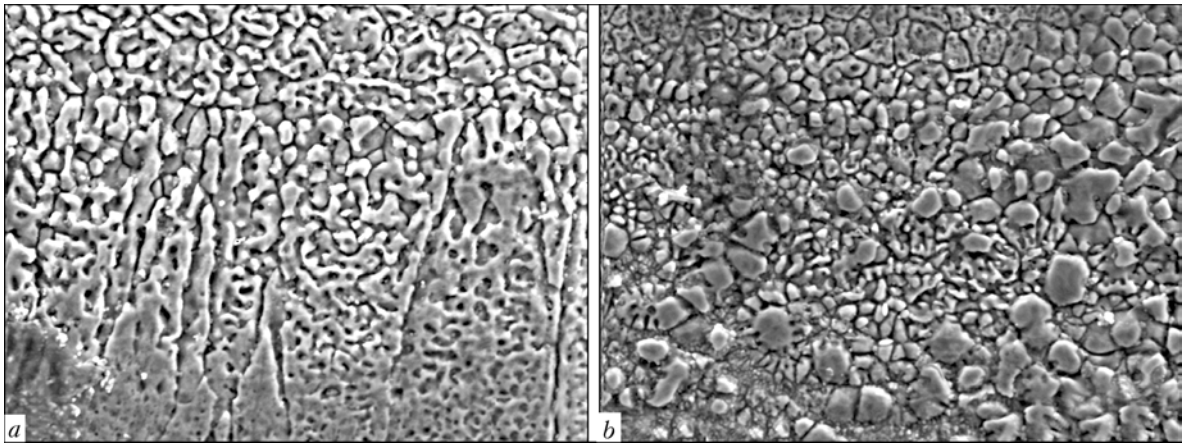

Figure 3. Microstructure of the boundary of a cast nugget with the base metal (*a*) and central part of the spot joint produced by capacitor-type welding (*b*) (×1000)

ible martensite transformation) the initial shape of the sample is restored. The extent of its restoration η was calculated by the following formula:

$$\eta = [(\varepsilon_h - \varepsilon_0)/\varepsilon_h]\cdot 100\ (\%),$$

where ε_h is the total deformation of the sample after direct martensite transformation; ε_0 is the residual deformation after reverse martensite transformation.

Table 6 gives the dependence of the degree of shape restoration on the deformation, induced by bending around a cylinder and calculated by the following formula:

$$\varepsilon = \frac{h}{2R}\cdot 100\ (\%),$$

where R is the radius of sample bending, mm; h is the sample thickness in the welding area for samples welded in different modes.

Table 5. Characteristic temperatures of martensite transformation (degree of shape restoration of samples is 100 %)

Modes acc. to Figure 4	M_s, °C	M_f, °C	A_s, °C	A_f, °C
I	–50	–60	–18	20
II	–50	–65	–21	25
III	–50	–60	–19	22

Table 6. Determination of the degree of shape restoration after deformation of spot-welded samples

Sample #	Individual plate thickness, mm	Welding area thickness, mm	Magnitude of specified deformation, %	Degree of shape restoration η, %
Capacitor-type welding				
À-1	0.18	0.40	1.80	100
À-2	0.20	0.43	1.95	98
À-3	0.19	0.41	1.58	90
À-4	0.19	0.51	1.96	90
À-5	0.18	0.39	1.77	90
Welding by alternating current of industrial frequency				
Â-1	0.26	0.70	2.5	90
Â-2	0.27	0.57	1.5	100
Â-3	0.28	0.61	1.9	95
Â-4	0.25	0.61	3.0	80

It is seen from the Table that only in samples # A-1 and B-2, which featured the lowest energy of welding heating, the degree of shape restoration was up to 100 %. In samples welded in modes with a higher heating intensity, shape restoration was incomplete, and in sample # B-4, welded at the greatest heating energy, shape restoration did not exceed 80 %.

Thus, heating by an inner heat source in spot welding leads to a slight local change of the structure, which is the smaller, the lower is the heating level. Therefore, as a result of the performed experiments, spot capacitor-type welding in stringent modes can be recommended for welding foils from alloys of Ni–Ti system. In this case, measures should be taken against electrode sticking to the surface of the welded foils by scraping the latter to remove a thick layer of titanium oxide.

Similar procedures were applied when studying the consequences of **laser welding** of wire samples of 0.28 mm diameter welded «into a cross» and «into a sphere» (Figure 5).

Analysis of welded joints with the magnification of ×400 and ×600 showed absence of cracks on the surface. Distribution of nickel and titanium in the cast metal of the joints, by the data of microprobe analysis, turned out to be uniform similar to resistance spot welding, and investigation of the sample shape restoration confirmed the above conclusion that pulsed heating does

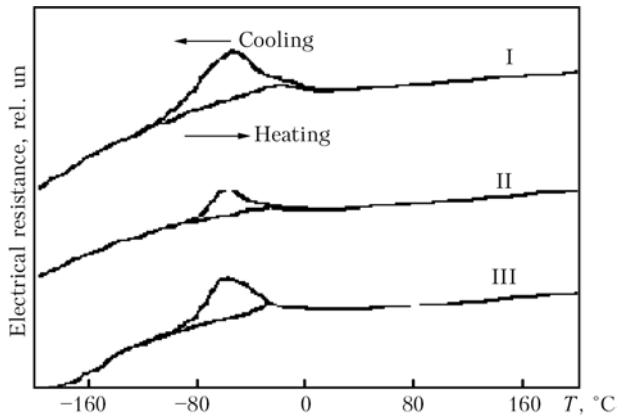

Figure 4. Temperature dependence of electrical resistance of samples welded in different modes: I, II — modes for sample # A-1 with a group and individual points, respectively; III — for sample # A-3 with a group of points

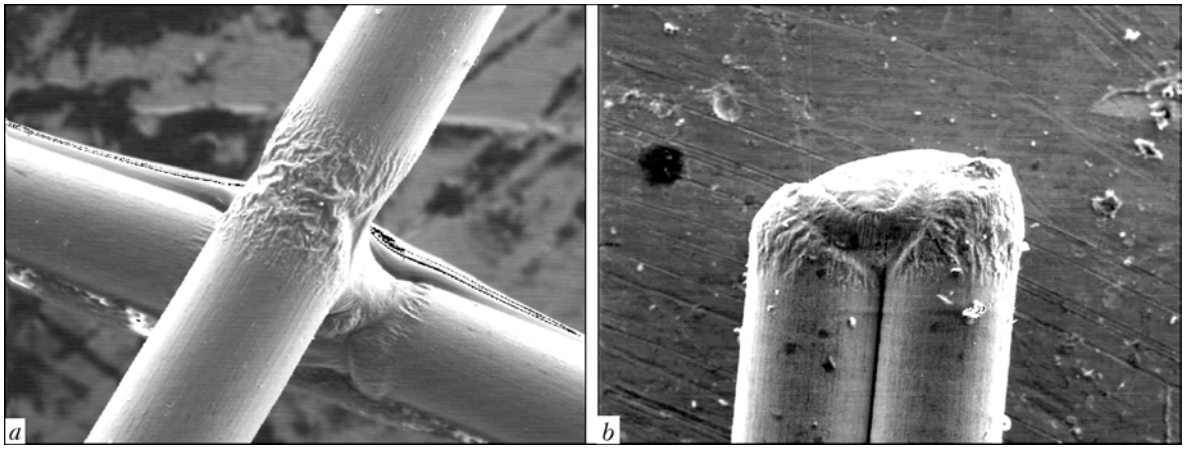

Figure 5. Nithinol samples welded by a laser beam «into a cross» (*a*) and «into a sphere» (*c*) (×100)

Table 7. Modes of capacitor-type welding of nithinol wire

Sample material	Capacitor capacitance, μF	Capacitor discharge voltage, V	Collision force, N	Discharge contour resistance, Ohm	Collision path length, mm	Length of wire protruding from the clamp, mm
Nithinol wire of 0.6 mm dia.	2850	900	30	1.0	6	1.5
Nithinol wire of 0.8 mm dia. + copper wire of 0.6 mm dia.	850	400	20	1.4	5	2.0
Nithinol wire of 0.6 mm dia. + nithinol plate 3 mm thick	2850	900	35	1.0	12	2.5
Wire from 10Kh18N9T steel of 0.8 mm dia. + nithinol plate 1.4 mm thick	3000	900	30	1.2	10	1.5

not lead to shifting of martensite transformation points.

Table 7 gives the modes of **shock capacitor-type welding** of nithinol wire. All the experiments on welding T-shaped joints were conducted at reverse polarity, considering that nithinol melting temperature is low (1240–1310 °C [16]).

A feature of nithinol (as a welded material), in addition to a relatively low melting temperature, also is a high electrical resistance and low ductility. Specific electrical resistance of nithinol is of the order of 70 μOhm·cm (for comparison, that of copper is 1.7, of stainless steel is 8 μOhm·cm), hardness is *HRC* 60, this corresponding to that of hardened steel. In shock capacitor-type welding this affects, on the one hand, the accelerated melting of nithinol due to heat evolution at current passage through the wire, and on the other hand ---- its insufficient deformation at collision.

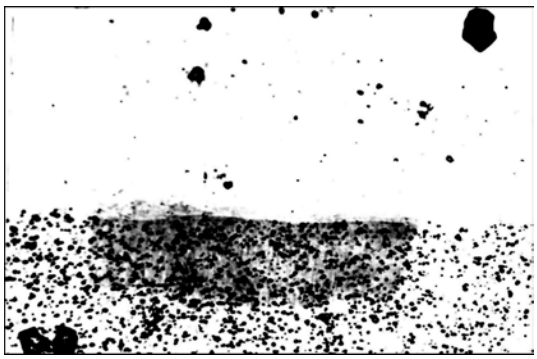

Figure 6. Microstructure of a joint of nithinol wire of 0.6 mm dia. to titanium nickelide plate 3 mm thick (×250)

Stresses which are manifested at phase transition during welded joint cooling, have an essential role in nithinol welding (both for joining two wires, and for T-joint of the wire with the plate surface), this causing an instability of the strength of the welded joint, produced by shock capacitor-type welding. This process of solid-phase joining of metals is characterized by a relatively low upset pressure. Therefore, depending on the random crystallographic orientation of the metal grains coming to the surface, stresses of the second kind can be added to a greater or smaller degree to external stresses applied in bend testing of the sample.

A much better result can be obtained in welding nithinol to a ductile metal, for instance, copper or stainless steel. In this case, the joint strength is influenced not so much by inner stresses, as by the relative position of the abutted crystalline blocks. Due to a low ductility of nithinol, one may anticipate only a rotation of the grains at deformation of the ductile metal. However, as shown by experiments, to achieve the joint strength higher than that of the soft metal, the butt cross-section has to be increased 2 times, compared to that of the soft wire.

Metallographic studies of welded samples demonstrated an absence of pores, cracks or other macrodefects, disturbing the butt discontinuity (Figure 6). Different «prehistories» of the wire and the plate led to different kinds of the structure and second phase content. In [17] it is assumed that its composition is Ti_4Ni_2O.

In the joints of the copper and nithinol wire welded in the optimum mode there is no mixing of the welded metals or loss of SMA components, which is indicated by coincidence of the butt shape in filming in the radiation of each of the elements present in the joint

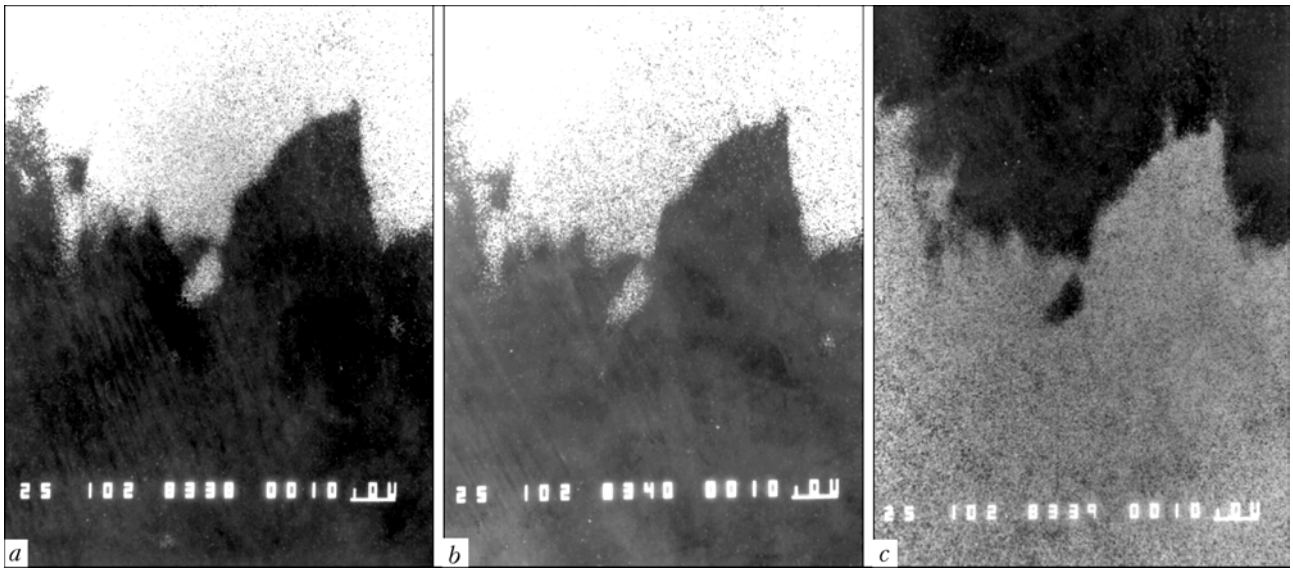

Figure 7. Radiographs of joints of nithinol with copper produced in the titanium (*a*), nickel (*b*) and copper (*c*) radiation (×1000)

(Figure 7), and the martensite structure in the joint of a regular metal with SMA is preserved (Figure 8).

CONCLUSIONS

1. There is no data in publications on the influence of thermomechanical impact in welding on the characteristics of the direct and reverse martensite transformations in SMA in Ni–Ti system or methods of welding thin wires and foil from these alloys. This restrains development of the technology of welding thermoelastic alloys and their application in engineering and medicine.

2. Analysis of the physical fundamentals of shape memory effect in thermoelastic alloys allowed selecting from the many welding processes those, which use pulsed heating, in particular, capacitor-type (spot and shock) and laser welding.

3. It is shown that in spot capacitor-type and laser welding of small cross-sections on nithinol, the temperature of SMA martensite transformation does not change, and the degree of shape restoration is the closer to 100 % the more rigid is the heating pulse.

4. Joints of nithinol made by shock capacitor-type welding do not have the required strength. However, satisfactory mechanical and thermomechanical characteristics of welded samples were obtained in welding nithinol to ductile metals.

5. Pulsed short-time heating of nithinol both with formation of the inner heat source, and of the surface zones of increasing the temperature above that of metal melting, does not impair the metal condition or change its thermomechanical properties near the welding area, so that it can be recommended for manufacturing products from this material.

The work was done with the financial support of the Ministry of Education and Science of Ukraine.

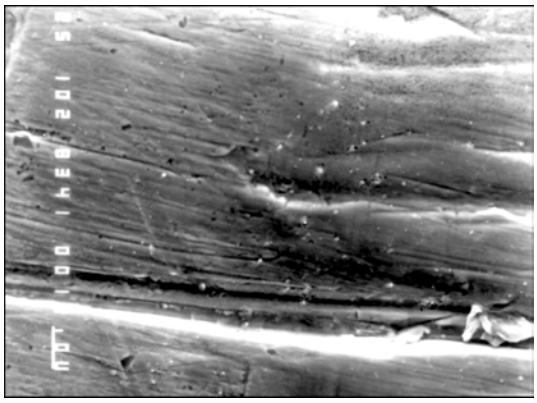

Figure 8. Surface of a section in the scanning mode (×1000)

1. Apaev, B.A., Voronenko, B.I. (1973) Shape memory effect in alloys. *Metallovedenie i Term. Obrab. Metallov*, **1**, 24–28.
2. Zhuravlyov, V.N., Pushin, V.G. (2000) *Alloys with thermomechanical memory and their application in medicine*. Ekaterinburg.
3. Kornilov, I.I. (1975) Metalloids with unique properties. *Metallovedenie i Term. Obrab. Metallov*, **10**, 19–22.
4. Ootsuka, K., Shimizu, K., Suzuki, Yu. et al. (1990) *Alloys with shape memory effect*. Moscow: Metallurgiya.
5. Gyunter, V.E., Kotenko, V.V., Mirgazizov, M.Z. et al. (1986) *Shape memory alloys in medicine*. Tomsk: TGU.
6. Mirgazizov, M.Z., Gyunter, V.E., Itin, V.I. et al. (1993) *Superelastic implants and structures of shape memory alloys in stomatologia*. Moscow-Berlin-Chicago-London-San Paulo-Tokyo: Quintessenz.
7. Shinoda, T., Tsuchia, T., Takachashi, H. (1992) Friction welding of shape memory alloy. *Welding Int.*, 6(**1**), 20–25.
8. Hirose, A., Araki, N. (1989) Welding TiNi shape memory alloys. *Metals*, 59(**8**), 61–68.
9. Nishikawa, M. (1985) Welding shape memory alloys. *Bull. Metals Sci.*, 24(**1**), 56–60.
10. Araki, T., Hirose, A., Uchihara, H. et al. (1989) Characteristics and fracture morphology of Ti–Ni type shape memory alloy and its laser weld joint. *Materials*, 38(**428**), 478–483.
11. (1999) Laserwerkstoffbearbeitung von Formgedaechtnislegierungen. *Schweissen und Schneiden*, 51(**12**).
12. Potluri, N.B. (1999) Joining of shape memory alloys. *Welding J.*, **3**, 39–42.
13. Rudakov, S.G. (2000) Development and research of welding process of titanium-nickelide-based alloys. In: *Proc. of 13th Sci.-Pract. Conf.* (Yurga, April 27–28, 2000). Tomsk: TGU.
14. Rudakov, S.G., Katunina, A.S., Petrichenko, O.V. (2001) Producing of welded structures from controllable shape memory alloys. In: *Proc. of 14th Sci.-Pract. Conf.* (Yurga, April 26–27, 2001). Tomsk: TGU.
15. (1997) Fabrication of titanium nickelide + aluminium alloy composite material by explosion welding. In: *Proc. of Russian Sci.-Techn. Conf. on Current Problems of Welding Science and Engineering «Welding-97»* (16–18 Sept., 1997). Voronezh.
16. Tikhonov, A.S., Gerasimov, A.P., Prokhorova, I.I. (1981) *Application of shape memory effect in current machine-building*. Moscow: Mashinostroenie.
17. Melton, K.N. (1990) *Ni–Ti based shape memory alloys. Engineering aspects of shape memory alloys*. Butterworth-Heinemann Ltd.

INFLUENCE OF ELECTRODYNAMIC TREATMENT ON THE STRESS-STRAIN STATE OF HEAT-RESISTANT STEELS

L.M. LOBANOV, N.A. PASHCHIN, V.Yu. SKULSKY and **V.P. LOGINOV**
E.O. Paton Electric Welding Institute, NASU, Kiev, Ukraine

Results of investigation into the effect of electrodynamic treatment (EDT) using single pulses on the kinetics of elastic strains and stressed state of heat-resistant steels are given. The experimental procedure is presented and a laboratory EDT unit is described. It has been established that treatment using single discharges initiates the fields of elastic compression-tension strains in the material treated, their values being in direct dependence on the discharge voltage. It is shown that EDT can be employed for relaxation of the stressed states of heat-resistant steel structures.

Keywords: electrodynamic treatment, heat-resistant steels, stress-strain state, electron-dislocation interaction, flat sample, cylindrical sample, specific pulse energy

Advance of modern mechanical engineering necessitates searching for new processes for improving the strength characteristics of high-strength steel welded structures. One of the promising directions is development of the process of treatment of metals and alloys by applying an electromagnetic field to them [1]. An example of such an interaction is treatment based on the effect which is manifested under the influence of electrodynamic forces on sheet materials. By varying the duration and energy of the current pulses, applied to an electrically conducting material, it is possible to influence the static and fatigue strength, ductility, hardness and stress-strain state of metals and alloys, as well as their welded joints through activation of dislocation displacements, phase changes and other processes [2]. The observed effects can be explained on the basis of the hypothesis of electron-dislocation interaction [3].

The purpose of this work is development of an experimental unit for electrodynamic treatment (EDT) of structural steels and their welded joints, as well as evaluation of the influence of such a treatment on performance of the studied materials.

The advantage of EDT over heat treatment and other kinds of treatment consists in mobility of the used equipment. In addition, owing to the small weight and overall dimensions of EDT units they can be used for treatment of large-sized welded structures in the operation sites of the latter.

EDT performance does not ask for high power units, as electric discharges of 0.005–1 ms duration are applied, which requires the availability of small-sized pulsed power sources, and the element base provides the following working parameters of the mode: pulse current $I_p \leq 10$ kA and voltage $U_p \leq 3$ kV. Under certain emergency conditions the values of current and voltage in the current-carrying elements of electric machines can rise by tens of times in a quite short period of time, so that a protection device should be in place [4]. However, in industrial electronic devices such transient processes (TP) are often regular, and not characteristic just for the emergency mode. TP associated with capacitor charging and discharge make up the principle of electronic generator operation; they arise in circuits which include inductive and capacitive elements. The developed EDT unit is a typical example of such instruments.

Processes running at EDT can be divided into TP in a circuit with a capacitance element and resistor (capacitor charging), TP in a circuit with a charged capacitor (capacitor discharge), as well as TP in the working circuit.

To study electrodynamic TP running at EDT, the working part of the circuit was connected to monitoring instrumentation, which allows recording the electrical and mechanical parameters of the performed treatment.

The unit end effector is the electrode, which is a coil placed into an insulated case and connected to a capacitor bank. The coil is connected to a cylindrical rod from electrical copper of M1 grade, the spherical end face of which is the zone of electrode contact with the treated surface of the welded joint, i.e. area where the electrodynamic discharge of the capacitor bank runs.

The block-diagram and the general view of the laboratory unit for EDT of metals and welded joints are shown in Figure 1. The monitoring instrumentation system for studying EDT consists of:

- bank of capacitors for accumulation and discharge of the current pulse at the frequency of 10 pulse / min;
- block of charging and control for charging the capacitor bank up to the working voltage;
- end effector-electrode fitted with a shunt to transfer the electrodynamic impact (current pulse) to the treated material with the concurrent measurement of current values (shunt);
- strain gauge unit for measurement of EDT component at the moment of the pulse action;
- strain gauge unit for measurement of the forces of the treated sample tension;

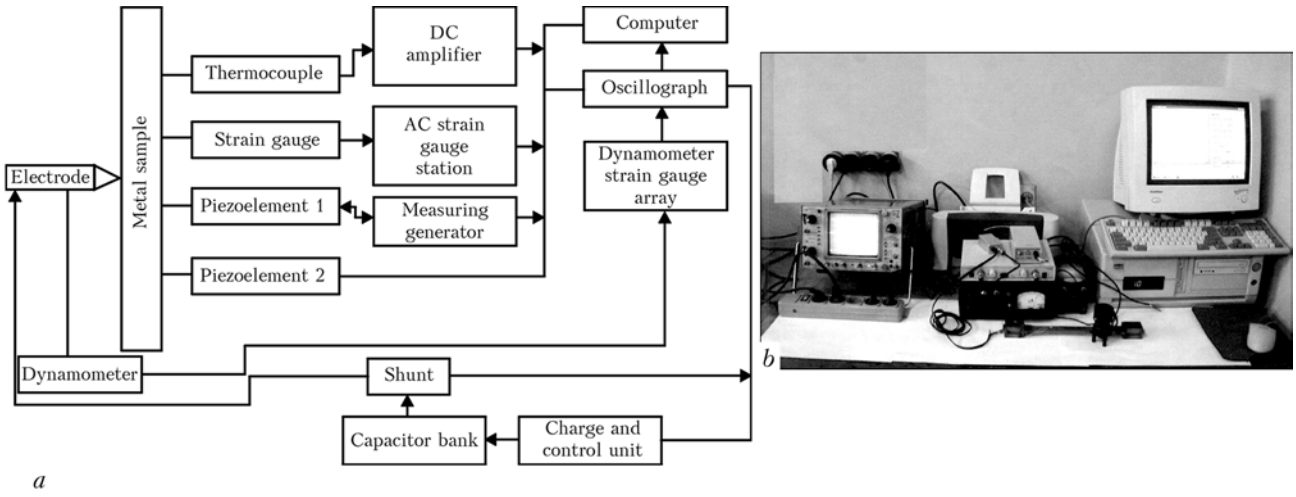

Figure 1. Block-diagram (*a*) and general view (*b*) of the laboratory unit for EDT of metals and welded joints

• thermocouple with a DC amplifier to measure the temperature component at the moment of the pulse action (integral Joule heating);

• piezoelements for conversion of mechanical displacements into an electric signal;

• signal generator for generation of electric oscillations and signal transfer to the metal sample;

• oscillograph for recording and displaying the electric and mechanical signals at EDT;

• computer for numerical processing of signals representing EDT parameters.

The main evaluation characteristic of EDT is variation of the initial stress-strain state of the metal sample, which results from treatment of its surface and is recorded by elements of the measuring system of the laboratory unit. Initial stress-strain state of the sample was induced by applying longitudinal uniaxial tension in a specialized force unit.

It is established that the impact of current pulses on the metal subjected to tension leads to relaxation of its stress-strain sate [5], which may be positive for increase of the welded structure life.

Investigation of the influence of EDT on relaxation of the stress-strain state of structural materials was conducted on samples from heat-resistant steels of different grades. The central part of the sample working zone was treated by series of pulses from one to three with the interval of 30 to 60 s.

The studied sample with the strain gauges and thermocouple fastened on it was fixed in the force device grips and stretched along the longitudinal axis, while controlling the values of initial relative deformations and temperature. The charging and control block was used to measure the pulse voltage.

At contact of the electrode end face with the sample surface the capacitor bank was discharged and the values of the relative deformations in the sample and of pulse current were recorded. After completion of the pulse action the values of residual deformations were determined, as well as the temperature of the studied sample surface.

Kinetics of deformation processes in the HAZ metal at EDT was studied on flat samples of blade type from steel 15 KhN with 120 × 15 × 3 mm working zone, which were fastened in the fixture without tension. EDT of the middle part of the sample working zone was performed by individual discharges with the following working parameters of the pulse: current I_p = = 2400 A, voltage U_p = 165 V, pulse frequency W_p = = 1600 Hz and their action time t_p = 0.3 ms. Relative deformations ε initiated by current discharge, were measured at the moment of the pulse action. Shape of current pulses and relative sample deformations induced by them are given in Figure 2.

It is seen from the Figure that the curve of relative deformations ε is of a pronounced sinusoidal nature, and electrodynamic impact causes a high-gradient elastic compression in the material, which is compensated by elastic tension with subsequent attenuation to zero ε values. Activation of mechanical action of the electric discharge starts with a certain (approximately 0.1 ms) delay from the moment of pulse current rise I_p, while increment of deformations in the compression-tension regions proceeds in a jump-like manner.

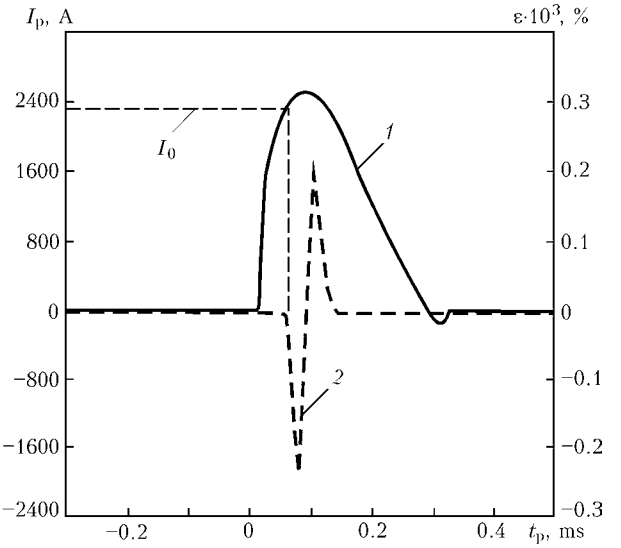

Figure 2. Change of the shape of current pulses I_p (*1*) and kinetics of relative deformations ε (*2*) at EDT of 15KhN steel samples

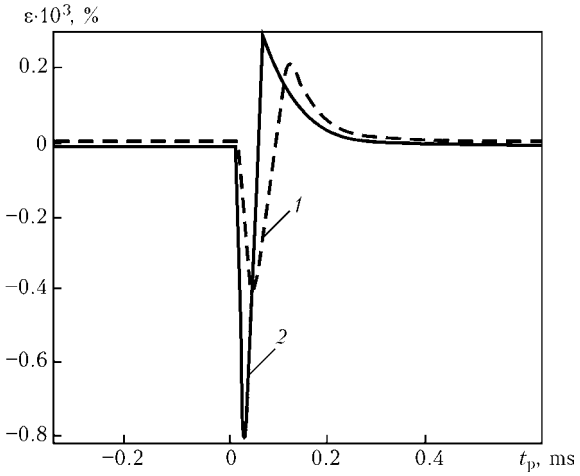

Figure 3. Kinetics of variation of relative deformations ε at EDT of 15KhN steel sample at the moment of action of individual discharge at U_{el} = 200 (*1*) and 400 (*2*) V

In terms of the hypothesis of electron-dislocation interaction [1], this is attributable to the fact that before the moment of increment of pulse current values from I_p to I_0 (start of the compression process), the dislocations are located on insurmountable stoppers for the given condition of the sample. After current has reached I_0 value, dislocation motion along the slip lines becomes more active in the sample metal, which is accompanied by the moving dislocations breaking through the obstacles in the form of discontinuities of different types and dislocation clusters [6].

In Figure 2 it is seen that the current pulse duration is equal to 0.3 ms, and the time of activation of the mechanical impact on the metal as a result of EDT is 0.10–0.15 ms. Maximum ε value corresponds to maximum values of current and discharge voltage, and, therefore, the effectiveness of EDT process is determined not by the time of current pulse action t_p, but its specific energy q per a unit of volume of the treated material.

To confirm the influence of q on the intensity of electrodynamic impact on the metal, the kinetics of ε variation at different values of electrode voltage U_{el} was studied at EDT of a sample from steel 15KhN. Flat samples were treated in the modes similar to those earlier used, but U_{el} was varied from 200 up to 400 V. Deformations ε (Figure 3) and temperatures T (Joule heat) were measured at the moment of action of the individual pulse. Analyzing function ε = f(U_p) one can see that increment of ε values is in direct dependence on voltage on the electrode and specific energy of the pulse, respectively. Increase of U_{el} leads to an increase of gradients of time deformations both in the region of compression and tension.

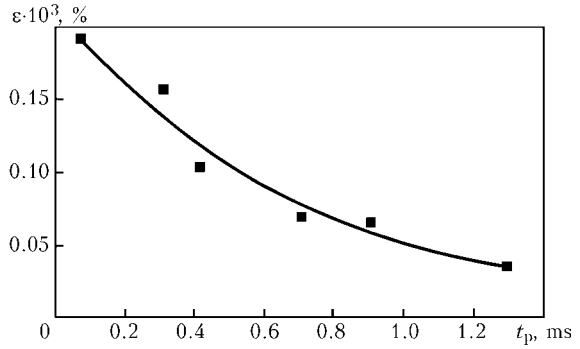

Figure 4. Dependence of maximum values of relative deformations ε in 15KhGMR steel samples on time t_p of the pulse impact at EDT

It should be noted that current measurements of metal temperature conducted in all the experiments to allow for the influence of sample heating at EDT showed that it does not change either at the moment of the discharge action, or after completion of treatment at T = (20 ± 5) °C.

Experiments were conducted to assess the influence of the duration of the time interval under the impact of the current discharge on EDT effectiveness. With this purpose a series of isolated discharges were run on a flat sample from steel 15KhGMR fastened without tension, in the above mode at U_{el} = 400 V, with t_p variation from 0.01 to 0.13 ms. The criterion of effectiveness of this process were the maximum values of elastic deformations ε determined by dependence ε = f(t_p) shown in Figure 4.

It is seen from the Figure that increase of pulse duration at stabilization of other EDT parameters lowers its relative deformations. This is indicative of lowering of the energy of the discharge impact on material, and, hence, has an adverse effect on EDT process. Therefore, at EDT it is rational to minimize the time of electrodynamic impact at a concurrent increase of power (specific energy q).

The influence of EDT on relaxation of longitudinal stresses was studied on cylindrical samples from steel 18KhGA (Figure 5). The sample was fastened in the grips of a specialized fixture and subjected to tension along the longitudinal axis, the values of which were recorded by the strain gauge. After achievement of the required load in the working zone, a series of individual discharges with the concurrent strain gauging of the relaxation processes in the material was conducted. EDT mode corresponded to that selected earlier for a flat sample from steel 15KhGA at U_{el} = = 400 V. The criterion for evaluation of the process efficiency was relaxation of the longitudinal tensile stresses $\Delta\sigma_t$ — the absolute value of the drop of sample tension level σ_t initiated by a pulsed current discharge. Dependence of $\Delta\sigma_t$ on the pre-tension level is shown in Figure 6, from which it can be seen that at application of small values of the tensile forces (up to 50 MPa) EDT allows lowering the level of tensile stresses in samples from 18KhGA steel by 50 %. On the other hand, at a higher loading level of $\Delta\sigma_t$ = = 200 MPa, $\Delta\sigma_t$ drops by 10–15 %. It should be also

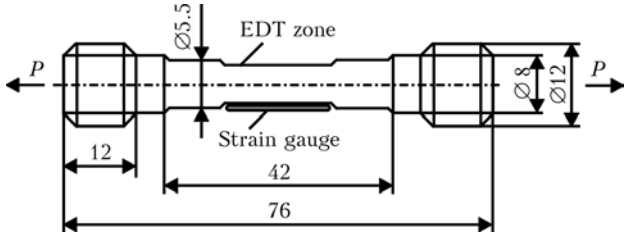

Figure 5. Schematic of 18KhGA steel sample for evaluation of EDT influence on the longitudinal tensile stresses: P — tensile load

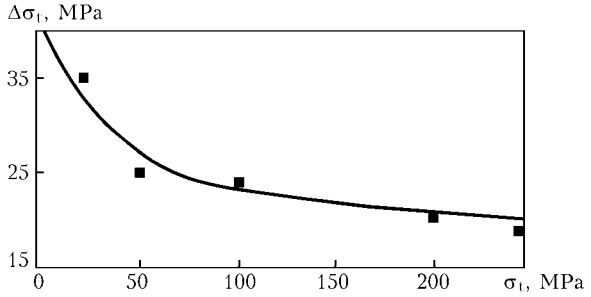

Figure 6. Variation of tensile stresses $\Delta\sigma_t$ in 15KhGA steel samples after EDT at different levels of pre-tension σ_t

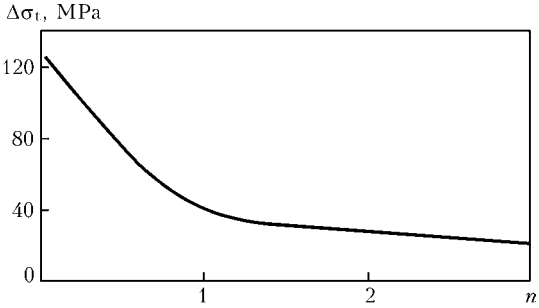

Figure 7. Influence of number n of current pulses on tensile stresses σ_t in 18KhGA steel samples after EDT

noted that at sample pretension to 25 MPa, after EDT it was possible to obtain small (up to 10 MPa) compressive stresses.

To evaluate the influence of the number n of successively applied pulses on σ_t lowering, the sample from steel 18KhGA (see Figure 5) was subjected to tension to 130 MPa. Then it was successively treated by a series of three discharges in the above EDT mode. Based on the conducted strain gauging, it was established that EDT effectiveness does not rise with increase of the number of pulse discharges at a constant energy stored by the capacitor bank. The nature of the studied experimental dependence is shown in Figure 7. The greatest lowering of mechanical tensile stresses in the studied samples was obtained under the impact of the first pulse and it is equal to 65 to 70 % of the total level of voltage drop σ_t. At the repeated discharge the stress level decreases by not more than 10–15 %, and after the third ---- by not more than 1–5 % of the total level of tensile stresses.

The obtained results lead to the conclusion that EDT is a promising means to increase the life of metal structures, including welded structures. However, the issues of evaluation of EDT influence on the mechanical properties of welded joints of various structural materials should be studied further.

1. Baranov, Yu.V., Troitsky, O.A., Avraamov, Yu.S. et al. (2001) *Physical principles of electropulse and electroplastic treatment and new materials*. Moscow: MGIU.
2. Beklemishev, N.N., Gorbunov, N.M., Koryakin, N.I. et al. (1989) *Ductility and strength of metallic materials in pulse action of high power electromagnetic field*. Moscow: IMP AN SSSR.
3. Spitsin, V.I., Troitsky, O.A. (1985) *Electroplastic deformation of metals*. Moscow: Nauka.
4. Aleksandrov, G.I. (1985) *Theory of electric apparatuses*. Moscow: Vysshaya Shkola.
5. Semeshko, N.A., Krupsky, R.F., Kupov, A.V. et al. (2004) Acoustic emission in electropulse deformation of titanium alloys. *Materialovedenie*, **7**, 29–33.
6. Finkel, V.M. (1997) *Physical principles of fracture retardation*. Moscow: Metallurgiya.

EFFECT OF PHOSPHORUS ON CRACK RESISTANCE OF LOW-CARBON DEPOSITED METAL

I.I. RYABTSEV, Yu.M. KUSKOV and **D.P. NOVIKOVA**
E.O. Paton Electric Welding Institute, NASU, Kiev, Ukraine

The paper presents results of investigation into the effect of phosphorus at its content of 0.3–3.5 wt.% on crack resistance of low-alloyed carbon deposited metal of the Fe–Mn–Si–Cr system. It is shown that cold cracks in the deposited metal of the type under investigation form at a phosphorus content of > 1.2 %. Brittle phosphide eutectics are the centres of initiation and propagation of cold cracks. In a multilayer deposited metal, the cracks can propagate from layer to layer, but they do not transfer into the base metal.

Keywords: arc cladding, low-alloy deposited metal, alloying with phosphorus, crack resistance, technological test, phosphide eutectics

Phosphorus has a positive effect on tribotechnical properties of low-carbon low-alloyed deposited metal [1, 2]. However, wide application of phosphorus as an alloying element of cladding consumables is hindered by an established opinion that it has a negative effect on crack resistance of the deposited metal, although the consumables in point have, as a rule, a relatively low phosphorus content, i.e. no more than 0.05 % [3–6]. The purpose of this study was to assess the effect of phosphorus at its content of 0.3–3.5 wt.% on crack resistance of low-carbon deposited metal of the Fe–Mn–Si–Cr alloying system. The content of manganese, silicon and chromium in the deposited metal was kept constant, the total content of these elements being no more than 5 %.

Many methods and technological tests were developed to study susceptibility of the deposited metal to cracking [7]. In our studies, a rigid technological test suggested by the Central Institute of Welding Engineering (ZIS) in Halle (Figure 1) [8] was used to assess crack resistance of the deposited metal. This test is simple in use and allows fixing a difference in crack resistance of metals containing brittle components in their structure.

According to this test, one to three beads are deposited in one or several layers with or without preheating. After cooling to room temperature at preset cooling parameters, the deposited metal surface is subjected, if necessary, to cleaning or grinding. Cracks

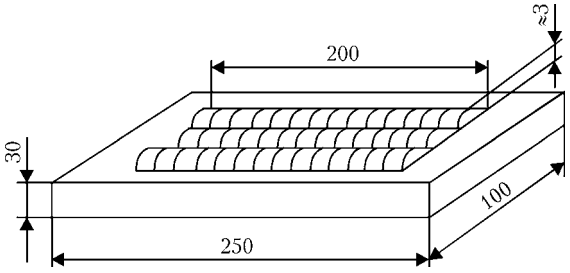

Figure 1. Schematic of technological test for assessment of crack resistance of deposited metal [8]

are detected by examinations using a magnifying glass with a four-fold magnification, dye penetrant or magnetic powder methods can also be applied. The quantity of cracks is counted, and their length and width are measured.

The scale of points was developed to assess sensitivity of the deposited metal to cracking: crack-free deposited metal has the lowest sensitivity (point 1), and metal containing cracks (more than 0.1 mm wide) extending to the base metal and having a total length of more than 60 mm is estimated at point 5. The deposited metal containing cracks of a smaller width (≤ 0.1 mm) and smaller length is estimated at intermediate points (2–4).

The experiments were conducted on steel St3 plates measuring 40 × 150 × 250 mm. The plates were clad by the automatic submerged-arc method using experimental wires and flux AN-348. The plates were not preheated before cladding. Individual beads about 200 mm long were deposited on them in four layers. After cladding, the plates were cooled in air. Flux-cored wires 2.0 mm in diameter were used for cladding, the cladding parameters being as follows: current 220–240 A, voltage 26–28 V, cladding speed 20 m / h.

After complete cooling, the plates were examined to detect cracks using a magnifying glass with a four-fold magnification. No hot cracks were detected in cladding using all experimental wires. It is likely that a large amount of low-melting point eutectics contained in the deposited metal provide healing of the hot crack embryos [9].

The first transverse cold cracks were fixed in the deposited metal containing 1.58 % P (Table, PP-1.6-F). In cladding samples using flux-cored wires with a higher phosphorus content, the quantity and total length of the cracks accordingly increased. The cracks present in the deposited beads were counted, and their maximal width was estimated using probes, while the length was measured with a calliper. Then the sensitivity of the deposited metal to cracking was assessed by points (see the Table).

After visual examination and counting of cracks, the clad plates were cut by the anode-mechanical method at the centre along the axis of the deposited beads. The resulting specimens were polished and

Assessment of sensitivity of deposited metal to cracking

Flux-cored wire grade	Phosphorus content of deposited metal, wt.%	Deposited metal hardness *HB* (*HRC*)	Quantity of cracks with width, mm		Point of crack resistance of metal depending upon total crack length, mm				
			> 0.1	≤ 0.1	0	1–20	21–40	41–60	> 60
PP-0-F	0.035	229	0	0	1	–	–	–	–
PP-0.3-F	0.32	229	0	0	1	–	–	–	–
PP-0.6-F	0.59	302	0	0	1	–	–	–	–
PP-0.9-F	0.98	302	0	0	1	–	–	–	–
PP-1.2-F	1.23	321	0	0	1	–	–	–	–
PP-1.6-F	1.58	(38)	0	8	–	–	3	–	–
PP-2.0-F	2.02	(41)	2	8	–	–	–	–	5
PP-2.5-F	2.46	(44)	2	11	–	–	–	–	5
PP-3.5-F	3.35	(46)	2	12	–	–	–	–	5

etched for a more precise estimation of the quantity of cracks and determination of the character of their propagation in the deposited metal layers (Figure 2). Dye penetrant inspection of sections was also performed. No new cracks were detected, compared with the initial assessment. No propagation of cracks from the deposited to base metal was fixed either.

No cracks were detected in the deposited metal at a phosphorus content of about 1.2 %. Thus, its sensitivity to cracking was estimated at point 1 (Table, Figure 2, macrosections 2–5). The first cold cracks were fixed in the deposited metal at a phosphorus content of 1.58 %. Eight cracks not less than 0.1 mm wide, which did not propagate from the base to deposited metal (Table and Figure 2, macrosection 6), were revealed over a length of about 200 mm. According to recommendations of the applied test, sensitivity of this metal to cracking was estimated at point 3. The deposited metal containing 2.02, 2.46 and 3.35 % P had cracks more than 0.1 mm wide with a total length of more than 60 mm. Sensitivity of this metal to cracking was estimated at point 5 (Table, Figure 2, macrosections 7–9).

To determine causes of cracking, the metal deposited with all experimental wires (Figure 3), as well as metal with a phosphorus content of 2.46 and 3.35 % in locations of cracks (Table, wires PP-2.5-F and PP-3.5-F; Figure 4, *a–d*), was examined by metallography. As shown by the metallographic examinations, structure of the deposited metal containing no phosphorus (Figure 3, *a*) consisted of ferrite (microhardness *HV* 0.01-185–199), pearlite (*HV* 0.01-205–288) and bainite regions (*HV* 0.01-205–254). Structure of the deposited metal was refined at a phosphorus content of 0.32 % (Figure 3, *b*). Like in the previous case, it consisted of a mixture of ferrite (*HV* 0.01-201–205), pearlite (*HV* 0.01-257–290) and bainite (*HV* 0.01-257–290). In addition, there were regions identified as a bainite-martensite mixture with microhardness *HV* 0.01-378. No free phosphides were detected. It is likely that all phosphorus was dissolved in the deposited metal matrix.

As the phosphorus content increased to 0.59 % (Figure 3, *c*), structure of the deposited metal became still finer. Microhardness of individual structural components increased: *HV* 0.01-205–239 (ferrite), *HV* 0.01-283 (pearlite), and *HV* 0.01-482–515 (bainite-martensite mixture). At the same time,

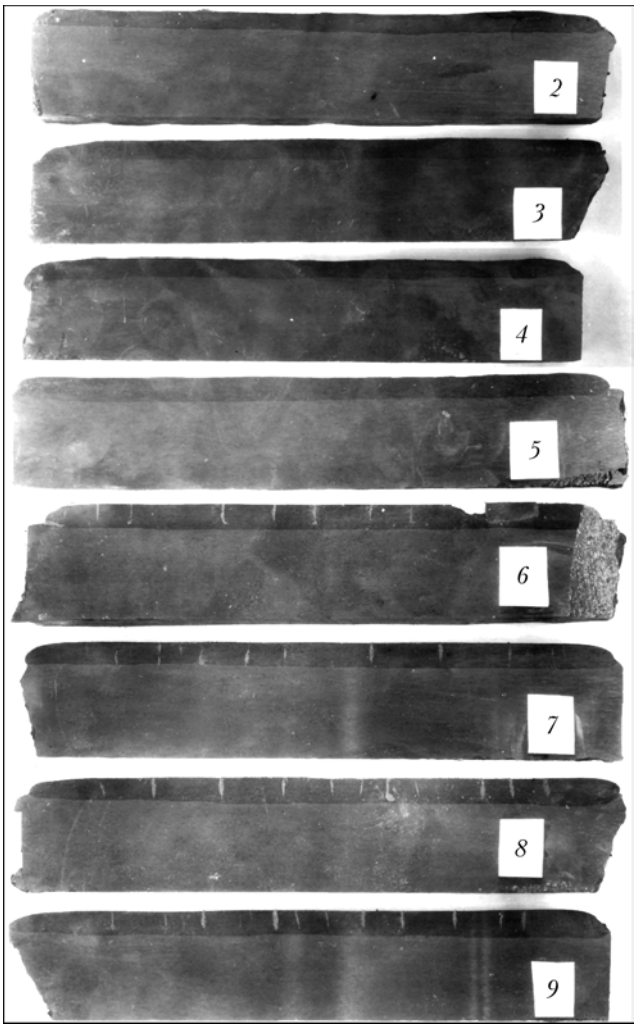

Figure 2. Longitudinal macrosections of plates deposited with flux-cored wires with a different phosphorus content, wt.%: *2* — 0.32; *3* — 0.59; *4* — 0.98; *5* — 1.23; *6* — 1.58; *7* — 2.02; *8* — 2.46; *9* — 3.35

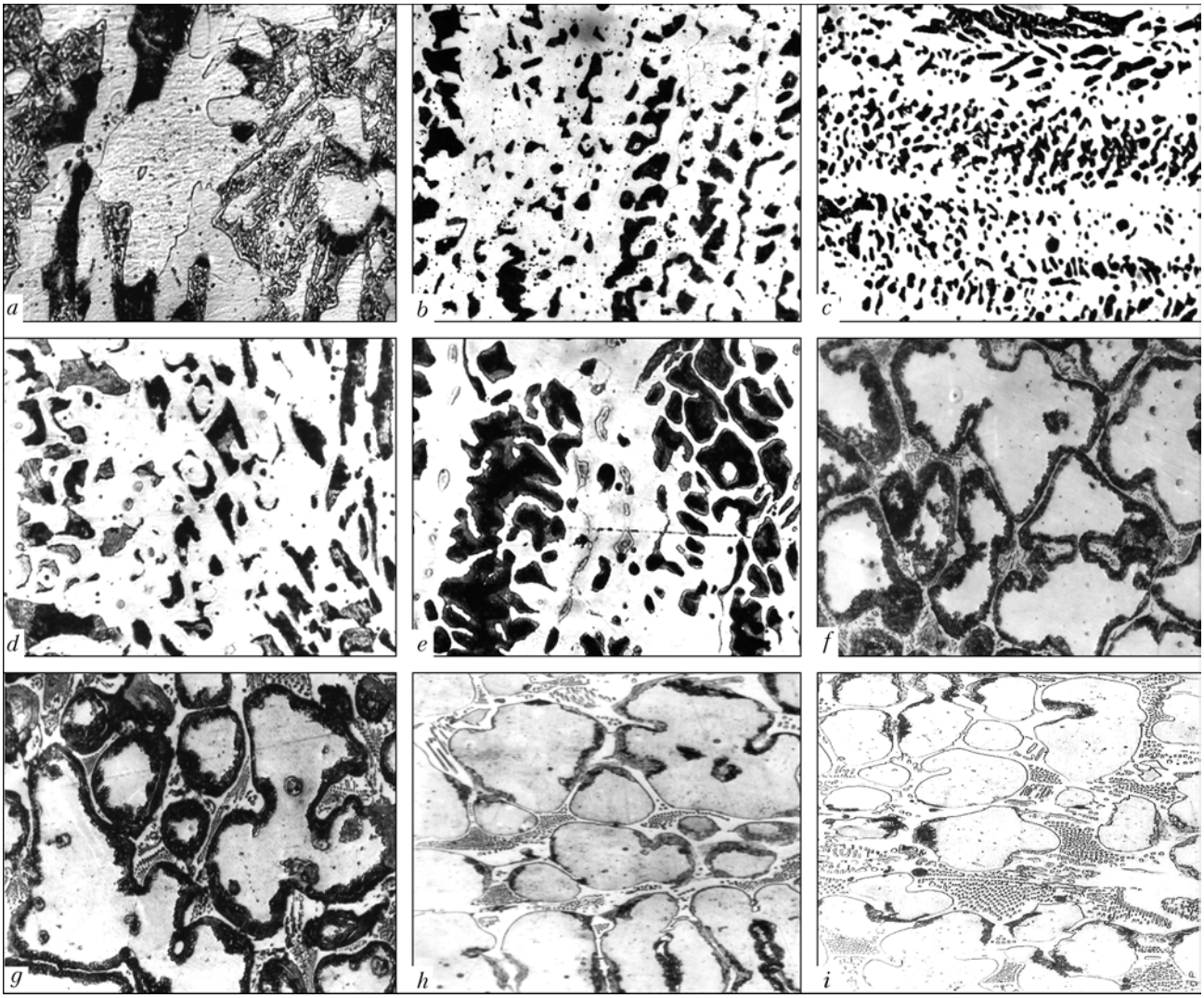

Figure 3. Microstructures of deposited metal 20KhGSP with different phosphorus content, wt.%: *a* — without phosphorus; *b* — 0.32; *c* — 0.59; *d* — 0.98; *e* — 1.23; *f* — 1.58; *g* — 2.02; *h* — 2.46; *i* — 3.35; *a*–*c* — ×400; *d*–*i* — ×800

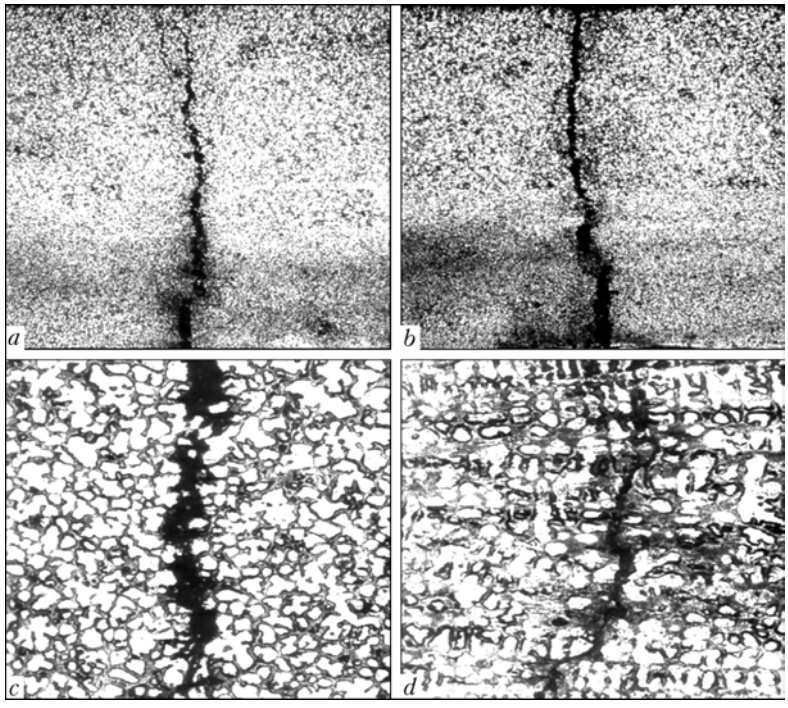

Figure 4. Macro- (*a*, *b*) and microstructures (*c*, *d*) of 20KhGSP type deposited metal with phosphorus content of 2.46 (*a*, *c*) and 3.35 (*b*, *d*) wt.%: *a*, *b* — ×50; *c*, *d* — ×250

macrohardness grew to *HB* 302 (see the Table). No marked structural changes occurred in the deposited metal structure at a phosphorus content of 0.98 % (Figure 3, *d*). However, microhardness of structural components increased: *HV* 0.01-299–309 (ferrite), *HV* 0.01-330–378 (pearlite), and *HV* 0.01-591–613 (bainite-martensite mixture). Metallography revealed no free phosphide inclusions at a phosphorus content of 0.59 and 0.98 %. Line inclusions of phosphides were fixed at a 1.23 % P content of the deposited metal (Figure 3, *e*). Microhardness of main structural components (ferrite, pearlite-bainite and bainite-martensite mixtures) remained at a previous level, and microhardness of phosphide inclusions was *HV* 0.01-330–378. Structure of the deposited metal significantly changed at its phosphorus content of 1.58 % (Figure 3, *f*). A continuous network of phosphide eutectic with high microhardness equal to *HV* 0.01-876–916 was fixed in the structure. Microhardness of the ferrite matrix increased (*HV* 0.01-358), and macrohardness of the deposited metal grew to *HRC* 38. Structure of the deposited metal containing 2.02 % P was of a similar character (Figure 3, *g*).

As the phosphorus content was further increased to 2.46 (Figure 3, *h*), and then to 3.35 % (Figure 3, *i*), the network of the phosphide eutectic along the grain boundaries became thicker, and its structure changed. Its microhardness remained at a sufficiently high level (*HV* 0.01-860–916), and macrohardness of the deposited metal was *HRC* 44–46.

Metallographic analysis was conducted in crack locations of the deposited metal with a phosphorus content of 2.46 and 3.35 %, which evidenced (Figure 4, *a–d*) the formation of cold cracks. The cracks initiated in the upper deposited layer. They propagated through all deposited layers, but did not transfer into the base metal (Figure 4, *a, b*). Fracture occurred along the grain boundaries (Figure 4, *c, d*). It is likely that initiation and propagation of such cracks was associated with a continuous network of brittle phosphide eutectic of a very high hardness, precipitating along the primary grain boundaries.

Therefore, no hot cracks form in the low-carbon deposited metal of the Fe–Mn–Si–Cr type at a phosphorus content of 0.3–3.5 %. No cracks form at a phosphorus content of less than 1.0 % either, as all phosphorus is dissolved in the matrix, and the deposited metal structure contains almost no free phosphides that may act as hot crack embryos. At a higher phosphorus content (> 1.2 %), low-melting point phosphide eutectics heal the forming microcavities, thus preventing formation of cracks.

Cold cracks form in the deposited metal of the type under investigation at a phosphorus content above 1.2 %. As shown by the investigations, centres of initiation and propagation of cold cracks are brittle phosphide eutectics, which precipitate along the grain boundaries at the above phosphorus content. In the multilayer deposited metal, the cracks may propagate from layer to layer, but they do not transfer into the base metal.

1. Ryabtsev, I.I., Kuskov, Yu.M. (2003) Prospects for applying phosphorus in iron-base surfacing consumables (Review). *The Paton Welding J.*, **1**, 12–16.
2. Ryabtsev, I.I., Kuskov, Yu.M., Grabin, V.F. et al. (2003) Tribological properties of the Fe–Cr–Si–Mn–P system deposited metal. *Ibid.*, **6**, 16–20.
3. Kiriakov, V.M., Degtyar, A.A., Podgaetsky, V.V. (1970) Effect of sulphur and phosphorus content in wire Sv-08G2S on weld properties. *Avtomatich. Svarka*, **12**, 19–21.
4. Potapov, N.N. (1973) Effect of sulphur and phosphorus on ductility and toughness of weld metal. *Ibid.*, **1**, 8–11.
5. Alekseev, A.A., Yavdoshchin, I.R., Vojtkevich, V.G. et al. (1989) Effect of phosphorus on structure and properties of weld metal in welding of low-alloy steels. *Ibid.*, **4**, 7–10.
6. Pokhodnya, I.K., Vojtkevich, V.G., Alekseev, A.A. et al. (1992) Effect of phosphorus on impact toughness and chemical microheterogeneity of weld metal. *Ibid.*, **2**, 3–7.
7. Shorshorov, M.Kh., Chernyshova, T.A., Krasovsky, A.I. (1972) *Weldability tests of metals*. Moscow: Metallurgiya.
8. Krechmar, E. (1979) Methods for testing deposited metal. In: *Theoretical and technological principles of surfacing. Properties and tests of deposited metal*. Kiev: PWI.
9. Kuskov, Yu.M., Ryabtsev, I.I., Doroshenko, L.K. et al. (2002) Peculiarities of melting and solidification of 20KhGS type deposited metal alloyed with phosphorus. *The Paton Welding J.*, **8**, 21–24.

OPTIMIZATION OF TRANSFORMER WITH DEVELOPED TRANSVERSE MAGNETIC LEAKAGE FLUXES AND MAGNETIC SHUNT

S.V. RYMAR
E.O. Paton Electric Welding Institute, NASU, Kiev, Ukraine

Optimization model of single-phase transformer with developed transverse magnetic leakage fluxes and mobile magnetic shunt is proposed for ensuring smooth adjustment of welding current. The model allows calculating transformers of optimum mass, volume and cost while ensuring assigned minimum and maximum values of leakage inductance.

Keywords: transformers, optimization model, leakage fluxes, magnetic shunt, leakage inductance, welding parameters, welding equipment

Single-phase transformers with developed transverse magnetic fluxes (hereinafter leakage fluxes), which pass from the rod to the rod of the magnetic conductor, and magnetic shunt are widely used in power sources for manual welding. Advantage of the transformer is its compactness and possibility of leakage inductance adjustment by the structure itself. Theory of the transformer calculation is developed in PWI by Prof. V.K. Lebedev [1]. Theory of leakage inductance was further developed in [2]. Optimization of transformers with transverse leakage with possible consideration of magnetic shunt is considered in [3]. However, it requires for calculation of a great number of intermediate versions.

It is known that in case of complete separation of dependent and independent variables in optimization model optimum version is determined unambiguously. In case of analytical approach to optimization of a transformer with rigid external characteristic such task was solved in [4–7], but in relation to the considered transformer optimization model does not guarantee obtaining of an optimum version of the transformer with necessary level of leakage inductance. Introduction into the mentioned model of a rigidly fixed parameter ---- assigned value of leakage inductance ---- causes occurrence of a problem in differentiation of the optimization function. That's why this task was not solved by analytical method. Scientists managed to solve it using developed optimization model designed for numerical methods of optimization.

The goal of this work is description of the developed optimization model of a single-phase transformer with developed transverse leakage fluxes and magnetic shunt, with rigid limitation of assigned minimum and maximum values of leakage inductance and complete separation of dependent and independent variables. The model allows unambiguous calculating optimum transformer with minimum mass, volume or cost of its active materials. This article is the last one in a number of publications [8, 9] relating to optimization of main types of single-phase welding transformers.

Development of transverse leakage fluxes in the considered transformer is formed by means of spacing primary and secondary windings over length of magnetic conductor rods, and smooth adjustment of leakage inductance is performed by moving magnetic shunt in / out between the windings (Figure), whereby leakage fluxes pass from one rod of the magnetic conductor to the other and through the magnetic shunt. If the shunt is moved in, the leakage inductance increases (welding current reduces), while during its moving out leakage inductance reduces (welding current increases).

Let us consider a two-winding transformer powered by industrial mains with sinusoidal voltage. We assume that current driving to the winding conductor surface is absent, and the magnetic shunt is not saturated. At optimization we will only take into account the active materials of the transformer, namely electrical steel of the magnet core, copper or aluminium of winding conductors.

Optimization model of the transformer with transverse leakage and magnetic shunt is similar to great degree to the model with transverse leakage [9]. That's why presented here formulas and blocks may be found by a reader in [9].

Optimization model is a global cycle procedure, which starts from assignment to the intermediate variable F' of optimization function start value F, and during subsequent addresses to this value assignment of the optimization function value, calculated at the previous step of the cycle, is performed:

$$F' = F. \qquad (1)$$

Than follows without changes block of formulas (2)–(14) of the first local cycle from [9]; whereby values of the transformer leakage inductance with completely moved out shunt $L_c^{\min}$, $L_s^{\min}$ and ΔL_{fr} are calculated in the same way as in [9] at assigned distance between the windings $\Delta h_{1,\,2} = \Delta h_{1sh} + b_{sh} + \Delta h_{2sh}$.

For ensuring the highest assigned value of leakage inductance $L_{sh.c}^{\max}$ it is necessary to determine non-mag-

netic gap δ_{sh} between rods of the magnetic conductor, when magnetic shunt is completely moved in. For this purpose the second local cycle is used.

Start value δ_{sh} is assumed equal 2 mm, and assigned initial value of step of this value in regard to the gap is $\Delta\delta_{sh} = 0.3\delta_{sh}$.

Using formulas (1), (23)–(26) from [9] (without taking into account inductance of magnetization current circuit of magnetic shunt $L_{\mu sh}$) and (21) from [2] with shunt being completely moved in, maximum values of the transformer leakage inductance L_c^{max} and leakage inductance L_s^{max}, stipulated by leakage fluxes passing between magnetic conductor rods in the area of primary and secondary windings $L_{s1, 2}$, leakage inductance, stipulated by leakage fluxes passing in the magnetic shunt zone $L_{s, sh}$, leakage inductance between the magnetic conductor rods and magnetic shunt $L_{\delta, sh}$, and inductance ΔL_{fr} are calculated.

If value L_c^{max} turns out to be less than the assigned value, it is impossible to get the highest value of inductance L_c^{max} in the transformer being calculated, and in this case value δ_{sh} is assumed equal to 2 mm, and value L_c^{max} is less than the assigned one. This recommendation is based on the fact that in practice when non-magnetic gap $\delta_{sh} / 2 < 1$ mm significant forces occur between the magnetic shunt and the magnetic conductor rod, which cause the magnetic shunt vibration and increased noise level. In addition, it is very difficult to ensure gap less than 1 mm in a mobile shunt.

Non-magnetic gap between the magnetic conductor rods and the magnetic shunt will be

$$\delta_{sh} = \begin{cases} \delta_{sh} + \Delta\delta_{sh}, \text{ if } L_c^{max} > L_{fr}^{max}, \\ \delta_{sh} - \Delta\delta_{sh}, \text{ if } L_c^{max} < L_{fr}^{max} \text{ and } \delta_{sh} \geq 2 \text{ mm}. \end{cases} \quad (2)$$

Expression (2) forms a sub-cycle, after entrance into which the program works only with of its current values and unchangeable value $\Delta\delta_{sh}$ with recalculation of vales L_c^{max} at each step. The sub-cycle is fulfilled till current condition of the sub-cycle is valid. After this step $\Delta\delta_{sh} = 0.2\Delta\delta_{sh}$ is reduced and fulfillment of the conditions on exit from the second local cycle are checked:

$$|L_{fr}^{max} - L_c^{max}| / L_{fr}^{max} < \varepsilon_2 \text{ or } \delta_{sh} < 2 \text{ mm}, \quad (3)$$

where ε_2 is the assigned accuracy of calculations in the second local cycle consisting of (2) and (3).

Then length of the magnetic shunt

$$l_{sh} = l_{op} - \delta_{sh} \quad (4)$$

and height of the magnetic conductor

$$h_{op} = \Delta h_1 + h_{c1} + \Delta h_{1sh} + b_{sh} + \Delta h_{2sh} + h_{c2} + \Delta h_2 \quad (5)$$

are calculated.

Mean length of magnetic line of force in the magnetic conductor l_{av} is determined according to (18) from [9].

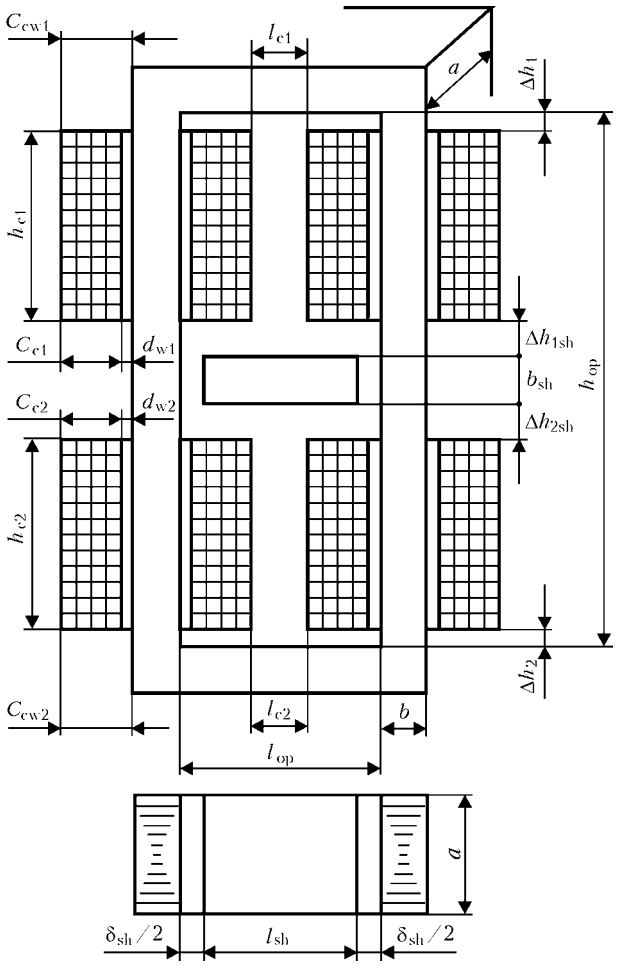

Single-phase transformer with transverse magnetic leakage fluxes and magnetic shunt: $\Delta h1_{sh}$, Δh_{2sh} — assigned distances between coil ends and primary and secondary windings and magnetic shunt, respectively; l_{sh}, b_{sh} — shunt length and width, respectively; δ_{sh} — non-magnetic gap between magnetic conductor rods and magnetic shunt; for the rest designations see Figure in [9]

Volume of the magnetic conductor active material is

$$V_s = l_s S_s + l_{sh} S_{sh}, \quad (6)$$

where $S_{sh} = k_s a b_{sh}$ is the active cross section of the magnetic shunt; $b_{sh} = k_{sh} b$ is the width of the shunt; $k_{sh} \leq 1$ is the coefficient of shunt width.

Volume, mass and cost of the magnetic conductor active materials, windings, and the whole transformer are calculated according to (19)–(21) from [9].

Optimization of the transformer function has the view [4]

$$F = M_s + k_g M_w, \quad (7)$$

where k_g is the generalized weight coefficient, which assigns ratio between masses of active material of the magnetic conductor and the windings. Value k_g is chosen depending upon optimization criterion, for which the calculation is performed [4, 8, 9].

Condition for exit from the global cycle has the following view:

$$|F - F'| / F < \varepsilon, \quad (8)$$

where ε is the assigned accuracy of calculations in the global cycle.

In optimization model of transformer (1)–(8) (and included into it formulas from [2, 9]) independent variables are two values ---- b and C_{c1}, while all other are assigned or dependent ones. Independent variables are determined during optimization of function F. Minimum values of optimization function may be found by any numerical methods of optimization, for example, coordinate-wise descent method, at assigned initial values of independent variables b and C_{c1}. As a result of the function F optimization, optimum values of variables b, C_{c1} and the rest values, which enter into the optimization model, are determined, whereby optimum version for some of the coefficient k_g values may be only one of the same assigned parameters of the transformer.

Developed optimization model was used for calculating transformers of welding power sources developed in PWI. Here are given data on the welding transformer with magnetic shunt, which was calculated using developed optimization model for getting minimum mass of active materials. These data may be used in manufacturing of designated for repair workshops and household purposes transformer for manual welding with smooth adjustment of current.

The transformer has the following parameters (designation of values see above and in [9]): U_1 = 220 V; U_2 = 60 V; f_{mains} = 50 Hz; X = 30 %; k_{tr} = 3.674; L_c^{min} = 9.925 mH; L_c^{max} = 31.28 mH (the parameters are reduced to the primary winding). The transformer makes it possible to adjust welding current within the range I_2 = 75–160 A. Values of parameters for the rated current 160 A are as follows: I_1 = 45.7 A; I_{1l} = = 25 A; J_{1l} = 2.874 A / mm^2; J_{2l} = 2.883 A / mm^2; open-circuit current ---- 2.154 A (4.71 %); power of the transformer ---- 9.6 kV·A; arc voltage ---- 26.4 V; efficiency ---- 94.2 %; B_m = 1.63 T; k_{sh} = 0.5; electrotechnical steel 3414 of 0.35 mm thickness; c_s = = 1.4 c.u. / kg; windings from copper; c_w = = 3.3 c.u. / kg; M_s = 17.5 kg; M_w = 8.7 kg; M = = 26.2 kg; C_s = 24.5 c.u.; C_w = 28.7 c.u.; C = 53.2 c.u.

The windings have the following parameters: parallel connection of primary winding coils, w_1 = 169 (number of turns in one coil is 169, in one layer is 19, in the last layer is 17, number of layers is 9); parallel connection of secondary winding coils, w_2 = = w_1 / k_{tr} = 46 (number of turns in one coil is 46, number of turns in one layer is 10, number of turns in the last layer is 6, number of layers is 5); size of the primary winding conductor is 1.7 × 2.8 mm (thickness of insulation on two sides is 0.27 mm); size of the secondary winding conductor is 3.1 × 5.0 mm (thickness of insulation on two sides is 0.5 mm); thickness of the interlayer insulation is 0.15 mm; length of the primary winding wire is 115; length of the secondary winding wire is 32 m.

Geometric dimensions of the transformer: a = = 85 mm; b = 45 mm; h_{op} = 155 mm; l_{op} = 60 mm; h_{c1} = 61 mm; C_{c1} = 18 mm; C_{cw1} = 21 mm; h_{c2} = = 61 mm; C_{c2} = 19 mm; C_{cw2} = 22 mm; l_{c1} = 16 mm; l_{c2} = 15 mm; d_{w1} = d_{w2} = 3 mm; Δh_1 = Δh_2 = 3 mm; Δh_{1sh} = Δh_{2sh} = 3 mm; b_{sh} = 23 mm; l_{sh} = 56.8 mm; δ_{sh} = 3.2 mm; dimensions of the transformer are 195 × 130 × 245 mm.

Thermal characteristics of the transformer are as follows, °C: mean temperature of primary winding is 140; secondary winding ---- 130; magnetic conductor ---- 75 at ambient temperature 40 °C, insulation class «F» [10].

It should be noted that for simplicity of presentation the simplest optimization models of single-phase welding transformers are considered in this work and in [8, 9]. When it is necessary the models may be modified by introducing into them calculation blocks of other parameters.

So, optimization model of a single-phase transformer with developed transverse leakage fluxes and mobile shunt with complete separation of dependent and independent variables is developed. It allows unambiguous optimizing a transformer for getting minimum mass, volume, and cost of its active materials, while ensuring assigned values of leakage inductance. Optimization model will be useful for developers of new welding power sources.

Presented data on the welding transformer with magnetic shunt, calculated for getting minimum mass according to the developed optimization model, may be used in manufacturing transformers with smooth adjustment of current for manual welding, designed for repair workshops and household purposes.

1. Paton, B.E., Lebedev, V.K. (1966) *Electric equipment for arc and slag welding*. Moscow: Mashinostroenie.
2. Pentegov, I.V., Rymar, S.V. (2004) Peculiarities of calculation of stray inductance of transformers with developed magnetic stray fluxes. *Elektrotekhnika i Elektromekhanika*, **2**, 38–45.
3. Feder, E.S., Pesenson, A.E. (1965) On calculation of transformers with mobile windings for arc welding. *Avtomatich. Svarka*, **7**, 7–10.
4. Pentegov, I.V., Rymar, S.V., Stemkovsky, E.P. (2002) Optimization mathematical model of three-phase transformer and selection of its calculated option in multicriteria optimization. *Tekhn. Elektrodinamika*, **1**, 22–28.
5. Pentegov, I.V., Stemkovsky, E.P., Shejkovsky, D.A. (1983) Determination of optimal parameters of welding transformers for resistance machines with preset resistance of windings. *Avtomatich. Svarka*, **11**, 35–40.
6. Pentegov, I.V., Stemkovsky, E.P., Shejkovsky, D.A. (1981) Determination of optimal number of secondary windings for AC resistance and percussion welding transformers. *Ibid.*, **4**, 11–15.
7. Pentegov, I.V., Stemkovsky, E.P., Shejkovsky, D.A. (1980) Calculation of welding transformer for resistance percussion welding. *Ibid.*, **3**, 26–30.
8. Rymar, S.V. (2005) Optimization of a transformer with developed yoke magnetic stray fluxes. *The Paton Welding J.*, **7**, 27–30.
9. Rymar, S.V. (2005) Optimization of transformer with developed transversal magnetic stray fluxes. *Ibid.*, **9**, 19–22.
10. Tikhomirov, P.M. (1986) *Calculation of transformers*. Moscow: Energoatomizdat.

DEVELOPMENT AND CERTIFICATION OF AUTOMATIC NARROW-GAP ARGON-ARC WELDING TECHNOLOGY OF MCP Dn850 ELEMENTS AT NPP

A.K. TSARYUK[1], V.Yu. SKULSKY[1], I.L. KASPEROVICH[2], A.I. BYVALKEVICH[2], T.V. OSTASHKO[2], V.V. ZHUKOV[2], S.N. DUDKIN[2], N.A. IVANOV[2], A.P. MIROSHNICHENKO[3], N.V. NEMLEJ[3] and A.V. BAZHUKOV[3]

[1]E.O. Paton Electric Welding Institute, NASU, Kiev, Ukraine

[2]Company «Atomremontservis», «Energoatom», Slavutich, Ukraine

[3]Company «Yuzhno-Ukrainskaya NPP», «Energoatom», Yuzhno-Ukrainsk, Ukraine

Automatic narrow-gap argon-arc welding in gas mixture of 70 % He + 30 % Ar using 0.8–0.9 mm diameter welding wire Sv-08G1NMA was employed to join elements of the main circulation piping (MCP) Dn850 of clad steel 10GN2MFA to steam generator branch pipes. The technology suggested passed the research and industrial certification to advantage, was approved by the State Inspection Body of the State Nuclear Regulatory Committee of Ukraine and recommended for joining elements of MCP Dn850 when replacing steam generators at NPP. The automatic narrow-gap argon-arc welding technology will allow significant reducing labor content of welding operations, increasing productivity, reducing amount of deposited metal and level of residual welding stresses, and ensuring high quality of welded joints and significant reducing dose of radiation action on the personnel performing welding operations.

Keywords: automatic argon-arc welding, welding technology, narrow-gap groove, nonconsumable electrode, helium, argon, weld metal, welded joints, physical-mechanical properties of metal, steam generator, piping

As showed analysis of existing methods of mechanized welding, application of automatic argon-arc welding (AAAW) is the most efficient method for joining elements of the main circulating piping (MCP) with branch pipes of a steam generator (SG) [1]. It is recommended to use filler wire Sv-08G1NMA (TU 14-15-373–95) when performing AAAW with standard groove. Application of standard groove [2] (Figure 1, *a*) is stipulated by absence of a specialized equipment for machining edges of SG branch pipes for narrow-gap groove under NPP conditions (the manufacturer supplies SG with standard groove of branch pipes). Due to developed at present specialized portable equipment for machining real possibility occurred to use narrow groove (Figure 1, *b*) when joining MCP elements with SG branch pipes. Performance of narrow-gap AAAW will allow significant reducing labor content of welding operations, increasing their productivity, reducing amount of deposited metal and level of residual welding stresses and ensuring high quality of welded joints and significant reducing dose of radiation action on the personnel performing welding operations. Development and certification of narrow-gap AAAW technology in replacement of SG is

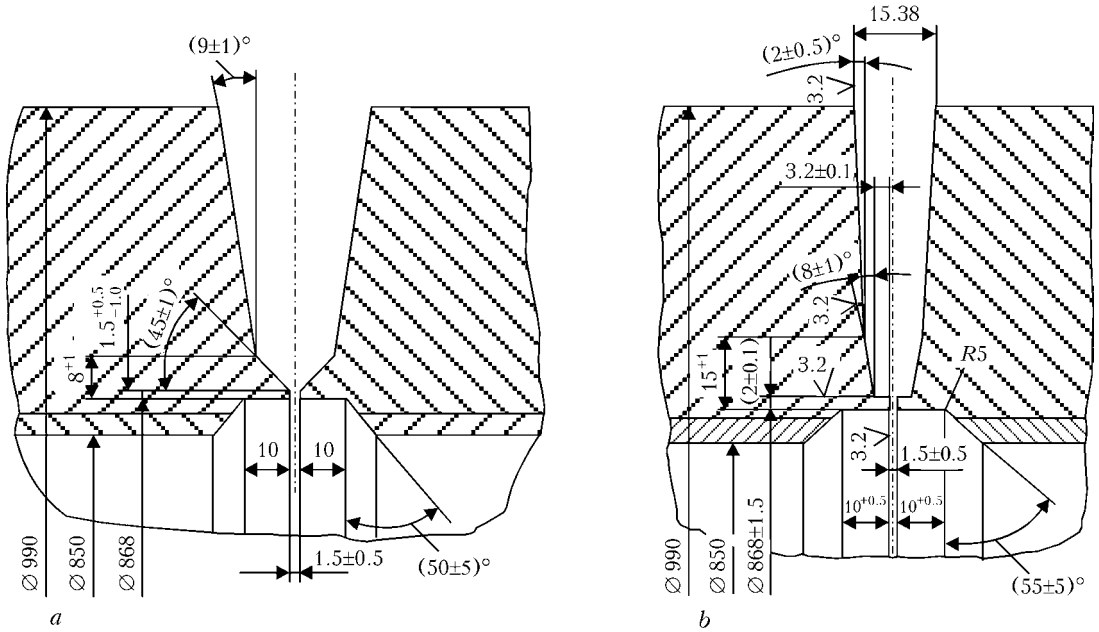

Figure 1. Schemes of standard (*a*) and narrow (*b*) groove of joints produced by AAAW using nonconsumable electrodes and filler wire

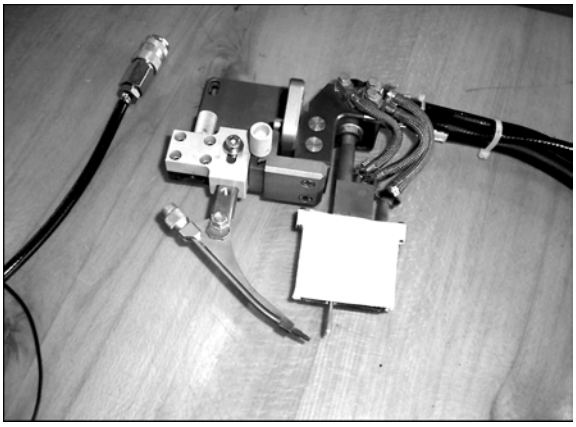

Figure 2. General view of torch for narrow-gap AAAW

an important and actual task for solving the issue of service life extension of NPP equipment in Ukraine.

According to TACIS project U2.02 / 96 «Application of Narrow-Gap Automatic Welding in Replacement of Steam Generators», French narrow-gap AAAW technology in gas mixture of He + 30 % Ar for Dn850 piping was proposed and welding equipment was supplied. However, recommendations of mentioned project relate exclusively to welding technique in case of using the supplied welding equipment. As far as properties of welded joints performed using narrow-gap AAAW are concerned, information on this issue is not available. In addition, application of narrow-gap AAAW is not envisaged by valid in nuclear power engineering norms and rules. In this connection it is necessary to carry out complex of certification tests of welded joints of steel 10GN2MFA, which were made using narrow-gap AAAW, in correspondence with requirements to application and certification of new technologies and materials [3].

Preliminary investigations. Preliminary investigations were carried out for obtaining initial data for development of narrow-gap AAAW technology and estimation of physical-mechanical properties of welded joints. For this purpose narrow-gap circular butt specimens (see Figure 1, *b*) of MCP Dn850 from steel 10GN2MFA of 990 mm diameter with wall thickness 70 mm were welded. The welding was performed with the joint axis in vertical position (welding of a horizontal seam on vertical plane). Welding wire Sv-08G1NMA (TU 14-1-2869–79) of 0.9 mm diameter was used as a filler material in AAAW in the mixture of He + 30 % Ar [1].

Peculiar feature of welding with nonconsumable electrodes in the mixture of helium and argon [4, 5] is change of the penetration depth. So, in case of welding in the mixture of He + 30 % Ar depth of penetration is higher than in case of welding in pure argon or mixture of Ar + 30 % He. It is stipulated by a higher ionization potential of helium (U_1 = 24.5 V) in comparison with similar parameter of argon (U_1 = = 15.7 V). Significant (up to 70 %) content of helium in the mixture causes increase of arc voltage, due to which temperature of the weld pool and penetration of the base metal increase. That's why for guaranteed fusion of the deposited metal with narrow-gap edges it is advisable to perform AAAW in the mixture of He + 30 % Ar. In case of standard-gap AAAW (see Figure 1, *a*) such mixture can not be efficient because of poor shielding of the pool against ambient air. In case of narrow-gap welding the edges being welded directly enable good shielding of the pool. In addition, for ensuring reliable and efficient gas shielding of the pool in AAAW of circular butt joints from steel 10GN2MFA a special welding torch was used for narrow-gap welding (Figure 2). The welding was performed with preliminary and accompanying heating up to 170 °C [2].

AAAW of the root part was performed with minimum axial gap and feeding of the welding wire into tail of the pool, which ensured required penetration and backward formation of the root weld. The welding conditions were as follows: welding current I_w = = 150 A; arc voltage U_a = 11 V; welding speed v_w = = 6 m / h; filler wire feed rate v_f = 152 m / h; shielding gas mixture flow 1000–1200 l / h. Welding conditions for filling the groove were selected allowing for reliable fusion of the weld with the gap walls and formation of the beads and depending upon the diameter of an item, on which the layer is deposited. As a result of the technology development optimum modes of narrow-gap AAAW of circular thick-wall butts Dn850 from steel 10GN2MFA were established (Table 1).

In the process of welding of butts layer-by-layer 100 % visual and measurement check (VMC) was performed. After filling of the root part of the gap at the height 8–10 mm thermal «rest» at the temperature 150 °C for 8 h with subsequent VMC, radiographic (RGC), and capillary check (CC) from inside were performed. After filling 50 % of the gap and thermal «rest» again 100 % VMC and RGC were performed. After termination of the groove filling and subsequent thermal «rest» 100 % VMC, CC, RGC, and ultrasonic check (USC) were performed.

After welding and check welded joints were subjected to heat treatment according to the final high-temperature tempering mode [2]; heating up to 650 °C, soaking at 650 °C for 8 h, cooling down to 450 °C at the rate 40 °C / h, and down to 250 °C at the rate not more than 80 °C / h. Further cooling down to the ambient temperature was performed under the layer of isolation.

After performance of heat treatment 100 % VMC, CC, RGC and USC, as well as CC of austenite deposit and USC of the deposit (for checking lamination of the cladding layer) were performed. Results of the checks showed that defects in heat treated welded joints were absent.

From the performed welded butt joints of steel 10GN2MFA billets of the specimens were cut out for determining chemical composition, mechanical properties, and structure of the weld metal. Results of spectral analysis of the weld metal (at 14–15 mm interval beginning from the weld root) with estimation of distribution of the alloying elements over

Table 1. Welding conditions of circular butt joints from steel 10GN2MFA

Run No.	Program No.	Time, μs	Welding current, A	Arc voltage, V	Welding wire feed rate, mm / min	Welding speed, mm / min
1	1	225 / 275	150 / 50	11	2540 / 1000	99
2	2	125 / 375	160 / 90	10	Without welding wire	86
		Lower edge fusion (bent electrode is directed downwards)				
3	3	125 / 375	175 / 100	10	Without welding wire	86
		Upper edge fusion (bent electrode is directed upwards)				
4	4	225 / 275	220 / 130	11.5	2000 / 1000	91
5	5	225 / 275	250 / 150	11.5	2600 / 1300	89
6	6	225 / 275	300 / 180	11.5	3400 / 1620	89
7–11	7	225 / 275	350 / 170	12.1	2100 / 920	84
		Weld width is 7.5–8.5 mm				
12–29	8	225 / 275	360 / 180	11.5	2290 / 1020	84
		Weld width is 8.5–9.5 mm				
30–34	12	225 / 275	370 / 190	11.5	2450 / 1150	84
		Weld width is 9.5-10.5 mm				
35–43	13	225 / 275	330 / 140	11.5	2050 / 850	89
		Finish layer (last 10–15 % of gap)				
44–45	14	175 / 325	260 / 110	11.5	1520 / 760	89
		Facing layers				

Note. In numerator values of parameters in pulse, and in denominator values in pause are given.

height of the joint are given in Table 2. One can see from the Table that weld metal of the butt joint is characterized by uniform chemical composition all over the welded joint height. Rather interesting are gas analysis data on oxygen content. It turned out to be very low (0.0032 wt.%), which proves minimum content of non-metallic inclusions in the weld metal and its high impact toughness and is explained by refining action of helium on molten metal. It is known that during blow-down of liquid metal by helium dissolved in the metal gases and non-metallic impurities in the form of slag are removed [4, 5].

Results of performed mechanical tests of deposited metal at room temperature and 350 °C are presented in Table 3. As one can see from the Table, strength characteristics and indices of the weld metal ductility at room and working temperatures are significantly higher than that of valid requirements [6].

Determination of critical temperature of the weld metal brittleness was performed by impact bend tests of the Charpy specimens with V-shape sharp notch in the weld center (type IX according to GOST 6996–66). Results of the impact bend tests are given in Table 4. In Figure 3 change of impact toughness (KCV) and share of ductile fibers B in the fracture depending upon the test temperature are shown. According to [7], as critical temperature of brittleness T_c the temperature is accepted, for which the following conditions are fulfilled:

- at T_c mean arithmetic value of impact toughness should be not less than 59 J / cm^2, and minimum value ---- not less than 70 % of the mentioned one, i.e. not less than 41.3 J / cm^2;
- at T_c + 30 °C mean arithmetic value of impact toughness should be not less than 89 J / cm^2, and minimum value ---- not less than 70 % of the mentioned

Table 2. Chemical composition (wt.%) of welding wire, base metal and weld metal of steel 10GN2MFA welded joint

Investigation object	Ñ	Si	Mn	Ni	Mo	V	S	P	[O]	[N]	H_{res}
Wire Sv-08G1NMA	0.06	0.40	1.60	0.70	0.80	0.01	–	–	–	–	–
Steel 10GN2MFA	0.11	0.24	0.78	1.89	0.52	0.01	0.003	0.01	–	–	–
Part of weld metal:											
root	0.098	0.268	1.11	0.85	0.62	0.01	0.009	0.011	0.0032	0.005	0.22
intermediate	0.087	0.290	1.17	0.80	0.64	0.01	0.011	0.010			
	0.086	0.288	1.17	0.68	0.64	0.01	0.010	0.010			
	0.081	0.302	1.21	0.72	0.63	0.01	0.010	0.010			
upper	0.078	0.305	1.22	0.70	0.63	0.01	0.009	0.011			

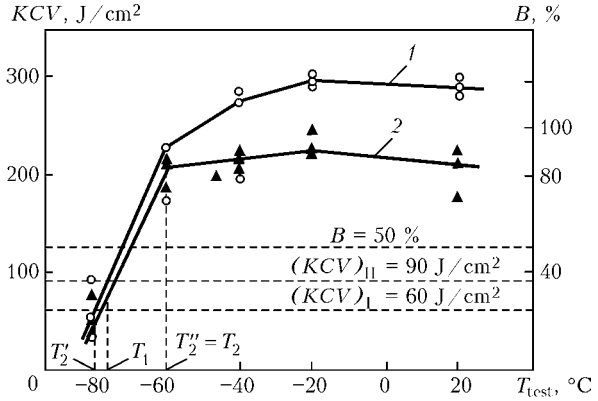

Figure 3. Influence of test temperature of weld metal of welded joints performed by narrow-gap AAAW on impact toughness *KCV* (*1*) and share of ductile fiber *B* in fracture (*2*): ○, ▲ — experimental points; for the rest designations see [7]

one, i.e. not less than 62.3 J / cm^2, whereby minimum value of ductile component in the fracture should make up at least 50 %.

When considering the data obtained one can see that as follows from [7] critical brittleness temperature corresponds to –72 °C.

So, mechanical properties and critical brittleness temperature of weld metal of welded joints of steel 10GN2MFA performed by narrow-gap AAAW in mixture of He + 30 % Ar completely meet existing requirements [6].

Investigation of macro- (Figure 4) and microstructure of the welded joints showed that pores, cracks, lack of fusion, slag inclusions, and other defects were absent in the weld metal. Deposited metal has bainite structure, which in addition to the required mechanical properties is characterized by high ductility and crack resistance. Non-metallic inclusions in the weld metal are finely dispersed and have arbitrary arrangement. Analysis of HAZ metal showed that its structure is characterized by mainly bainite component. Ferrite-pearlite component is almost always located on the phase interface, whereby its content is insignificant. Hardness of the weld metal is *HV* 240–250, which is characteristic of the tempered bainite structure. By means of the distance increase from the fusion line hardness somewhat reduces (*HV* 225–235). Hardness of the base metal is *HV* 215–220. Hardness deep in HAZ metal are not observed. One can see from the data obtained that microstructure character of the weld metal and HAZ of welded joints of steel

Table 3. Mechanical properties of weld metal of steel 10GN2MFA welded joint

T_{test}, °C	σ_t, MPa	σ_y, MPa	δ_5, %	ψ, %
20	447.2–486.7 / 465.2	568.9–591.6 / 538.4	27.0–28.0 / 27.4	75.0–76.6 / 76.0
350	609.6–638.8 / 626.0	473.0–497.6 / 488.8	18.8–21.3 / 20.0	65.7–72.0 / 69.2

Note. In nominator mean values are given, which were obtained after testing three specimens.

Table 4. Results of impact bend tests of Charpy specimens with V-shape sharp notch

Specimen No.	T_{test}, °C	*KCV*, J / cm^2	*KCV*, J / cm^2 (mean value)	*A*, %
1	20	304.8	292.8	70
2		284.3		89
3		289.4		85
4	–20	299.6	301.5	89
5		303.5		88
6		301.4		98
7	–40	277.0	253.4	86
8		199.6		87
9		283.7		81
10	–60	225.6	217.8	75
11		174.0		85
12		254.0		88
13	–80	31.6	57.0	21
14		51.2		17
15		88.2		33

10GN2MFA matches well data on distribution of hardness and mechanical properties of the weld metal.

So, results of preliminary tests prove high quality and availability of the required mechanical properties of welded joints of steel 10GN2MFA produced by narrow-gap AAAW in the mixture of He + 30 % Ar and complete correspondence to the valid requirements and norms [6].

Research certification. In order to have possibility to include narrow-gap groove into the list of main types of welded joints produced by AAAW [2] it is

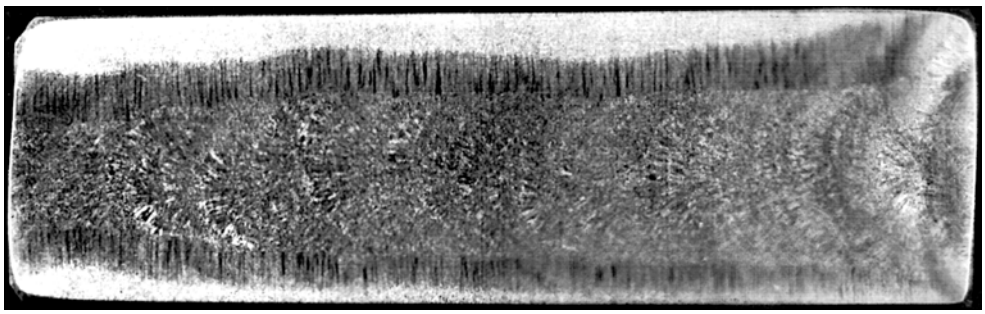

Figure 4. Macrostructure of weld metal of welded joint of steel 10GN2MFA produced by narrow-gap AAAW in mixture of He + 30 % Ar using welding wire Sv-08G1NMA (×1.7)

Table 5. Mechanical properties of weld metal and welded joints of steel 10GN2MFA produced by AAAW using welding wire Sv-08G1NMA

Investigation object	T_{test}, °C	σ_t, MPa	σ_y, MPa	δ_5, %	ψ, %
Weld	20	66.4–71.8 / 69.0	58.8–63.9 / 61.5	23.0–25.6 / 24.2	71.7–74.6 / 73.3
	350	59.5–64.4 / 61.7	49.0–56.4 / 52.2	21.3–22.4 / 22.0	69.8–71.7 / 70.8
Welded joint	20	55.3–56.0 / 55.6	–	–	75.5–77.9 / 76.9
	350	50.3–50.9 / 50.5	–	–	74.9–76.1 / 75.3

necessary to pass certain certification tests envisaged in [3].

Circular butt with external diameter 990 mm and wall thickness 70 mm from clad steel 10GN2MFA was prepared in «Atomremontservis» (Slavutich). The shape of groove corresponds to the one presented in Figure 1, *b*. Specialized welding equipment «AutoTIG 600PC» of French company «Polysoude» was used for welding. Before welding preheating of joints up to the temperature 150–200 °C at the rate not more than 150 °C / h using unit «Standard Europe 82 / 6» (company «Weldotherm») was performed. When the root weld was made welding wire Sv-08G1NMA of 0.9 mm diameter was fed into the pool tail, due to which necessary penetration and backward formation of the root weld metal were ensured.

Modes of welding of the root weld and subsequent layers during filling of the groove corresponded to those given in Table 1. During filling of the groove welding wire was fed into the pool head. In the process of the groove filling fettling of the weld metal surface by metal brush and external inspection of each run were performed. After termination of welding of the butt thermal «rest» at temperature 150 °C for 8 h (according to [2]) and 100 % USC, RGC and CC of welded joints were performed. After non-destructive testing of quality the welded butt was subjected to heat treatment according to final high-temperature tempering mode at temperature 650 °C for 6 h [2, 8].

According to PM-T. 38.001–04 «Program of Certification Tests of Welded Joints of Piping Dn850 from Steel 10GN2MFA (clad) Performed by Narrow-Gap AAAW», samples were taken from the welded butt and billets of specimens were cut out for studying physical-mechanical properties of welded joints, characteristics of brittle failure resistance, indices of cyclic strength, intercrystalline corrosion resistance, and sections for metallographic studies were taken.

Investigation of distribution of alloying elements over height of the weld metal of a welded joint of steel 10GN2MFA performed by narrow-gap AAAW in mixture of He + 30 % Ar using welding wire Sv-08G1NMA showed that it had practically constant chemical composition (see Table 2) over the whole height of the weld metal cross-section.

Results of tests of mechanical properties of the weld metal and welded joints of steel 10GN2MFA (Table 5) prove that strength characteristics and indices of ductility of welded joints are higher than in the base metal. Failure of all the welded joint samples ran through the base metal.

Bend angle of the tested specimens of welded joints of 35 × 45 mm section was at least 120°, which exceeded required values (according to [6] it should be at least 40°). It should be noted that tested specimens didn't fail and even didn't have cracks (Figure 5).

Determination of the weld metal and HAZ critical brittleness temperature was performed according to [7] when the weld metal was tested on impact bend using Charpy specimens with V-shape sharp notch over the weld center and fusion zone (type IX according to GOST 6996–66). On the basis of performed calculation critical temperature of the weld metal brittleness should make up –77 °C, and of HAZ not lower

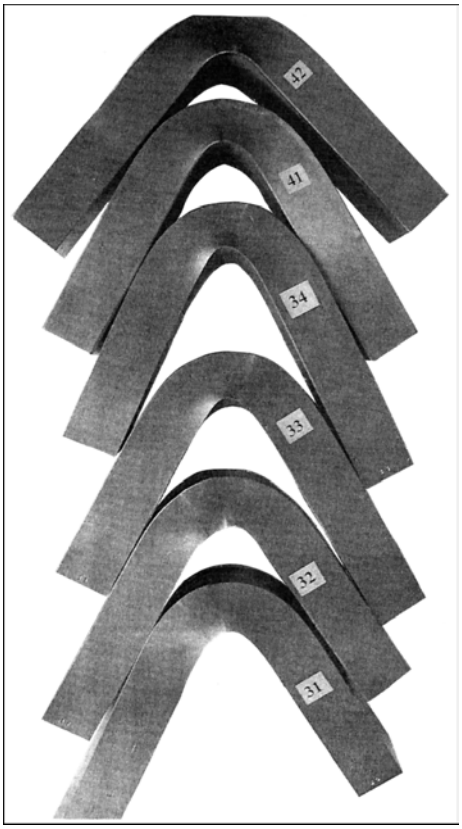

Figure 5. View of specimens of reference joint after static bend tests

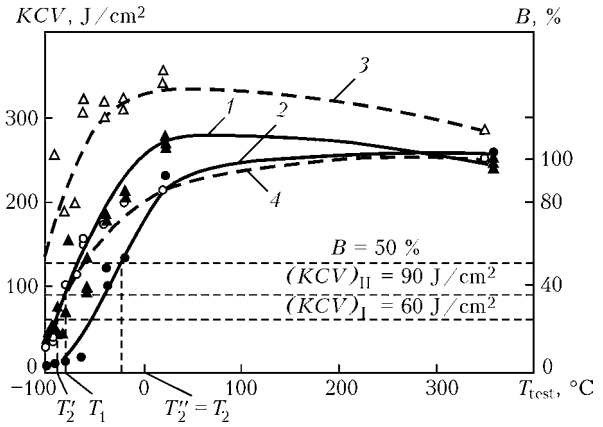

Figure 6. Influence of reference welded joint metal test temperature T_{test} on impact toughness *KCV* (*1, 3*) and share of ductile fiber *B* in fracture (*2, 4*): solid curves — weld metal; dash lines — HAZ; ●, ▲, ○, Δ — experimental points

than –100 °C (Figure 6), which completely meets established requirements [6].

Low-cycle fatigue tests were performed in the Institute for Problems of Strength of the NAS of Ukraine on standard universal electro-hydraulic machine 3201 UE-20 using axial extension-compression (strain) and checking of the full strain amplitude of working part of a specimen. Main geometric parameters of the specimen were chosen according to recommendations of GOST 25.502–79 «Methods of Mechanical Tests of Metals. Methods of Fatigue Tests». Specimens were loaded according to the symmetrical cycle (coefficient of strain cycle asymmetry R_ε = –1), i.e. tests were performed in robust mode. In the process of cyclic loading of the specimens longitudinal strain was assigned and measured using special strain gage. Tests were carried out at frequency of cyclic loading f = = 0.3 Hz. As criterion of cyclic durability of a specimen, occurrence and development on the specimen surface of a fatigue crack of 0.5–2.0 mm length was accepted according to [7]. After the fatigue crack achieved assigned length a specimen was withdrawn from the tests.

In Figure 7 results of low-cycle fatigue tests of welded joints of steel 10GN2MFA performed by narrow-gap AAAW at room and working temperatures, and for comparison the results obtained in testing of the base metal are given. One can see from the Figure that both at room and at working temperature insig-

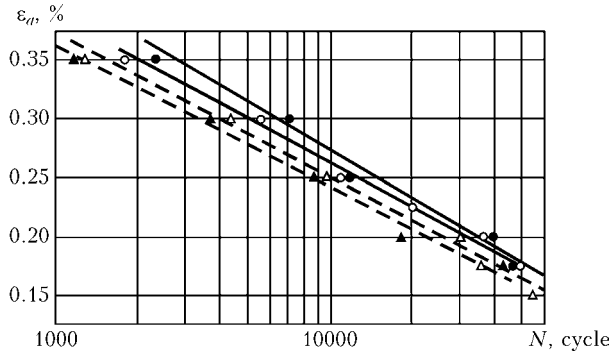

Figure 7. Fatigue curves of base metal (solid) and welded joints (dash) obtained according to results of reference welded joint tests for low-cycle fatigue: ●, ▲ — 350; ○, Δ — 20 °C

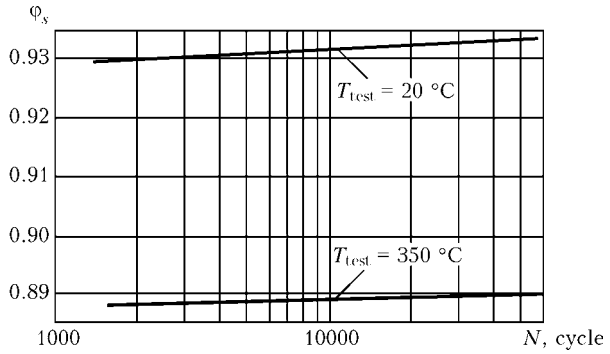

Figure 8. Curves of change of coefficient φ_s of welded joint cyclic strength

nificant reduction of the failure strain amplitude ε_a occurs at assigned durability of welded joints in comparison with the steel 10GN2MFA base metal. Reduction of cyclic strength is insignificant when duration of tests is more than $1 \cdot 10^4$ cycles, and in the area of lower durability, where low-cycle fatigue resistance is mainly affected by ductile properties of welded joints, fatigue curves of welded joints at 20 and 350 °C are located close to each other and to the base metal curves. In Figure 8 curves of change of cyclic strength coefficient φ_s of welded joints depending upon number of cycles prior to occurrence of crack, which were determined according to the methodology recommended in [7], are given. For investigating durability range within interval from $1 \cdot 10^2$ to $1 \cdot 10^8$ cycles minimum value φ_s at room temperature is 0.93, while at working temperature φ_s is 0.88. So, results of low-cycle fatigue investigation showed that welded joints of steel 10GN2MFA performed by narrow-gap AAAW have insignificant (5–7 %) reduction of cyclic strength at room temperature and 350 °C in comparison with the base metal.

Intercrystalline corrosion resistance tests of a welded joint of steel 10GN2MFA were performed according to GOST 6032–89 using AM method without a provoking heating on specimens of type 1. Detection of intercrystalline corrosion was performed by method of bending at 90° angle. Results of tests completely met established requirements [6].

For study of the macrostructure templates cut out across a welded joint were used. Lamellar structure of the weld metal was investigated for detecting interlayer and interbead faults, as well as its crystal macrostructure, for estimating its continuity and homogeneity. Analysis of the weld metal macrostructure showed that beads in the weld metal had homogeneous structure and approximately the same section, and in HAZ they had constant width over the whole height of the weld. This allows assuming that welding mode during the whole process of the welded joint production was stable, faults between beads and layers in the weld metal, as well as in fusion zone, were not detected, and the weld metal was dense. Faults in the form of cracks, pores, inadmissible accumulations of slag inclusions, and lack of penetration were not detected either. During investigation of the welded joint metal microstructure our attention was drawn to very

high level of purity in regard to non-metallic inclusions. Available non-metallic inclusions of complex manganese oxy-sulfide type are peculiar for fine (not more than 0.001 mm) dispersity and are solitary. Structure of the weld metal consists of tempered bainite and ferrite component, peculiar feature of which is fineness (grain size is Nos. 8–9 points).

In the HAZ metal microstructure near fusion boundary of the welded joint areas of coarse grain are absent; instead of them fine-dispersion bainite-ferrite structure is formed. By means of distance increase from the fusion boundary size of grains somewhat reduces and metal structure represents fine-dispersion bainite.

The weld metal hardness is *HV* 235–240, which is characteristic of the tempered bainite structure. Hardness of HAZ metal near fusion boundary is somewhat increased (up to *HV* 250–255) and by means of distance increase from the fusion boundary it reduces down to the base metal hardness level ---- *HV* 180–185.

One can see from presented data that character of the weld and HAZ metal structure of welded joints of steel 10GN2MFA matches well parameters of hardness distribution and mechanical characteristics of the deposited metal and welded joints.

So, results of performed investigations and data on metallographic investigations of welded joints of steel 10GN2MFA performed by narrow-gap AAAW using welding wire Sv-08G1NMA proved that physical-mechanical properties, brittle failure resistance, cyclic strength, and corrosion resistance completely met established requirements.

On the basis of results obtained technical decision TR-N.1234.ARS.72–04 was made on possibility of application of nonconsumable electrode narrow-gap AAAW for repairing (mounting) main circulation piping Dn850 of power units with WWER-1000 reactors.

Industrial certification. For the purpose of checking possibility of practical performance of narrow-gap AAAW for joining elements of MCP Dn850, at Yuzhno-Ukrainskaya NPP primary industrial certification of the technology for producing welded joints was carried out (in certification also participated employees of «Avtoremontservis» V.N. Adamenko, V.I. Podiachev, F.F. Melnik, A.V. Begun, and employees of «Yuzhno-Ukrainskaya NPP» S.I. Shmalko and I.D. Dolmatov). In correspondence with developed technological guidelines on narrow-gap AAAW of the piping Dn850 element edges from clad steel 10GM2MFA under industrial conditions a reference circular butt of shells of 990 mm diameter having wall thickness 70 mm was produced. The welded butt was subjected to heat treatment recommended in [5]. Results of nondestructive testing demonstrated high quality of the reference welded joint. All used methods of 100 % check (VMC, etching, CC, USC, and RGC) confirmed absence of faults and correspondence of the quality of welded joints to existing requirements [6].

Destructive testing was performed on the specimens cut out from the reference welded joint, whereby strength of the welded joint and intercrystalline corrosion resistance were determined and static bend tests and metallographic studies were carried out in correspondence with [6].

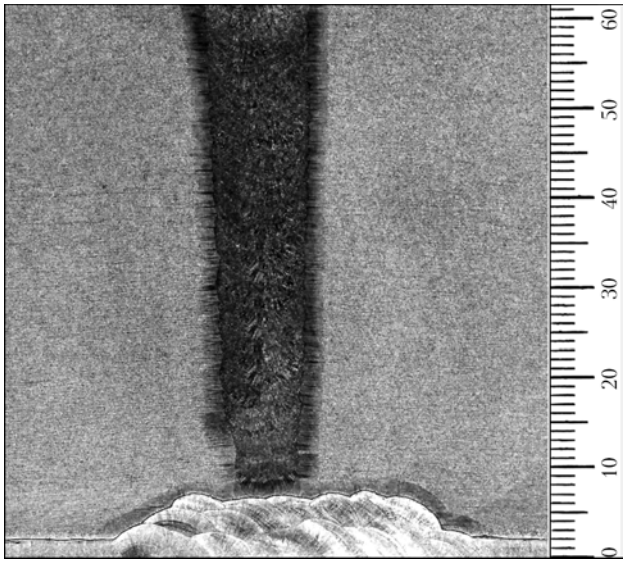

Figure 9. Macro-section of reference welded joint of steel 10GN2MFA produced by narrow-gap AAAW in mixture of He + 30 % Ar

Results of destructive testing showed that the reference welded joint completely met all established requirements in regard to all parameters [6]. View of the industrial reference welded joint section of steel 10GN2MFA produced by narrow-gap AAAW in mixture of He + 30 % Ar is presented in Figure 9.

Proceeding from mentioned above one may state that for joining elements of MCP Dn850 from steel 10GN2MFA with SG branch pipes narrow-gap AAAW in mixture of He + 30 % Ar using welding wire Sv-08G1NMA of 0.8–0.9 mm diameter is recommended. Mentioned technology ensures high quality and necessary service properties of welded joints of steel 10GN2MFA. Developed and certified narrow-gap AAAW technology is approved by the State Nuclear Regulatory Committee of Ukraine is recommended for application at NPP.

1. Tsaryuk, A.K., Skulsky, V.Yu., Volkov, V.V. et al. (2005) To the problem of selection of the technology for welding elements of MCP Dn 850 in replacement of steam generators PGV-1000M at NPP. *The Paton Welding J.*, **10**, 39–45.
2. *PN AEG-7-009–89*: Equipment and piping of nuclear power plants. Welding and surfacing. Main regulations. Moscow: Energoatomizdat.
3. *PN AEG-7-008–89*: Rules of arrangement and safe operation of equipment and piping of nuclear power plants. Moscow: Energoatomizdat.
4. Brodsky, A.Ya. (1951) *Technology of inert-atmosphere arc welding*. Moscow: Mashgiz.
5. Brodsky, A.Ya. (1956) *Argon-arc tungsten-electrode welding*. Moscow: Mashgiz.
6. *PN AEG-7-010–89*: Equipment and piping of nuclear power plants. Welded joints and deposits. Testing regulations. Moscow: Energoatomizdat.
7. *PN AEG-7-002–89*: Codes of strength calculation of equipment and piping of nuclear power plants. Moscow: Energoatomizdat.
8. Kuran, R.I., Tzyba, V.I., Tsaryuk, A.K. (2004) Heat treatment of welded joints of main circulation piping Dn850 in replacement of steam generators PGV-1000M at Yuzhno-Ukrainskaya NPP. *Svarshchik*, **1**, 32–34.

GAS-ABRASIVE WEAR RESISTANCE OF THERMAL SPRAY COATINGS OF Al–Cu–Fe SYSTEM ALLOYS CONTAINING QUASI-CRYSTALLINE PHASE

Yu.S. BORISOV, A.L. BORISOVA, V.F. GOLNIK and **Z.G. IPATOVA**
E.O. Paton Electric Welding Institute, NASU, Kiev, Ukraine

Wear resistance of detonation and plasma coatings of powders based on Al–Cu–Fe alloy with scandium and chromium additions was studied under conditions of gas-abrasive wear at different angle of attack by an abrasive. Dependence of wear of the coatings upon the abrasive attack angle, deposition method, coating composition, and quasi-crystalline content was established.

Keywords: thermal spray coatings, Al–Cu–Fe system alloy, quasi-crystalline phase, gas-abrasive wear

Since discovery of the quasi-crystalline state of the matter, it has been a challenge to practically apply this class of materials that combine such unique properties as high hardness and wear resistance, low values of friction coefficient and surface energy, capability of elastically restoring, high-temperature superplasticity, etc.

More than 200 quasi-crystalline alloys have been discovered up to now. However, they failed to find a wide practical acceptance so far, one of the reasons being insufficiently studied properties of practical interest. One of the important service characteristics is their behaviour under different wear conditions. Information on such characteristics of quasi-crystalline materials is scanty, and it relates mainly to materials of the Al–Cu–Fe system.

High wear resistance of thermal spray coatings of the Al–Cu–Fe system alloy under abrasive wear conditions is related, first of all, to their content of the quasi-crystalline ψ-phase, whose hardness may exceed *HV* 1000 MPa [1]. At the same time, such characteristics of the coatings as crack resistance, porosity, grain size, and presence of oxide inclusions, are taking on high significance, depending upon the conditions of tribotechnical tests. Study [2] gives results of investigation of tribotechnical properties of the $Al_{63}Cu_{25}Fe_{12}$ alloy plasma coatings under abrasive wear conditions (fixed abrasive of a grinding cloth containing SiC with grit 400, P = 10 kPa, v = = 240 rpm). Under these conditions, the powder grain size (d_p = 25–45 and 45–75 μm) had an insignificant effect on wear resistance, whereas annealing at a temperature of 700 °C for 2 h in argon led to a substantial (4–5 times) increase in wear resistance of a coating, and its friction coefficient also grew from 0.1 to 0.4. Increase in wear resistance of the coatings as a result of annealing is provided by an almost complete transformation of structure from the two-phase (ψ + β) to single phase ψ one, accompanied by decrease in porosity and healing of cracks. The authors attribute growth of the friction coefficient after annealing of a coating to increase in adhesion wear and decrease in the role of the wear products (secondary structures) acting as lubricants within the friction zone.

Study [3] gives results of investigation of wear of thermal spray coatings of the Al–Cu–Fe system alloy under the dry friction conditions. The tests were conducted by the pin-on-dick method under a load of 50 N and sliding velocity of 0.01 m / s, a steel ball with hardness of *HV*1-750 being used as a mating body. Three types of coatings were tested: plasma (APS) coatings containing a mixture of the ψ- and β-phases; APS coatings annealed at a temperature of 700 °C for 4 h, containing only the ψ-phase; and high-velocity oxy-flame (HVOF) coatings consisting only of the β-phase. The annealed APS coatings had a maximal hardness, and the HVOF coatings had a minimal hardness. That is, there was a correlation of hardness of the coatings with their content of the ψ-phase. The friction coefficient of the coatings differed but insignificantly and ranged from 0.09 to 0.11. However, the HVOF coatings consisting of the ψ-phase, which is softer than the β-phase, exhibited the highest wear resistance. As shown by metallographic examinations, these coatings had the highest density and contained almost no cracks. Annealing of the two-phase (ψ + β) plasma coatings led to increase in their density. However, that was accompanied by increase in the quantity of cracks, which was associated with volume changes as a result of the ψ–β transformation. Therefore, the annealed APS coatings consisting of the ψ-phase exhibited the lower wear resistance than the single-phase HVOF ones containing the softer β-phase.

The authors of study [4] note that wear of coatings under the dry sliding friction conditions (P = 250 g, linear velocity ---- 2.5 cm / s) strongly depends upon their density and topography of the surface, and, to a lesser degree, upon their chemical composition. This conclusion is proved by the results of tests of the coatings produced by the APS, vacuum plasma (VPS) and HVOF methods. The coatings differed in the content of the ψ-phase, density and hardness. Maximal hardness and content of the ψ-phase were exhibited by the VPS coatings, and maximal density ---- by the

HVOF coatings. The coatings can be arranged as follows in an order of growth of the friction coefficient: APS → VPS → HVOF, the values of f differing by almost an order of magnitude from those given in study [3] (0.6–1.2, compared with 0.09–0.11). Investigations of tribotechnical properties of thermal spray coatings of alloys $Al_{65}Cu_{20}Fe_{15}$, $Al_{64}Cu_{18}Fe_8Cr_8$ and $Al_{67}Cu_9Fe_{10.5}Cr_8Si_3$ by the sclerometry method at a constant load of 20 N resulted in fixing a dependence of the friction coefficient upon the material, diameter of a spherical indenter and degree of roughness of the coating surface. Increase in the latter decreases the friction coefficient in the case of a diamond indenter, and increases it in a case of steel indenter [5].

The studies considered, dedicated to investigations of tribotechnical properties of thermal spray coatings containing the quasi-crystalline phase, prove that they hold much promise for use to protect light alloy parts from wear, and that it is necessary to continue investigations to expand their practical application fields. However, no data are available so far on behaviour of these coatings under conditions of gas-abrasive wear, which is a common type of wear in practice.

There is a number of factors that affect the mechanism of gas-abrasive wear of coatings. Wear resistance of coatings under such conditions depends not only upon the hardness and brittleness of the coating material, but also upon the structure, size and distribution of its structural components. No direct relationship has been fixed between the wear resistance and hardness of thermal spray coatings (like in the case of porous powdered materials). Thus, as noted in study [6], at low attack angles an increase in hardness of a coating is accompanied by increase in its relative wear resistance, and at high attack angles it is accompanied by decrease in the relative wear resistance. At the same time, increase in elasticity modulus of the coating material leads to increase in the relative wear resistance both at low and high attack angles. This relationship is characteristic of materials having residual porosity. For almost pore-free materials (e.g. deposited coatings), increase in elasticity modulus at low attack angles leads to increase in wear resistance of coatings, and at high attack angles ---- to decrease in wear resistance. Any porosity in a material decreases its wear resistance under the impact by an abrasive jet, the degree of its effect depending upon the attack angle.

Initially, in wear of porous materials, they may be charged with abrasive particles in the abrasive jet, which does not only compensate for wear of a specimen, but also adds to its mass. Therefore, in this study the measurements during the tests were made after the end of some incubation period, i.e. after a stationary wear rate was established. At the same time, pores in a material, which act as stress raisers, may serve as crack initiation centres under the impact by abrasive particles.

Powder materials and coatings can be subdivided into two groups as to the degree of their resistance to abrasive wear (depending upon angle α of attack by abrasive particles [6]: $\alpha < 35°$ ---- maximal wear for plastic materials, and $\alpha > 45°$ ---- for brittle materials.

Studies were conducted to investigate wear resistance of detonation and plasma coatings of powders of the Al–Cu–Fe system ($Al_{63}Cu_{25}Fe_{12}$) alloy with no alloying additions, as well as of powders of alloys with scandium (0.265 and 0.440 at.% Sc) or chromium (8 at.% Cr) additions, under the gas-abrasive wear conditions. The powders for deposition of the coatings were produced by atomisation of melt in argon and high-pressure water (Table). Detonation coatings* were deposited using the «Perun-S» machine under the following conditions: working gas flow rate, m^3 / h: 0.35 (propane-butane), 0.95 (oxygen) and 0.4 (air); spraying distance ---- 110 mm. Size of the powder particles was 40–63 μm.

Plasma coatings were applied under the following technological parameters using the «Kiev-7» machine: current 200 A, voltage 340 V, spraying distance 200 mm, and plasma gas (air) flow rate 20 m^3 / h. Size of the powder particles was 40–63 and 25–40 μm. Coatings were deposited on a steel substrate having room temperature, and on a substrate preheated to 270 and 400 °C.

Coatings of the Al–Cu–Fe and Al–Cu–Fe–Sc systems consisted of a mixture of hard and brittle quasi-crystalline ψ- and softer crystalline β-phases. In all the cases, except for plasma spraying of the Al–Cu–Fe system alloy powder on the substrate preheated to 400 °C (pos. 5 of the Table), the content of the β-phase was lower, compared with the initial powder. In a case of detonation spraying of the $Al_{66}Cu_{18}Fe_8Cr_8$ powder (pos. 9), heating resulted not only in an increase of the ψ-phase content, but also in a formation of the crystalline approximant of decagonal quasi-crystal, i.e. O_1 phase, instead of the ψ-phase. No clear correlation was fixed between the amount of the quasi-crystalline ψ-phase and microhardness of a coating, this being related to the fact that it is determined not only by the phase composition, but also by the grain size and density of a coating, which, in turn, depend upon the characteristics of an initial powder, method and parameters of spraying.

Investigations of gas-abrasive wear of coatings were conducted using the centrifugal solid particle accelerating unit TsUK-3M [6, 7] in compliance with GOST 23.201–78. Quartz sand with a particle size of 0.5–0.9 mm and a relative moisture content of not more than 0.15 % was used as an abrasive material. Frequency of rotation of the unit rotor was constant and equal to 3000 ± 50 rpm, this corresponding to the linear rate of flow of the abrasive particles equal to 38 m / s. The investigations were carried out at fixed abrasive attack angles: 30, 45, 60 and 90°.

*Detonation coatings were produced under the leadership of Dr. E.A. Astakhov, and plasma coatings were deposited by M. Kolomytsev.

Gas-abrasive wear resistance of thermal spray coatings containing quasi-crystalline phase

Pos. #	Spray powder	Deposition method[1]	Substrate temperature, °C	Powder characteristics		
				Production method[2]	Particle size, μm	Content of quasi-crystalline ψ-phase, wt.%
1	$Al_{63}Cu_{25}Fe_{12}$	DS	20	ÀÐ	40–63	45
2	$Al_{63}Cu_{25}Fe_{12}$	DS	20	WÐ	40–63	53
3	$Al_{63}Cu_{25}Fe_{12}$	PS	20	ÀÐ	40–63	45
4	$Al_{63}Cu_{25}Fe_{12}$	PS	400	ÀÐ	40–63	45
5	$Al_{63}Cu_{25}Fe_{12}Sc_{0.265}$	PS	270	ÀÐ	25–40	50
6	$Al_{62.735}Cu_{25}Fe_{12}Sc_{0.265}$	DS	20	WP	40–63	72
7	$Al_{62.735}Cu_{25}Fe_{12}Sc_{0.265}$	PS	20	WP	40–63	72
8	$Al_{62.256}Cu_{25}Fe_{12}Sc_{0.44}$	DS	20	WP	40–63	73
9	$Al_{66}Cu_{18}Fe_{8}Cr_{8}$	DS	20	WP	40–63	42

[1]DS ---- detonation spraying; PS ---- plasma spraying.
[2]AP ---- powder atomised in argon; WP ---- powder atomised in water.

Table (cont.)

Pos. #	Coating characteristics		Mean wear at different abrasive attack angles (°), mg / kg			
	Content of quasi-crystalline phases (ψ), wt.%	*HV*, GPa	30	45	60	90
1	36	6.4 ± 1.0	49.9	104.4	113.7	118.2
2	17	5.5 ± 1.0	33.4	87.6	88.4	103.6
3	36	5.5 ± 0.9	148.0	220.9	227.9	238.2
4	45	6.6 ± 1.9	142.5	147.7	156.3	206.5
5	36	6.9 ± 1.5	105.2	186.4	260.6	269.4
6	35	5.7 ± 1.2	29.4	65.1	86.2	111.8
7	38	5.9 ± 1.7	75.2	140.6	149.0	236.8
8	32	5.6 ± 1.5	47.8	78.4	91.8	123.8
9	37 ($\hat{I}_1$)	5.8 ± 2.3	93.2	115.8	152.6	186.8

The intensity of wear in milligrams per kilo (mean loss of weight of specimens per kilo of the abrasive getting onto a specimen) was assumed to be the wear resistance indicator. The total amount of the abrasive spent for each series of specimens was 30 kg, and the quantity of specimens with the same type of a coating (coating thickness ~ 500 μm) was not less than three.

Analysis of the results allows the following conclusions to be made concerning the effect of characteristics of an initial powder and method used to deposit coatings on their resistance under the gas-abrasive wear conditions.

All coatings investigated, independently of their composition and spraying method, exhibited decrease in wear resistance with increase in the attack angle. The highest effect by the attack angle on wear resistance of coatings was seen on the detonation coatings of the Al–Cu–Fe system alloy with an addition of 0.265 at.% Sc (3.8 times decrease in wear resistance with increase of the attack angle from 30 to 90°), and the lowest effect was seen on the plasma coatings sprayed on the substrate preheated to 400 °C, a decrease being no more than by a factor of 1.5 (pos. 6 and 4, respectively, of the Table).

Again, no clear correlation was fixed between the gas abrasive wear resistance of the coatings and their content of the ψ-phase. However, the coatings produced from the powder with the same particle size by the same spraying method exhibited decrease in wear resistance with increase in the ψ-phase content, this being associated with increase in brittleness of the coatings. Thus, for a detonation coating with 36 % ψ-phase, compared with 17 % ψ-phase (pos. 1 and 2 of the Table), wear resistance was lower by a factor of 1.1–1.5, depending upon the attack angle.

At the same time, preheating of the substrate to 400 °C in plasma spraying, which leads to increase in cohesion strength and density of the coatings, in addition to increase in the ψ-phase content, provides also increase in their wear resistance (pos. 3 and 4 of the Table).

As a whole, detonation coatings are superior to plasma ones in gas abrasive wear resistance. For example, the detonation coatings of the Al–Cu–Fe sys-

tem powder with a particle size of 40–63 μm are 2–3 times superior in wear resistance to the plasma ones produced from the same powder, their ψ-phase content being also the same, i.e. 36 wt.% (pos. 1 and 3 of the Table).

Alloying with 0.265 at.% Sc provides increase in wear resistance of the detonation coatings, especially at low attack angles (pos. 6 and 1), while with an increase of up to 0.44 at.% in the content of the alloying element its effect on wear resistance is much lower and shows up at attack angles of up to 60° (pos. 8 of the Table).

The lowest wear resistance among the detonation coatings under the gas abrasive wear conditions at all attack angles was exhibited by the coatings alloyed with chromium. This is attributable to the fact that they are characterised by the highest brittleness and low cohesion strength, this leading, as proved by metallographic analysis, to partial separation of a coating from the substrate.

Therefore, coatings with the quasi-crystalline phase wear out as brittle materials: wear resistance decreases with increase in the attack angle, going down to minimal values at a head-on collision of the abrasive particles with the coating surface ($\alpha = 90°$). At low attack angles, the kinetic energy of the abrasive particles getting on the surface causes micro cutting and precipitation of wear products. High attack angles lead to formation of recesses covering several grains of a coating, which is caused by detachment of slightly bonded particles. The main criterion of wear resistance of such brittle coatings is their crack resistance, which can be increased by providing a pore-free or low-porosity structure with uniformly distributed equilibrium pores in the fine-grained structure of a coating. Another important factor of the structural state of thermal spray coatings is their cohesion strength, which reflects the strength of bond between individual structural elements of a coating (lamellae). This structure of a coating can be provided by selecting optimal technological variants and deposition parameters.

Based on the results of this study, the maximal gas-abrasive wear resistance of thermal spray coatings containing the quasi-crystalline phase was achieved with the detonation method of depositing unalloyed powders of the Al–Cu–Fe system alloys, or powders alloyed with a small amount of scandium (~ 0.3 wt.%). Increase in the ψ-phase content of a coating, or its alloying with chromium, has no marked effect on wear resistance of the Al–Cu–Fe system alloy under the gas-abrasive wear conditions.

The team of the authors expresses gratitude to the Science and Technology Centre in Ukraine for its financial support rendered to perform this study under Project 1630.

1. Borisov, Yu.S., Borisova, A.L., Adeeva, L.I. et al. (2005) Thermal-spray coatings containing the quasi-crystalline phase, peculiarities and applications (Review). *Fizika i Khimiya Tv. Tila*, **1**, 124–136.
2. De Palo, S., Usmani, S., Sampath, S. et al. (1997) Friction and wear behavior of thermally sprayed Al–Cu–Fe quasicrystal coatings. In: *Thermal Spray A*: Proc. of United Forum for Sci. and Technol. Advances. Ohio: ASM Int. Materials Park.
3. De Palo, S., Usmani, S., Kishi, K. et al. (1998) Thermal spray quasicrystalline coatings. Part 2: Relationships among processing, phase assemblage and tribological response. In: *Proc. of 15th Int. Thermal Spray Conf.* (Nice, France, May 25–29, 1998).
4. Sordelet, D.J., Krotz, P.D., Daniel, Jr. R.L. et al. (1995) Microstructure and wear behavior of quasicrystalline thermal sprayed coatings. In: *Proc. of 8th Nat. Thermal Spray Conf.* (Houston, USA, Sept. 11–15, 1995).
5. Dubois, J.-M., Kang, S.S., Massiani, Y. (1993) Application of quasicrystalline alloys to surface coating of soft metals. *J. Non-Crystalline Solids*, **153 / 154**, 443–445.
6. Kulu, P. (1988) *Wear resistance of powder materials and coatings*. Tallinn: Valgus.
7. Klejs, I.P. (1970) Centrifugal accelerator TsUK-3M for determination of relative wear resistance of materials during abrasive erosion. In: *Transact. of the Tallinn Polytechn. Inst.*, Series A.

COMPARATIVE ANALYSIS OF APPLICATION OF COVERED ELECTRODES FOR MAJOR REPAIRS AT MAIN OIL PIPELINES

D.A. ZAVALINICH[1], **V.M. DZYUBA**[2], **V.G. LOZOVOJ**[2] and **D.L. STOROZHIK**[3]

1Open Joint Stock Company «Chernomortransneft», Novorossijsk, Russia
[2]Limited Liability Company «Welding Consumables», Krasnodar, Russia
[3]Novorossijsk Ship Yard, Novorossijsk, Russia

Results of comparative tests of Russian and imported covered electrodes applied to repair main oil pipelines are presented. Recommendations based on the experience gained at the Joint Stock Company «Transneft» are given for application of electrodes.

Keywords: arc welding, main oil pipelines, repair, strength group of steels, covered electrodes, qualification tests, application experience, recommendations

Russia and other CIS countries widely apply general-purpose electrodes complying with GOST 9466–75 for welding of metal structures. However, this standard disregards technological peculiarities of welding and repair of oil pipelines, which does not allow using such electrodes without special testing and certification. In Russia, qualification tests of imported and domestic electrodes to be applied at Joint Stock Company «Transneft» are carried out at VNIIST (Moscow), while those of electrodes to be applied at Russian Joint Stock Company «Gazprom» and «Strojtransgaz» ---- at VNIIGAS (Moscow). Additionally, the domestic electrodes to be qualified for repair and construction of pipelines are tested to meet requirements of RD 03-613–03 of the National Association of Testing and Welding of Russia. This cross certification system makes assessment more stringent and provides high objectiveness of the test results.

Qualification tests of welding consumables determine the level of welding-technological characteristics and assess correspondence of welding consumables to special requirements for quality of their manufacture and required package of mechanical properties.

This article generalises experience gained in major repairs of main pipelines using imported and domestic electrodes and, on this basis, gives some of the recommendations.

Welding consumable is chosen for each particular case on the basis of strength classes and dimension types of pipes welded, requirements for mechanical properties of welded joints, conditions of laying an oil pipeline and availability of special requirements to welded joints, welding-technological properties of specific grades of electrodes, arrangement of welding-assembly operations, and required rate of their performance.

Table 1 gives a regulation directive for electrodes intended for butt welding of oil pipelines depending upon the strength class of steels.

In the case of butt welding of pipes made from steels of different strength groups, welding consumables should be chosen on the following basis: at different values of pipe wall thicknesses ---- on the basis of thickness of pipe made from steel of a higher strength class, and at the same values of pipe wall thicknesses ---- on the basis of thickness of pipe made from steel of a lower strength class.

As follows from Table 1, basic electrodes corresponding to type E50A (E7016), or cellulose electrodes of the E42A and E46A (E6010 and E6010+) types should be used to make the root weld layer in butt joints on pipes made from steels of strength groups 1–4.

The following types of cellulose electrodes are used for welding of the hot pass (the first filler pass in welding of the root weld layer):

- E42A, E46A (E6010 and E6010+) ---- to make the hot pass in butt joints on pipes of steels of the first and second strength groups;
- E50A (E7010 according to AWS A5.1 and E6010+) ---- to make the hot pass in butt joints on pipes of steels of the third strength group.

Welding consumables for deposition of filler and cover layers of the weld should provide strength of the weld metal equal to that of the base metal. The following basic electrodes (see Table 1) are mainly used in Russia to deposit the above weld layers:

- type E50A (E7016, E7018) ---- for welding butt joints on pipes of strength groups 1 and 2;
- type E60 (E8015, E8016, E8018) ---- for welding butt joints on pipes of strength group 3;

*The publication is based on the paper presented at the 2nd Workshop «Arc Welding. Consumables and Quality» (26–30 September 2005, Magnitogorsk, Russia).

Table 1. Specifications of electrodes for welding oil pipelines, depending the strength class of steels

Application	Type of covering, type acc. to GOST 9467–77 (AWS A5.1)	Strength group of steel; rated tensile strength, MPa (kgf / mm^2)
Root weld	Basic, E50A (E7016)	1–4; up to 637 (65)
	Cellulose, E42A, E46A (E6010)	
Hot pass	Cellulose, E42A, E46A (E6010)	1, 2; up to 530 (54)
	Cellulose, E50A (E7010)	3; 539 (55)–588 (60)
Filler and cover weld layers	Basic, E50A (E7016, E7018)	1, 2; 530 (54)
	Basic, E60 (E8018, E8016, E8015 — acc. to AWS A5.5)	3; 539 (55)–588 (60)
	Basic, E70 (E9016, E9018 — acc. to AWS A5.5)	4; 637 (65)
	Cellulose, E42A, E46A (E6010)	1; up to 490 (50)
	Cellulose, E50A (E7010)	2; 490 (50)–530 (54)
	Cellulose, E55A (E8010 — acc. to AWS A5.5)	530 (54)–550 (56)
	Cellulose, E60A (E9010 — acc. to AWS A5.5)	3; 539 (55)–588 (60)

• type E70 (E9016, E9018) — for welding butt joints on pipes of strength group 4.

Cellulose electrodes may also be used for depositing filler and cover weld layers. However, the necessary conditions in this case are development and harmonisation of appropriate welding flow charts and instructions for each specific construction facility, qualification tests of the welding technology, and special training and certification of welders. In addition, this requires using the following cellulose electrodes:

• type E42A, E46A (E6010 and E6010+) — for welding butt joints on pipes of strength group 1;

• type E50A (E7010) — for welding butt joints on pipes of strength group 2;

• type E55 (E8010) — for welding butt joints on pipes with strength ranging from 530 (strength class of pipe steel K54) to 550 MPa (strength class K56);

• type E60 (E9010) — for welding butt joints on pipes of strength group 3.

Basic electrodes qualified and recommended for manual arc welding of pipes of different strength groups of steels, and manufacturers of these electrodes, are listed in Table 2, while cellulose electrodes and their manufacturers are listed in Table 3.

Open Joint Stock Company «Chernomortransneft» tested new electrodes of the LB-52TRU grade (TU 1272-018-01627014–2002) manufactured by the Krasnodar Electrode Limited Liability Company «Research and Production Centre «Welding Consumables», which were certified by the Russian Register of Shipping, Lloyd's Register (Great Britain) and DNV (Norway). Difference in thickness of coverings of the 3 mm diameter electrodes is 0.04–0.08 mm, and that of the 4 mm diameter electrodes is 0.06–0.10 mm. Coverings of electrodes of both diameters were not destroyed in tests with falling from a height of 1 m onto a cast iron plate. Welding-technological properties of the electrodes were tested in welding of root, filler and cover layers of the weld joining coils of the 530×9 and 720×10 mm pipes of steel 17GS1. X-ray inspection revealed no inadmissible defects, and slag could be easily removed from the weld groove. The back bead of the root weld was free from undercuts, had minimal gradient between ripples, and the internal (top) surface of the root bead had no overlaps and no large reinforcement. The cover layer had a ripple surface, meeting the most stringent requirements. Providing that the manufacturing quality is kept to, electrodes LB-52TRU will seriously compete with the best foreign samples of pipe welding electrodes, which will dramatically decrease dependence of the CIS countries from import, the electrode price being substantially reduced. The tests of electrodes LB-52TRU conducted at the Tyumen Training Centre of the Open Joint Stock Company «Sibnefteprovod» confirmed the test results obtained at the Open Joint Stock Company «Chernomortransneft».

New Russian cellulose electrodes «Kuban 6010» and «Kuban 7010» of series E6010 and E7010 according to AWS A5.1, respectively, were tested in qualification of the technology for welding the «Blue Stream» pipeline between Russia and Turkey in a region of 56–92 km. Electrodes «Kuban 6019» with a diameter of 4 mm were used for welding the root weld of a pilot joint between the 1420×18.7 mm pipe sections, and the same diameter «Kuban 7010» electrodes were used for making the hot pass in this joint. In parallel, the root weld and hot pass of a similar joint were welded using the 4 mm diameter electrodes «Fleetweld 5P+». The groove was filled and cover layers in both cases were made using self-shielding wire NR-202 (Lincoln Electric, USA). In terms of technology, electrodes «Kuban 6010» and «Kuban 7010» were found to be superior to electrodes «Fleetweld 5P+». They are advantageous, in particular, in a smaller stub permitted for welding, compared with imported electrodes, which provides saving of quite expensive cellulose electrodes. 100 % X-ray inspection revealed no inadmissible defects in welded joints made using these electrodes. It is a common opinion of specialists and welders that, after beginning of commercial manufacture of electrodes «Kuban 6010» and «Kuban 7010», and their certification by VNIIST and

Table 2. Basic electrodes for welding and repair of position and roll butt welded joints in construction, reconstruction and repair of oil pipelines

Application	Electrode grade	Diameter, mm	Manufacturing company
Welding and repair of root weld, and making back layer* on pipe joints of steel with rated tensile strength of up to 588 MPa (strength groups 1–4)	LB-52U	2.6; 3.2	Kobe Steel (Japan)
	Phoenix K50R Mod	2.5; 3.2	Boehler-Thyssen Schweisstechnic (Germany)
	OK 53.70	2.5; 3.2	ESAB AB (Sweden)
	OK 53.70	2.5; 3.0	ESAB-SWEL (St.-Petersburg, Russia)
	OK 53.70**	2.5; 3.0	SIBES (Tyumen, Russia)
	Fox EV Pipe	2.5; 3.2	Boehler-Thyssen Welding (Austria)
	Lincoln 16P	2.5; 3.2	Lincoln Electric (USA)
	MTG-01K	2.5; 3.0	Sychevsky Electrode Factory (Sychevka, Russia)
	LB-52TRU	3.0	Research and Production Enterprise «Welding Consumables» (Krasnodar, Russia)
Welding and repair of filler and cover layers on pipe joints of steel with rated tensile strength of up to 530 MPa (groups 1, 2)	LB-52U	3.2; 4.0	Kobe Steel (Japan)
	Phoenix K50R Mod	3.2; 4.0	Boehler-Thyssen Schweisstechnic (Germany)
	OK 53.70	3.2; 4.0	ESAB AB (Sweden)
	OK 53.70	3.0; 4.0	ESAB-SWEL (St.-Petersburg, Russia)
	OK 53.70**	3.0; 4.0	SIBES (Tyumen, Russia)
	Fox EV Pipe	3.2; 4.0	Boehler-Thyssen Welding (Austria)
	Lincoln 16P	3.2; 4.0	Lincoln Electric (USA)
	MTG-01K	3.0	Sychevsky Electrode Factory (Sychevka, Russia)
	MTG-02	4.0	Same
	OK 48.04	3.0; 4.0	SIBES (Tyumen, Russia)
	LB-52TRU	3.0; 4.0	Research and Production Enterprise «Welding Consumables» (Krasnodar, Russia)
	OK 48.04**	3.2; 4.0	ESAB AB (Sweden)
Welding and repair of filler and cover layers on pipe joints of steel with rated tensile strength from 539 to 588 MPa (group 3)	OK 74.70	3.2; 4.0	Same
	Lincoln 18P	3.2; 4.0	Lincoln Electric (USA)
	Kessel 5520 Mo	3.2; 4.0	Boehler Schweisstechnic Deutschland (Germany)
	OK 74.70**	4.0	SIBES (Tyumen, Russia)
	MTG-03	3.0; 4.0	Sychevsky Electrode Factory (Sychevka, Russia)
	Schwarz-3K Mod	3.2; 4.0	Boehler-Thyssen Schweisstechnic (Germany)
Welding and repair of filler and cover layers on pipe joints of steel with rated tensile strength of up to 637 MPa	OK 74.78**	4.0	ESAB AB (Sweden)

*It is recommended to use electrodes #1–8 with diameters of 3.0, 3.2 or 4.0 mm for depositing a back layer.
**Electrodes OK 53.70 (SIBES), OK 74.70 (SIBES), OK 48.08 and OK 74.78 can be allowed for use only after their periodic qualification tests following an established procedure.

VNIIGAZ, they will realistically find very wide application in welding of pipelines, provide substantial savings in pipelines construction, given their much lower costs, and decrease dependence of demand for cellulose electrodes upon the import.

Of certain interest is an experimental assessment of welding-technological properties of imported electrodes intended for pipeline construction, mechanical properties of welded joints and chemical composition of deposited metal, which were determined in qualification tests of electrodes and generalisation of experience of their application at organisations of the Joint Stock Company «Transneft» for position butt welding of pipelines of different diameters, wall thicknesses and assembly conditions. This assessment (Tables 4–7) can serve as a guideline for developers of welding consumables in Russia and other CIS countries, as well as for specialists and welders of all pipeline organisations.

As seen from the data given in Tables 4–7, electrodes with the highest points of welding-technological properties may have a low level of toughness and ductility of the weld metal. In turn, high values of impact toughness of the weld metal, which is characteristic of some electrode grades, may mismatch with the same indicators of welding-technological properties. Therefore, the choice of electrodes should be based on specific tasks and conditions of repair, type

Table 3. Cellulose electrodes for position and roll butt welding of pipes in construction, reconstruction and repair of oil pipelines

Application	Electrode grade	Diameter, mm	Manufacturing company
Welding of root weld in butt joints on steel pipes with rated tensile strength ≤ 588 MPa (strength groups 1–3), and hot pass in butt joints on pipes with rated tensile strength ≤ 530 MPa (strength groups 1 and 2)	Fleetweld 5P+	3.2; 4.0	Lincoln Electric (USA)
	Fox Cel	3.2; 4.0	Boehler-Thyssen Welding (Austria)
Welding of hot pass in butt joints on steel pipes with rated tensile strength ≤ 588 MPa (strength group 3), filler and cover layers in butt joints of steel pipes with rated tensile strength of 490–530 MPa (strength groups 1 and 2)	Fleetweld 5P+	4.0	Lincoln Electric (USA)
	Fox Cel	4.0	Boehler-Thyssen Welding (Austria)
Welding of filler and cover layers in butt joints on steel pipes with rated tensile strength < 490 MPa (strength group 1)	Fox Cel	3.2; 4.0	Same
Welding of filler and cover layers in butt joints on steel pipes with rated tensile strength < 530 MPa (strength groups 1 and 2)	Fleetweld 5P+	3.2; 4.0	Lincoln Electric (USA)
Welding of hot pass, filler and cover layers in butt joints on steel pipes with rated tensile strength of 530–550 MPa (K54–K56)	Shield Arc 80	4.0	Same
Welding of hot pass, filler and cover layers in butt joints on steel pipes with rated tensile strength of 539–588 MPa (strength group 3)	Fox Cel	4.0; 5.0	Boehler-Thyssen Welding (Austria)

Table 4. Welding-technological properties of 3.2 mm basic electrodes for deposition of root weld*

Welding-technological properties	Electrode grades					
	LB-52U	Phoenix K50 Mod	Lincoln 16P	OK 53.70	Firma 5520R Mod	UONI-13 / 55M (for comparison)
Practicability	5	4	5	4	4	3
Penetrating power of arc, no sensitivity to formation of lacks of fusion and undercuts	5	4	4	4	4	3
Softness and stability of arc	5	5	5	5	5	3
Shape and surface of root weld on groove side	5	4	5	5	4	3
Detachability of slag	5	5	5	5	5	3
Sensitivity to formation of pores in variations of gap size	5	4	5	4	3	3

*Expert numerical estimation was performed with electrode LB-52U (Kobe Steel, Japan) taken as reference (point 5).

Table 5. Chemical composition and mechanical properties of deposited metal made by using basic electrodes for welding root, filler and cover layers in butt joints of pipes on steels of strength groups 1 and 2

Electrode grade, type acc. to GOST (AWS)	Typical chemical composition of deposited metal	Typical mechanical properties of metal					
		σ_t, MPa	σ_y, MPa	δ, %	ψ, %	*KCV*, J / cm^2, at temperature, °C	
						–20	–40
LB-52U, E50A (E7016)	0.08 C; 0.86 Mn; 0.64 Si	563	447	24	65	40	40
Lincoln 16P, E50A (E7016)	0.07 C; 1.15 Ì n; 0.60 Si	530	417	29	70	88	48
Phoenix K50R Mod, E50A (E7016)	0.07 C; 1.28 Ì n; 0.51 Si	520	418	28	63	73	47
OK 53.70, E50A (E7016)	0.05 C; 1.34 Ì n; 0.29 Si	524	420	32	75	121	59
Firma 5520R Mod, E50A (E7018)	0.05 Ñ; 1.07 Ì n; 0.56 Si	525	410	27	76	72	35
OK 48.04*, E50A (E7018)	0.06 C; 1.15 Ì n; 0.50 Si	504	418	30	79	90	55

*Welding of only filler layers.

Table 6. Welding-technological properties of 4.0 mm diameter cellulose electrodes for welding root weld layers*

Welding-technological properties	Electrode grades				
	Fox Cel	Thyssen Cel 70	Fleetweld 5P+	Pipeweld 6010	Kobe 6010
Penetrating power of arc, back bead formation	5	5	5	4	5
Back bead shape	5	5	5	5	4
No sensitivity to formation of lacks of fusion and undercuts	5	5	5	4	4
Sensitivity to arc sticking during welding	4	4	5	3	3

*Expert numerical estimation was performed with electrode Fox Cel (Boehler-Thyssen Welding, Austria) taken as reference.

Table 7. Typical mechanical properties of deposited metal made with cellulose electrodes for welding root, filler and cover layers in butt joints of pipes on steels of strength groups 1 and 2

Electrode grade, type acc. to GOST (AWS)	σ_t, MPa	σ_y, MPa	δ, %	ψ, %	*KCV*, J / cm^2, at temperature, °C	
					–20	–40
Fox Cel, E46 (E6010)	495	425	26	66	65	–
Fleetweld 5P+, E46 (E6010)	520	410	29	67	72	46
Pipeweld 6010, E42 (E6010)	450	360	30	58	45	30
Pipeweld 7010, E50 (E7010)	565	435	25	57	48	27
Thyssen Cel 70, E46 (E6010)	505	385	25	61	25	13

of oil pipelining, climatic conditions where the operations are to be performed, presence or absence of special requirements to toughness and ductility levels (e.g. impact toughness) of welded joints in oil pipelines, etc.

Experience gained by the Company «Transneft» in performing welding operations allows distinguishing also a number of technological peculiarities in application of basic and cellulose electrodes for major repairs of main oil pipelines, the most important of them being considered below.

Welding of the root weld layer using basic electrodes should be performed at a direct current of straight or reverse polarity, and at a minimum possible arc length. The best results are obtained at the straight polarity, as in this case the penetrating power of the arc is increased, and a more complete penetration of edges is achieved.

Welding at the reverse polarity current by keeping to the recommended conditions of fit-up (gap and root face sizes) on the welded joint perimeter can also provide a sound root weld. But this requires a higher-skill welder to ensure a complete penetration of edges than in welding at the straight polarity current. Penetration in welding at the reverse polarity current can be increased by adjusting an electrode inclination angle (making it closer to normal to the pipe surface), increasing the current by 10–20 A, and weaving the electrode. Values of the welding current recommended for basic electrodes used to deposit the root weld at the reverse polarity direct current are given in Table 8.

Table 8. Welding current in deposition of root weld layer using basic electrodes

Electrode dia., mm	Spatial position		
	Flat	Vertical	Overhead
2.50	50–80	70–90	80–90
3.25	80–90	80–100	90–110

Only 2.5 mm diameter electrodes should be used to deposit the root weld at a pipe wall thickness of up to 7 mm, while at larger thickness the use should be made of the 3 and 3.2 mm diameter electrodes.

Welding of the root weld layer with cellulose electrodes should be performed by the downward method at a direct current of reverse or straight polarity using power supplies with special characteristics. The use of the straight polarity arc current allows the probability of undercuts to be reduced, and formation of elongated pores in back beads to be avoided.

For pipes with a diameter of 530 mm or more, and with a wall thickness of up to 7 mm, the 4 mm diameter cellulose electrodes should be used to weld the root weld layer.

Welding of the hot pass should be performed only at a reverse polarity current.

The amperage in welding depends upon the specific electrode grade and diameter, wall thickness of a pipe welded, spatial position in welding, and welder's skill.

Recommended values of the welding current for deposition of the root weld layer and hot pass using 4 mm diameter cellulose electrodes are given in Table 9.

Procedure for manipulating an electrode in deposition of the root weld layer by the downward method allows no oscillating movements when the electrode crate contacts the weld edges. In this case a hole (proc-

Table 9. Parameters of welding using cellulose electrodes

Electrode grade	Root layer		Hot pass	
	Kind of current, polarity	Welding current, A	Kind of current, polarity	Welding current, A
Fleetweld 5P	DCRP	130–150	DCSP	150–170
Fleetweld 5P+		120–140		140–160
Thyssen Cel 70		130–160		170–190
Pipeweld 6010		120–140		140–160
Fox Cel		120–150		150–180

ess window) corresponding to the electrode rod diameter is formed in the weld edges.

Welding speed should be maximum possible (14–18 m / h), this allowing undercuts to be avoided, and the weld bead to be formed over the process window.

With proper implementation of the process, the welding arc penetrates through the gap between the weld edges in such a way that the gas flow of the arc and slag spatters are directed to inside a pipe and can be seen on the external surface, this providing through penetration of the weld edges.

Inclination angle of an electrode during welding should be close to normal to the pipe surface in the welding zone (10°, Figure). This provides an easy formation of the weld bead. An oval hole of a large size is formed at an inclination angle of more than 10°, this leading to violation of the stable-size bead formation process.

Welding of the root layer with cellulose electrodes is characterised by formation of slag-filled undercuts on both sides of the weld. The weld bead on the outside has a substantial reinforcement at the centre.

To ensure the reliable quality of the weld, deposition of the root weld layer should be followed by grinding to open the slag-filled undercuts (pockets) and remove an excessive weld reinforcement.

Welding of the hot pass should be performed not later than 5 min after completion of the root layer. This is associated with the fact that the welds made with cellulose electrodes are characterised by a high content of diffusible hydrogen, which increases the risk of cold cracking in the weld and HAZ metal. Because of a high rate of diffusion of hydrogen into different (potentially dangerous for initiation of cracks) regions of the HAZ metal, diffusible hydrogen should be removed as much as possible from the root weld metal. This is achieved by making the hot pass, which is performed immediately after completion of the root weld.

Therefore, the main purpose of the hot pass is to remove diffusible hydrogen from metal of a previous layer and slag from pockets opened after grinding of the root weld layer.

Peculiarities of the hot pass deposition procedure consist in the following:

- welding should be performed at a maximum permissible welding current for a specific electrode grade;
- electrode should not contact the weld edges, but should be separated from the weld pool, and then, for a short time, be again immersed into it in the location of the lower boundary of the crater;
- during the above manipulation, the electrode is imparted a rotational movement at a variable arc length, thus allowing removal of slag from the welding zone;
- the electrode inclination angle depends upon the spatial welding position. In a vertical position it should be 70–80° (3 h), in a horizontal position it should be 30–40°, and in overhead position — 10° (see the Figure).

With a proper hot pass deposition procedure, a welder can easily melt out slag from the slag-filled undercuts (pockets) that are opened by grinding the root weld, thus providing the smooth surface of the weld for subsequent welding.

Main defects formed in welding of the root weld layer and hot pass using cellulose electrodes are given in Table 10.

Electrodes intended for welding of filler and cover layers should also meet special requirements as to welding-technological characteristics, mechanical properties of welded joints and deposition efficiency.

The main welding-technological characteristics are as follows:

- penetrating power of electrodes and capability of removing defects from the previous layer;
- deposition efficiency;

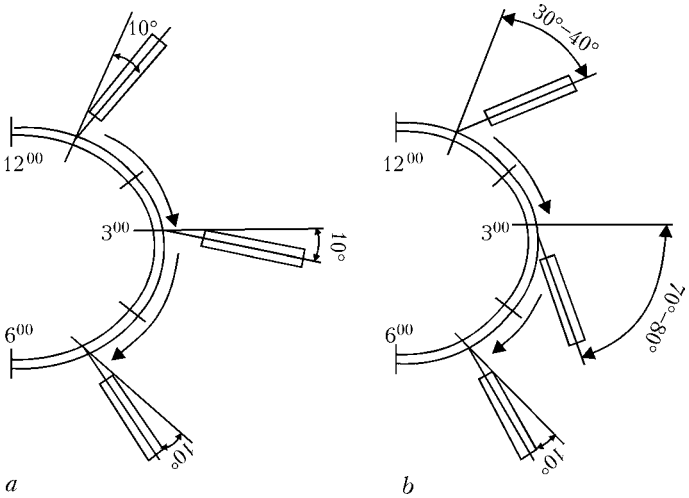

Electrode inclination angle in welding using cellulose electrodes: *a* — root layer; *b* — hot pass

Table 10. Defects and their causes in welding of root weld layer and hot pass

Defect	Cause
Lack of fusion between edges in root layer	Small gap between edges Large root face Presence of edge displacement Low current High welding speed
Undercut in root layer	Large gap between edges High current Arc is too long Improper welding procedure Wrong current polarity
Formation of longitudinal plane in back bead (shrinkage cavities)	Gap is too small (degassing is difficult because of intensive dilution of deposited metal in base metal) Gap between edges is too large
Slag inclusions between root layer and hot pass	Not all weld reinforcement is removed by grinding Slag remained in pockets Current is too low Electrode inclination angle is wrong
Porosity in welding of hot pass	Reinforcement of root weld layer is too large Slag remained in pockets Current is too high Arc is too long

Table 11. Chemical composition and mechanical properties of basic electrodes for welding root, filler and cover layers in butt joints on pipes of increased strength steels (group 3)

Electrode grade, type acc. to GOST (AWS)	Typical chemical composition of deposited metal	Typical mechanical properties of weld metal					
		σ_t, MPa	σ_y, MPa	δ, %	ψ, %	*KCV*, J / cm^2, at temperature, °C	
						–20	–40
Kessel 5520 Mo, E60 (E8018-A1)	0.08 C; 1.20 Ì n; 0.30 Si; 0.5 Mo	640	523	24	66	–	38
OK 74.70, E60 (E8016-03)	0.07 C; 1.43 Ì n; 0.41 Si; 0.38 Mo	625	525	27	72	79	51
Lincoln 18P, E60 (E8018-0)	0.05 C; 1.33 Ì n; 0.30 Si; 0.77 Ni; 0.32 Mo	645	535	27	71	85	66
Schwarz 3K Mod, E60 (E8015-A1)	0.08 C; 1.20 Ì n; 0.30 Si; 0.45 Mo	620	530	23	68	53	39

- detachability of slag;
- ripple weld;
- practicability of electrode in welding of cover layers;
- spattering factor.

The main requirement to mechanical properties is providing the weld metal with strength equal to that of the base metal. It means that actual tensile strength of metal should be not lower than rated tensile strength of a pipe steel being welded, as specified in corresponding standards for pipes or pipeline components.

An additional requirement is providing the necessary level of toughness and ductility of the weld metal, if such requirements are imposed on welded joints of a specific pipeline.

Data on chemical composition of the deposited metal and mechanical properties of the weld metal for welding filler and cover layers in butt joints on pipes of increased strength steels using basic electrodes are given in Table 11.

The deposition efficiency of electrodes for welding filler layers in butt joints on pipes of steels of strength groups 1–3 for 4 mm diameter electrodes at a welding current of 160 A is 1.34 (OK 53.70), 1.27 (Lincoln 16P), 1.45 (Phoenix K50R Mod), and 1.54 (OK 48.04). At a current of 180 A, it is 1.50 (Kessel 5520 Mo), 1.40 (OK 74.70), 1.65 (Lincoln 18P), 1.50 (Schwarz 3K Mod), and 1.42 (VSF-65M).

Welding of filler layers should be performed without interruptions. Also, it is necessary to control the inter-layer temperature ranging from 20 to 120 °C. Layer-by layer cleaning should be carried out using grinding devices with round metal brushes. The cover layer should have a 1–3 mm reinforcement. Width of the cover layer is determined by width of the edge opening from +1.0 to 1.5 mm in overlapping the base metal on each side.

Implementation of the above data on selection of electrodes for construction, reconstruction and major repairs of main oil pipelines on the basis of peculiarities of their application, combined with mandatory certification of welders and stringent control of quality of welded joints, allows organisations of the Joint Stock Company «Transneft» a high-reliability failure-free service of oil pipelines in Russia and abroad, and raises a general level of pipeline construction in Russia and other CIS countries.

APPLICATION OF RECONDITIONING TECHNOLOGIES TO EXTEND THE LIFE OF GAS TURBINE ENGINES (analysis of state-of-the-art and development)

A.M. ZHADKEVICH
E.O. Paton Electric Welding Institute, NASU, Kiev, Ukraine

Advances in development of welding, brazing and coating technologies for repair of components of the hot section of gas turbine engines are noted. Causes limiting the wide-scale application of new technologies are considered. Prospects for arrangement of repair operations to recondition the blades of gas-pumping units in the gas industry of the CIS countries are substantiated.

Keywords: brazing, welding, coating deposition, turbine blades, casting alloys, casting and service defects, reconditioning repair, advanced technologies, cost effectiveness, prospects for application

In the last third of the previous century the advance of science and technology was closely connected to development and manufacturing of new equipment in different industrial sectors, namely aerospace, shipbuilding, power, mechanical, electronic engineering, instrument-making, etc. That period is characterized by development and introduction into production of technologies and equipment for brazing various metal materials, ceramics, glass, graphite, diamonds, semiconductors and other materials.

Technological capabilities of brazing are huge. This process enables making permanent joints in the most diverse combinations without any essential change of their initial structures or physical properties, with the capability of simultaneous joining of several components or parts of a complex geometrical shape with a considerable extent of braze welds, also in difficult-of-access places. The high efficiency and low cost, compared to other joining methods, make the brazing technology one of the promising, cost-effective and competitive processes [1–6].

Despite these advantages, brazing has not taken an appropriate place in the technologies of manufacturing advanced equipment, because of incomplete evaluation of its capabilities. Lower strength of the brazed joint compared to a welded joint, need for a thorough fit-up of the surfaces being joined, use of expensive metals in the brazing filler metals and low corrosion resistance of the weld compared to the base metal, are usually regarded as the disadvantages of brazing. Lack of specialized enterprises producing brazing consumables and equipment should be considered as objective disadvantages slowing down a wide-scale introduction of brazing.

New grades of nickel-based brazing filler metals developed over the last two decades, provide the corrosion resistance of brazed joints equivalent to that of the base metal. Application of pressure brazing and special kinds of heat treatment provides the joint strength sufficient for the operation conditions [7–9].

A significant contribution to development and introduction of brazing into production and repair technologies of components of the hot section of gas turbine engines (GTE) was made by scientists and specialists of research institutes, turbine and engine construction associations and enterprises, aircraft and shipbuilding design bureaus, higher engineering establishments, and over the last years also gas industry enterprises [9]. A number of enterprises and organizations for the last 30 years have been and still are the leaders in development and introduction of advanced technologies, materials and equipment for brazing parts in turbine construction and repair production.

Special mention should be made of the great contribution of scientists and specialists of FSUE VIAM, K.E. Tsiolkovsky RTTU MATI, N.E. Bauman MSTU, SPA «Tekhnomash», E.O. Paton Electric Welding Institute, Admiral Makarov NUSB, N.E. Zhukovsky HAIA, FSUPE «Salyut», SI «Zarya-Mashproekt», OJSC NIAT, FSUE TsNII SM «Prometej», OJSC «Silovye Mashiny», OJSC «A. Lulka-Saturn», OJSC «N.D. Kuztensov SNTK», etc. The results of research, design and applied developments performed in these organizations in the directions of development of the most advanced brazing technologies for aircraft, rocket and mechanical engineering, deposition of protective coatings and reconditioning of the turbine parts by brazing, are widely known and used in production not only in Ukraine, and Russia, but also in the foreign countries [10].

In 1984 the E.O. Paton Electric Welding Institute put into operation the Pilot Plant of Special Electrometallurgy (advanced technology plant), in which the shops of electron beam technology of welding and coating deposition were opened in addition to the shops of electroslag and ion-plasma technology. The initiator, ideological and scientific supervisor for establishing such an enterprise [11] in the system of the Academy of Sciences of Ukr. SSR was academician B.E. Paton, and the scientific supervisors of individual technological areas were academicians B.A. Movhcan,

B.I. Medovar, D.A. Dudko; and O.K. Nazarenko, Dr. of Sci. (Eng.), who was elected the Corresponding-Member of the National Academy of Sciences of Ukraine in 1992.

In the period from 1985 to 1992 the Plant performed a large scope of work on EBW of GTE and assembly blade sets, and tens of thousands of GTE blades were restored after their scheduled operation period in service. Application of special heat treatment and deposition of protective high-temperature resistant coatings from the vapour phase under vacuum from nickel- and cobalt-based alloys with additives of aluminium, chromium and yttrium, allowed extending several times the operating life of many hundreds of GTE, assemblies, compressors and power turbines.

Blades are the most prone to failure during GTE operation. The main cause for that is the fatigue fracture and violation of the geometrical dimensions and shape of blades, operating under the conditions of high temperatures, under the aggressive impact of the fuel combustion products and high-temperature gas (sulphide-oxide) corrosion [12]. Despite the use of dispersion-hardening nickel-based casting alloys in blade manufacture, the turbine operating life is limited by the design operating life, based on the processes of equipment ageing as a result of accumulation of fatigue damage in structural materials. The ageing process usually consists of two stages. The first is related to accumulation of reversible phenomena and is characterized by a gradual change of the material properties, and the second is related to irreversible changes leading to accelerated fracture of the material [5, 9, 12, 13].

Fatigue fracture of the most critical GTE parts, namely blades, results from the inaccuracies of machining, mounting and fit-up; impact of bending and torque alternating loads not allowed for by calculations; metal wear and corrosion. Repair of GTE blades addresses the following two problems: restoration of the geometrical shape (dimensions) of the blade and structure (strength properties) of blade material.

Taking into account the data of [14], Table 1 gives a simplified classification of the main technologies (allowing for the level of complexity), applied in blade repair.

Reconditioning of parts of GTE hot section by brazing is a promising and energy-saving process [9, 15–17]. The cost-effectiveness of application of brazing in the technologies of manufacturing and repair of the hot section parts was proved by working experience of the leading local and foreign turbine and engine-construction companies and enterprises in the second half of 1970s. During this time many enterprises established repair production to eliminate the defects in cast GTE blades and restore the shape and dimensions of products of the aircraft turbine hot section, worn in service, namely blades, contact surfaces of root platforms, nozzle blocks, nozzle seal rings, sealing the marker holes, etc. [15–20].

Repair of casting and service defects in GTE products from wrought high-temperature nickel alloys does not run into difficulties. This is performed using argon-arc welding (AAW) with filler wires of a composition similar to that of the base metal [21, 22].

At restoration of GTE products from dispersion-hardening nickel-base alloys with the total content of aluminium and titanium above 5 %, the most widely accepted repair technology is brazing with vacuum heating in a controlled atmosphere [15, 19, 20]. This technology enables further operation of a large number of expensive GTE products for various purposes. Structural transformations in high-temperature nickel-base casting alloys proceed at the temperature of 1225–1260 °C with a change of not only the initial structure, but also operating characteristics of the products. In this connection, use of brazing with local heating (1170–1220 °C) enables minimizing the influence of thermal impact on the base metal [8, 9, 16, 20, 22–24].

Reconditioning repair of GTE blades enables extension of the service life and maintaining within the specified limits the basic technical characteristics of the turbine, namely the power and efficiency. By the data of [14], the cost effectiveness of reconditioning repair of turbine blades can be estimated with some assumptions, using the following indices: C_r — cost of repair; ΔT_r — extension of service life (residual) as a result of repair; C_{pr} — total cost of the program of blade supply during repair; C_s — total cost of the program of blade supply without repair; T_l — design life of the blade; $C_{n.bl}$ — cost of new blade; $\Delta T_r / T_l$ — relative increase of blade service after repair.

Condition $C_{pr} / C_s < 1$ limits the region, in which blade repair will be cost-effective. Ratio $C_r / C_{n.bl}$ should not exceed the relative extension of service life $\Delta T_r / T_l$, resulting from repair. If blade life is extended

Table 1. Classification of the main technologies applied in blade repair

Level of complexity	Kind of repair	
	Restoration of geometrical dimensions	Restoration of metal structure and strength properties of the blade
I	Welding-on in the locations of thinning and flanges, repair of small defects of AAW	Heat treatment in the atmosphere (annealing)
II	Vacuum brazing Microplasma welding AAW EBW Application of high-resistant coatings	Thermoplastic strengthening Ultrasonic strengthening Hydroshotblasting strengthening Hot isostatic pressing (HIP) Metallographic inspection

by 20 % relative to the design life of a new blade, the cost of repair should not be higher than 20 % of the new blade cost. Otherwise repair will turn out to be more expensive than purchasing a new blade [14].

At present the enterprises of aircraft, shipbuilding turbine and engine construction have technologies of restoration of the metal structure and geometrical dimensions of blades. These technologies were developed with participation of enterprises and applied-research institutes based on extensive studies and testing. Repair technology, successfully applied for about one third of a century now, envisages elimination of metal structure defects, developing in service and of considerable damage (more than 25 % of blade airfoil area).

Data on technological capabilities of enterprises of the aircraft, power and shipbuilding industry for GTE blade repair are given in Table 2.

Highly efficient and advanced technologies of extension of the operating life due to reconditioning repair of heavy-duty parts and components of hot section of aircraft and navy GTE using brazing are described in detail in [7–13, 15–20, 22–24].

Using extensive scientific, research, experimental and industrial potential in the market of the aircraft and navy turbine and engine construction, the leading companies and enterprises such as Rolls Royce, Boeing, General Electric, Pratt&Whitney, Salyut, Zarya-Mashproekt, Rybinskie Motory, Ufa Mechanical Engineering Association, N.D. Kuznetsov SNTK, Aviadvigatel, Motor Sich, PMZ, A. Lulka-Saturn, A.G. Ivchenko DB Progress (Ivchenko-Progress) and others started successfully working under a military conversion program to develop GTE complexes for the power and oil and gas industries [25–28].

The gas pumping system of CIS countries is currently operating several hundred stationary gas-pumping units (GPU). The total number of blades in stationary GPU turbines just in OJSC «Gazprom» is higher than 205 ths pcs. Average annual requirement for blades, which have to be replaced during repair and maintenance, is up to approximately 30 ths pcs. The cost of blades in the general volume of annual supply of spare parts for GPU amounts to approximately one third. «Gazrpom» alone is currently operating more than 105 GKT-25I units of Nuovo Pignone, Italy. The operating time of 75 % of the gas-turbine compressors by the start of this century was equal to 70–80 ths h, this being essentially higher than the design operating life of 50 ths h [29].

During operation of gas turbine compressors (GTC) the protective coatings are partially or completely removed from the blade working surface as a result of the eroding action of the medium, this leading to acceleration of the corrosion processes in the blades

Table 2. Technological capabilities of aircraft industry enterprises

List of technologies	«Alstron Power Uniturbo», St.-Petersurg	«A.Lulka-Saturn», Moscow	«Salyut», Moscow	UMPO, Ufa	MPZ, Perm	«Pratt& Whitney-Paton», Kiev	SNTK, Samara	«Zarya-Mash-proekt», Nikolaev	«Motor Sich», Zaporo-zhie	«Silovye Mashiny», St.-Peter-sburg
Cleaning										
ultrasonic	+	+	+	+	+	+	+	+	+	+
sandblasting	+	+	+	+	+	+	+	+	+	+
Heat treatment										
HIP	+	–	–	–	–	–	–	–	–	–
in vacuum	+	+	+	+	+	+	+	+	+	+
in inert gas atmosphere	+	+	+	+	+	+	+	+	+	+
Welding, brazing										
AAW	+	+	+	+	+	+	+	+	+	+
microplasma	+	+	+	+	+	+	+	–	+	+
EBW	+	–	+	+	–	+	+	+	+	+
vacuum brazing	+	+	+	+	+	+	+	+	+	+
Coating deposition										
diffusion	+	+	+	+	+	+	+	+	+	+
electron beam evaporation and deposition in vacuum	+	–	–	–	–	+	+	+	–	–
plasma	+	+	+	+	+	+	+	+	+	+
electric spark	+	+	+	+	+	+	+	–	+	+
Strengthening										
thermoplastic	–	–	–	–	–	–	+	–	+	+
ultrasonic	–	–	–	–	–	+	+	+	+	–
hydrosandblasting	+	+	+	+	+	+	+	+	–	+

and vanes from zero to 3rd stage, variable incidence blade of the inlet guide vane and guide blades of the last stages (16th and 17th).

The main type of wear of the compressor blades is pitting corrosion, leading to «dimples» and «pits» on the blade surface and softening of the surface layer, this being hazardous in terms of fatigue strength in the near-weld area of the blade airfoil.

The above examples of the current situation with the GPU and GTC blades operated by «Gazprom», indicate that timely and correctly applied system of repair-reconditioning operations of the first and second level of complexity (see Table 1) may allow bringing back into operation a significant number of expensive turbine blades and obtaining an impressive cost effect due to reducing the scope of delivery of new blades. Blade cleaning after operation, performance of heat treatment, welding and brazing, deposition of protective coatings and blade strengthening allow extending the operating life of restored blades up to 70 % at the repair costs of up to 20–30 % of new blade cost.

Performed analysis [14] of production capabilities of repair enterprises of subsidiary gas transportation companies demonstrated that they currently have technologies, production capacities and equipment to perform work of the first level of complexity. In addition, these enterprises also perform grinding, polishing and milling of blade surface, have in-coming luminescence inspection and hardness measurement, as well as blade weighing.

Despite the fact that welding and brazing technology has been used for repair of GPU and GTC blades in the gas industry for more than 20 years, performance of repair of the second level of complexity runs into great difficulties even now. A substantial drawback in repair organization is «depersonalization» of blades in repair complexes with loss of information about the total operating hours and number of earlier performed repairs, as well as limited capabilities of repair enterprises as regards ensuring the appropriate level of restoration of the metal strength properties [30]. As a result of that accidents related to failure of repaired blades are quite frequent. Conducting comparatively simple repair of blades should be concentrated in subsidiary enterprises of the gas industry, while repair of the second level of complexity requires introducing more complex technologies and expensive equipment, which it is rational to concentrate in the basic specialized enterprises of «Gazprom» and «Transgaz» of Russia, Ukraine, Turkmenia and Uzbekistan.

Table 3 shows the technological capabilities of specialized enterprises of «Gazprom», taking into account the data of [14], as regards performance of the necessary repair-restoration work.

Introduction of advanced technologies of reconditioning repair of blades of gas-pumping turbines requires development and implementation of a number of technical and organizational measures in the gas industry of CIS countries [14], including:

- development of the conditions and criteria for taking decisions on the location of blade repair as regards admissible defects (dimensions), taking into account the total operating life of the blades and number of earlier repair operations;
- introduction of special certificates (cards) for blades for repaired and assorted sets indicating the total operating time, number and kinds of conducted repairs;
- setting up the repair fund of blades in specialized enterprises, ensuring the quality at acceptable cost of reconditioning repair;
- substantiation of technical and economic feasibility of reconditioning repair of turbine blades and development of specialized enterprises on reconditioning repair of blades, having the technology and equipment for complex repair, including also metal structure restoration.

Table 3. Technological capabilities of «Gazprom» specialized enterprises in terms of repair performance

Kind of repair operations	List of technological operations	«Turbo-remont», Bryansk	«Rotor», Kamyshin, Volgograd distr.	«Turbodetal», Naro-Fominsk, Moscow region	Shchekinsky Zavod PTO, Shchekino, Moskow distr.	«Samaragaz-energo-remont», Samara	«Gaz-energoservis», Boyarka, Kiev distr.
Restoration of metal structure	Heat treatment						
	HIP	+	–	–	–	–	–
	vacuum HT	+	+	+	+	–	–
	gas-shielded HT (argon)	+	+	+	+	+	–
	HT in atmosphere	+	+	+	+	+	+
	Surface strengthening						
	ultrasonic	+	–	–	–	–	–
	hydroshotblasting	+	+	+	+	+	+
Restoration of geometrical dimensions	AAW	+	+	+	+	+	+
	AAW in a chamber	+	–	–	–	–	–
	microplasma	+	–	–	–	+	+
	vacuum brazing	+	+	–	+	–	–

The gas industry is economically stable and successfully developing sector. Development of innovation projects on repair of parts, assemblies and structures of GTE is believed to be highly promising. Practical innovation activity shows that regional plants on repair of GTE, innovation centers, technology incubators, innovation-consulting centers and technology parks can become the most widely accepted kind of national and regional innovation-technology centers in the gas industry. Centers for innovation transfer should facilitate technology purchase, perform technology auditing, render assistance in establishing technology partnerships, provide consultations on enterprise management and funding [31]. Innovation transfer means dissemination of systematized knowledge for releasing and application of high technologies in repair production.

CONCLUSIONS

1. Aircraft, navy and power turbine, and engine construction enterprises are fitted with the required equipment and technologies of reconditioning the components of GTE hot section.

2. Lack of enterprises, producing equipment and brazing filler metals limits the wide-scale introduction of highly effective brazing technology for reconditioning repair of blades after their operation.

3. The gas industry of CIS countries should have a wide network of repair subsidiary enterprises, capable of performing blade repair of the first degree of complexity. More complex blade repair, involving the use of welding, brazing, heat treatment and strengthening should be performed in the regional specialized enterprises of the gas industry, fitted with the necessary equipment, technologies and highly qualified personnel.

4. The conversion program of application of aircraft GTE in power generation and gas industry should provide a marked improvement of the quality, technological discipline and responsibility of the performers for the performed repair-reconditioning operations.

5. Innovation activity in repair production of the gas industry will enable fitting the regional and subsidiary enterprises with the required high technologies and equipment and acheiving a higher cost effect from introduction into industry.

1. (2002) *Machine-building*. Encyclopedia. Vol. IV.6: Welding equipment. Ed. by B.E. Paton. Moscow: Mashinostroenie.
2. (2006) Vol. III-4: Technology of welding, brazing and cutting. *Ibid*.
3. (2005) *Brazing: experience, art, science*: Proc. of Sci.-Techn. Conf. for the Period of 1967–2002. Moscow: Alfa Dominanta.
4. (2000) *Space: technologies, materials science, structures.* Transact. Ed. by B.E. Paton. Kiev: PWI.
5. Kvasnitsky, V.F. (1986) *Welding and brazing of heat-resistant alloys in shipbuilding*. Leningrad: Sudostroenie.
6. Khorunov, V.F. (1998) Brazing: achievements and prospects. *Avtomatich. Svarka*, **11**, 51–53.
7. Khorunov, V.F., Maksimova, S.V., Ivanchenko, V.G. (2004) Development of filler metal for brazing of heat-resistant Ni- and Ti-base alloys. *Ibid.*, **9**, 27–32.
8. Khorunov, V.F., Kudashev, A.V. (1991) Pressure brazing of high-temperature and heat-resistant alloys. In: *Transact. on Materials and Technologies of Brazing*. Kiev: PWI.
9. Zhadkevich, A.M. (2005) Brazing of defects of aircraft and ship turbine blades — challenging technology of extension of their life (Retrospective analysis of status and prospects of development). *Advances in Electrometallurgy*, **1**, 33–39.
10. Zhadkevich, A.M. (2006) For the 45th anniversary of Brazing Committee of welding section of TsP NTO Mashprom. *Avtomatich. Svarka*, **2**, 65–67.
11. Zhadkevich, M.L. (1989) Pilot plant of special electrometallurgy as the base of MNTK «E.O. Paton Electric Welding Institute» for the acceleration of industrial implementation of up-to-date technologies of special metallurgy. In: *Special electrometallurgy*. Issue 67.
12. Paton, B.E., Stroganov, G.B., Kishkin, S.T. et al. (1987) *Heat resistance of cast nickel alloys and their protection from oxidation.* Kiev: Naukova Dumka.
13. Nikitin, V.I., Komisarova, I.P., Movchan, B.A. et al. (1981) High-temperature corrosion and application of coatings for protection of gas-turbine unit blading. *Energomashinostroenie*, **9**, 44–52.
14. Zhdanov, S., Khoroshikh, A., Grabovsky, B. et al. (2001) Management and cost effectiveness of repair of turbine blades of stationary gas-pumping units. *Gazoturb. Tekhnologii*, June / Aug., 24–26.
15. Klyuchnikov, I.P., Gejkin, V.A. (2001) Repair of high-loaded parts and sub-assemblies of hot conveying system of gas-turbine engines by the brazing method. In: *Brazing. Current technologies, materials, structures.* Coll. 2. Moscow: TsRDZ.
16. Nerovny, V.M., Yampolsky, V.M., Rogov, R.M. (1989) Repair of gas-turbine blades by vacuum arc brazing. *Energomashinostroenie*, **2**, 22–24.
17. Kornienko, A.N., Zhadkevich, A.M. (2005) State-of-the-art and problems of brazing in repair of gas-turbine engine blades. *Zagotovit. Proizvodstvo v Mashinostroenii*, **9**, 9–12.
18. Klyuchnikov, I.P. (1997) Repair of parts and sub-assemblies of gas-turbine engines by brazing method with local heating. In: *Brazing and producing of current engineering items*. Moscow: TsRDZ.
19. Yampolsky, V.M., Nerovny, V.M. (1981) Strengthening and recovery of gas-turbine engine blades by brazing. In: *Transact. of N.E. Bauman MHTU*. Issue 383.
20. Khorunov, V.F., Maksimova, S.V., Samokhin, S.M. (2000) Brazing of current and prospective heat-resistant materials for gas-turbine manufacture. In: *Proc. of 4th Session of Sci. Council on New Materials of MAAN on Problems of Current Materials Science*. Kiev-Gomel: IMMS AN Belarus.
21. Yushchenko, K.A., Savchenko, V.S., Chervyakov, N.O. et al. (2004) Character of formation of hot cracks in welding cast heat-resistant nickel alloys. *The Paton Welding J.*, **8**, 34–38.
22. Kvasnitsky, V.F. (1985) Welding and brazing of heat-resistant alloys in shipbuilding. *Avtomatich. Svarka*, **6**, 26–30.
23. Zhadkevich, A.M. (2005) Advanced methods of brazing technology for repair of gas-turbine engines. *Problemy Metallurgii, Svarki i Materialoved.*, **4**, 9–17.
24. Orlov, A.V., Bereznikov, Yu.P., Samsonova, T.S. (1984) Repair of gas turbines by arc brazing method. *Energomashinostroenie*, **2**, 33–34.
25. Zinchenko, G., Morgunov, E. (2003) Talent multiplied by boldness, labor and persistence. *Gazoturb. Tekhnologii*, **2**, 30–32.
26. Glina, O., Tyuryakova-Matveeva, D. (2003) Pratt & Whitney — always in the right place. *Ibid.*, 38–40.
27. Muravchenko, A. (2004) Upgrading of gas-turbine engines «Ivchenko-Progress» for power units. *Ibid.*, **2**, 52–54.
28. Boguslaev, V. (2003) Gas-turbine units OJSC «Motor-Sich» for power engineering and oil-and-gas complex. *Ibid.*, **6**, 46–47.
29. (1999) Present and future of Russian turbine manufacture: Review of OJSC «A. Lyulka-Saturn». *Ibid.*, **1**, 34.
30. Ivanov, Yu., Kuzmenko, M., Mikhajlov, A. (2003) Heat treatment of heat-resistant nickel alloys. *Ibid.*, **1**, 51–53.
31. Bernadsky, V.N. (2006) Peculiarities of innovative process in development and transfer of high technologies. *Obzor-Inform. IES*, **1**, 19.

THERMAL SPRAY SCREEN COATINGS FOR PERSONAL COMPUTERS

A.P. MURASHOV[1], **I.A. DEMIANOV**[1], **A.I. DEMIANOV**[1], **A.P. PROVOZIN**[2] and **G.T. SOLDATENKO**[2]
[1]E.O. Paton Electric Welding Institute, NASU, Kiev, Ukraine
[2]CTZI «Barier», Company NII EMP, Kiev, Ukraine

A method was developed for deposition of screen coatings on office equipment elements (personal computer) by spay applying combined coatings produced by thermal spraying and subsequent impregnation. Thermal spray screen coatings ensure an essential lowering of the level of electromagnetic radiation.

Keywords: screen coating, thermal spraying, electromagnetic radiation, electric field intensity, information protection, biological protection

Personal computers (PCs), as well as other office equipment, containing processing, transmitting, receiving technical devices are characterized by electromagnetic radiation and inducing effects generated by working PC elements. There exists a possibility to intercept and decode speech, digital, TV and other information processed by PCs, communication channels and other hardware elements from the distance from several to hundreds of meters, by modern highly sensitive equipment [1]. Another important disadvantage of most presently used data processing equipment is its vulnerability to outer directional powerful electromagnetic radiation (pulses), which may distort or destroy information or even put out of order said devices. In this connection, there is a necessity to resort to various measures to protect office equipment from unauthorized read-out of information or undesirable outer effects.

There is some office equipment, including that made abroad, not meeting the requirements of information protection. In the case of imported hardware elements, the problem may be aggravated by presence of built-in devices: radio-microphones, other elements enabling unauthorized read-out of information. Besides, electromagnetic radiation generated by working office equipment adversely affects the health of operating personnel.

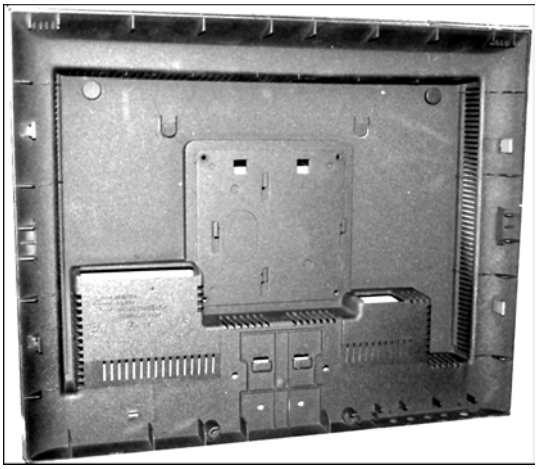

Figure 1. Appearance of rear panel of 17" monitor with protective coating

To protect PCs, exclude outer effects, special separated protected rooms are used, or office equipment is installed in protective metal cases.

Taking into consideration that in recent decades office equipment is widely used, and cases of PCs and of many communication means are made mainly from polymer materials, a reliable technical method of their protection is proposed, which is application of screening in the form of local or overall inner metal coating, without modification of outer appearance of the equipment.

The E.O. Paton Electric Welding Institute developed the technology for thermal spraying of coatings screening high- and low-frequency radiation of working units and elements of PCs. Such a solution enables protecting not only newly produced but also already operating PCs, irrespective of their geometry, dimensions and inner configuration. In so doing, also the issue of protection of users from electromagnetic radiation of their PC is automatically solved.

The difficulty in solving this problem lies in the necessity to deposit coatings onto plastic materials 0.5–2.0 mm thick having surfaces of different curvature, semi-open, with elements making the deposition process difficult. To solve this problem techniques have been developed and parameters chosen to prepare surfaces and obtain spray-on coatings with sufficient adhesion to plastic without evident deformation of the latter.

Technology of coating deposition includes jet-abrasive preparation of the surface, application of sublayer and subsequent deposition of the main functional two-layer coating 100–200 μm thick from materials on the basis of copper and iron, followed by application of impregnating layer.

Preparation of the surface was made using normal electro-corundum powder with particle size < 0.6 mm, with compressed air pressure not exceeding 0.3 MPa. Underlayer of zinc up to 50 μm thick was first deposited onto thus prepared surface by electric arc metallization, and then the main layer was sprayed-on. The

Values of electromagnetic field intensity generated by PC elements during operation

PC element	Frequency, mHz	Intensity, dB	
		Before coating deposition	After coating deposition
Monitor	12.6	11	7
	114	10	6.5
	164	8.5	3.5
Body of hard memory disk	1.50	47	4.5
	2.16	55	5.3
	3.12	51	5.4
Processing unit on floppy disks	4.52	47	4
	5.32	47	0.5
	270	22	5.5
Keyboard	0.01	1	–
	0.02	1.2	–
	0.05	5	3
	0.1	10	6
	0.2	15	10
	0.5	21	16
	1	26	24
	5	43	41
	8	50	–
	10	50	–

Note. Screening efficiency was evaluated as difference of electromagnetic field intensity before and after coating deposition. For the keyboard, results of measurement of electromagnetic field intensity are: in line «before coating deposition» electromagnetic field intensity was determined at the edges of measured specimen (keyboard bottom), in line «after coating deposition» — at the specimen center. Since the specimens had complex-shape surface, evaluation of screening efficiency was impossible.

said spraying method was chosen because of its very low thermal effect on the work and high strength characteristics of the coatings. Maximum spraying current did not exceed 100 A, while spraying distance was not less than 300 mm. Strength of adhesion of the coating with the substrate determined by the method used for measuring adhesive strength, was on the average 5 MPa. After impregnation adhesion value of the coating with plastic surface increased to 7 MPa. Silicon lacquer with addition of powdered Amotec-1 alloy developed by the E.O. Paton Electric Welding Institute, was used as impregnation agent. Such an operation, along with increasing adhesion strength with the substrate, lower the risk of separation of coating particles in the process of computer operation, and their getting into the area of operation of PC elements. Under this technology, protective coatings on the inner surfaces of the following PC elements were obtained: front panel of the processor, monitor, keyboard, mouse, printer, speakers, and body of plugged-in hard memory disk. Figures 1 and 2 show

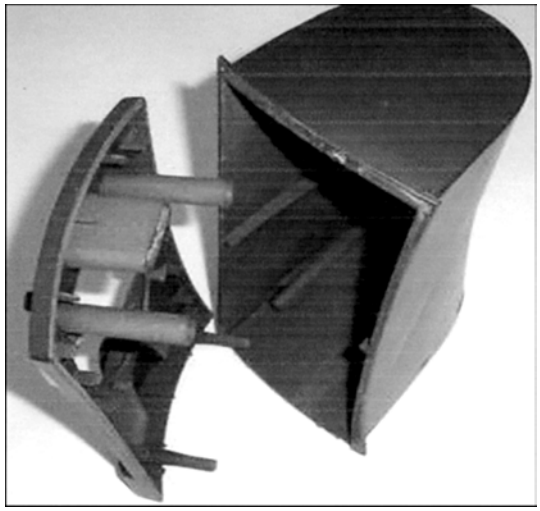

Figure 2. Elements of column speaker with internal screen coating

rear monitor panel and column speaker with protective coating.

Tests of screening efficiency of those elements were conducted using a special procedure «Method of Checking Screening Efficiency of Computer Equipment» under conditions of testing of respective PC elements, with selective nanovoltmeter and microvoltmeter SMV-11 and SMV-8.5, electrical circular antenna AE-1, magnetic antenna AM-2, and active antenna AIZ-3 [2]. Intensity of electric and magnetic fields radiated by PC elements: monitor, processing unit on floppy disks, signal keyboard within frequency range from 0 to 1000 MHz, was determined.

Measurements were made twice: on PC before and after application of coating onto the PC elements, screening and filtration of connecting cables. Results of the measurements are given in the Table.

Field tests of PCs with protective coatings have shown that application of the above information protection technique greatly reduces the chances of its unauthorized reading-out, due to considerable electromagnetic fields strength reduction. In so doing, such an effect was obtained without modification of PC outer appearance, promptness of access to it and its elements did not worsen, and operational control of PC functions did not become more complicated.

Thermal spraying of barrier coatings for screening of electromagnetic fields can be successfully applied for most of office equipment, mobile communication means, etc. The technology offered is one of the versatile means of protection of office equipment producing high- and low-frequency radiation.

1. Provozin, A.A., Gavrilchenko, V.V. (1998) Some aspects of protection of radioelectronic office equipment from outer electromagnetic influences. *Bizness i Bezopasnost*, **4**, 25–26.
2. Apollonsky, S.M. (1988) *Reference book on electromagnetic screen calculation*. Leningrad: Energoatomizdat.

NEWS

Technology for repair and restoration of mould plates of copper and copper alloys by friction stir surfacing

Friction stir welding (FSW) developed by TWI in 1991 is a solid-state joining method involving friction. It is applied in many industries for joining copper alloys, e.g. to manufacture copper containers for nuclear waste storage or copper strips (variety of heat sinks).

The E.O. Paton Electric Welding Institute developed, on the basis of FSW, the technology for friction stir surfacing (FSS) to repair plates of moulds for continuous casting of steel.

Workpiece to be surfaced and filler material in the form of a plate are fixed by hold-down mechanisms. The rotating tool is brought into contact with the filler plate up to the stop. Friction of the tool generates heat required to plasticize the filler material and part of the workpiece metal. Displacement of the tool results in formation of the overlap weld. Successive deposition of such welds with an overlap allows the workpiece to be fully restored.

The main FSS process parameters include:

- tool rotation and displacement speed;
- hold-down force;
- tool size.

Hardness of the stir zone metal is 10 % higher than that of the base metal. Distortions induced by welding stresses are absent.

FSS of copper and copper alloys provides welds of a high quality, free from defects and heterogeneities within the stir zone. The method developed for FSS of copper allows deposition of oxygen-free copper by eliminating oxidation and maintaining its initial thermal conductivity.

In addition, this method can be used for hardening of new mould surfaces and those being restored by depositing wear-resistant bronze of the BRKh and BRKhTs types.

FSS is performed using specially adapted metalworking machines equipped with a head, the spindle of which is rotated with an adjustable speed, powered from the 30 kW motor.

The welding tool is made from a heat-resistant material, the size and configuration of which depend upon the deposited layer thickness.

Plasma-arc spraying of wear-resistant coatings on shaft-type parts

Repair of shafts of ash pumps, rotors of electric motors, crankshafts and wheelset axle journals is usually performed in the CIS countries by the method of electric arc wire metallising.

The method is based on air spraying of metal of two steel wires molten by the electric arc. Wide acceptance of the method is limited by an insufficient density of the sprayed layer and its oxidation.

The E.O. Paton Electric Welding Institute developed a new technology and equipment for plasma metallising deposition of wear-resistant and other coatings on steel and cast iron shafts and parts of the shaft type.

The technology for spraying of wear-resistant coatings is based on plasma arc spraying of a current-conducting wire set as anode, which serves as a source material for formation of a coating layer and, at the same time, for activation of the sprayed layer using a special device.

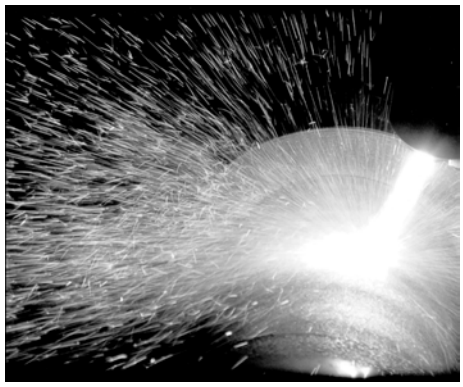

Specifications

Power of plasmatron, kW, not more than	24
Deposition efficiency, kg / h	4–8
Spray wire diameter, mm	1.2–1.8
Working current of plasmatron, A	160–300
Working voltage of arc, V	60–80
Plasma gas (argon) flow rate, m^3 / h	1.0–1.5
Flow rate of compressed air for plasmatron cooling, m^3 / h	16–20
Pressure of compressed air, Pa	5–7

The technology for repair of axle and shaft journals provides the following benefits:

- the spraying process does not decrease strength properties of workpieces (workpieces are heated to no more than 200 °C);
- the process causes no distortion of workpieces being repaired;
- coating to workpiece adhesion strength is above 50 N / mm^2;
- it is possible to deposit coatings up to 15–20 mm thick with a porosity of no more than 2–5 %;
- the spraying process is characterised by high stability (life of the plasma arc shaping nozzle is not less than 100 h of the machine time);
- plasmatron is cooled with air.

The set of plasma equipment includes the plasma metallising head with an activation device, control panel, control cabinet with a gas preparation unit, power supply, wet cleaning chamber with a ventilation device, rotation mechanism, plasma device movement unit, and noise-proof chamber.

Subject to repair are parts that failed due to wear (geometry changes or other defects causing no decrease in strength properties or reliability).

Experience of application of the technology for spraying of corrosion-resistant metallised coatings of Al, Zn and their alloys on large-size structures

The E.O. Paton Electric Welding Institute developed mobile equipment for deposition of corrosion-resistant coatings. The equipment has been applied for a couple of years to perform the work on corrosion protection of a number of major industrial facilities, such as:

- load-carrying longitudinal beams of the Vozdukhoflotsky Overpass in Kiev (600 m^2 of Zn–Al coating);
- orthotropic plate of the Yuzhny Bridge across the Dnieper River in Kiev (10,000 m^2 of Zn–Al coating);
- aviation fuel storage tanks;
- metal structures of hydraulic engineering equipment for Hydroelectric Power Plant in Al-Vahda, Morocco (24,000 m^2 of Zn–Al coating);
- smoke stacks of local heat power plants at the Chekhovsky Works «Gidrostal» (40,000 m^2 of Zn coating); etc.

Ni–Cr–Mo coatings were deposited on a number of facilities, where service conditions lead to development of high-temperature and chemical corrosion, the most obvious examples being a smoke stack 320 m high with a 4.4 m diameter at the Uglegorskaya Gas Distribution Power Plant, and boiler furnace of the Heat Power Plant at the Izmail Paperboard Factory.

As a rule, anticorrosive coatings are deposited on large-size structures under field conditions, which may involve electrical safety problems and difficulties related to delivery of a spray material and power to the spraying site. In this respect, a wide experience has been accumulated in application of different methods and types of equipment for thermal spraying (flame, electric arc, plasma), based on the service conditions and customer's requirements.

The exclusive flame spraying machine UGPN-005 proved to be most reliable and efficient. It allows deposition of sound coatings in compliance with GOST 9.304–87 «Thermal Spray Coatings. General Requirements and Testing Methods», and GOST 28302–89 «Thermal Spray Zink and Aluminium Coatings for Metal Structures. General Requirements to Standard Technological Process».

The source of thermal energy in thermal spraying is flame formed as a result of combustion of the oxygen + fuel gas mixture. Movement of spray particles in the flame body is accompanied by their continuous heating. Having passed through the flame body, the particles in the molten (softened) state get to the substrate surface, where they are mechanically bonded to the surface irregularities.

Coating to substrate adhesion strength is 25–30 N / mm^2.

Specifications of the machine

Size of powder material particles, μm	0.04–0.20
Fuel gas (propane-butane) flow rate, l / min	20–30
Oxygen flow rate, l / min	30–60
Powder consumption, kg / h	2–15
Compressed air flow rate, l / min	20–50
Weight of the machine, kg	30

Electron beam remelting of high-speed steel

Research and Production Company GEKONT developed the commercial technology for electron beam remelting of high-speed steel, where the tool production wastes and used tools are employed as a source charge. The technological process is performed by the electron beam cold hearth remelting (EBCHR) method.

The use of EBCHR eliminates the need to manufacture consumable electrodes. Refining of high-speed steel in vacuum during remelting, high homogeneity of chemical and phase compositions across the entire section of ingots, and high degree of dispersion of structure allow the operations of thermomechanical treatment (forging) to be excluded from the technological cycle of tool production, and the resulting ingots to be utilised immediately after annealing to manufacture tools from them.

Appearance of 140 × 160 mm slab and 70 mm diameter cylindrical ingot of EBCHR high-speed steel R6M5

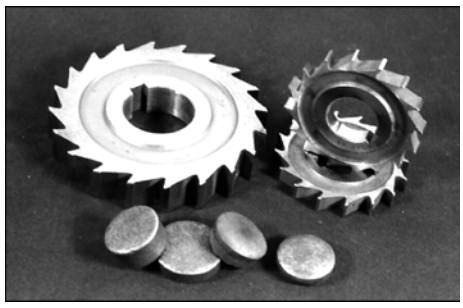

Cutting tools of EBCHR high-speed steel R6M5

Sizes of EBCHR high-speed steel ingots:

cylindrical:

- diameter 60–150 mm
- length up to 1900 mm

slabs:

- cross section 14 × 160 mm
- length up to 1900 mm

THESIS FOR A SCIENTIFIC DEGREE

E.O. Paton Electric Welding Institute of the NAS of Ukraine

S.M. Teslevich (Zaporozhie Titanium-Magnesium Industrial Complex) defended Candidate's thesis on March 15, 2006 on the subject «New Technologies and Equipment for Obtaining Spongy Titanium and its Remelting into an Ingot».

Solving the problem of spongy titanium quality improvement and its remelting is considered in the thesis, as well as creation of fundamentally new installation for obtaining spongy titanium with cycle output of 3.8 t in comparison with 0.87 t / cycle, which is functioning in industrial production in Ukraine.

The procedure was developed for many times speed increase for the reaction of titanium reduction from its tetrachloride by magnesium on periodically renovated surface of titanium-containing melt.

Temperature parameters were determined for smooth transportation of titanium reduction reaction products by steam line from reduction vessel to condenser vessel.

A complex of heat engineering and technological engineering studies led to development of new technologies of titanium reduction from titanium tetrachloride by magnesium and of vacuum separation of reaction mass formed in the process of reduction with obtaining of spongy titanium of high grade in the new installation.

Detailed studies were carried out to obtain high quality spongy titanium in laboratory and pilot plants. Conditions for controlled removal of residual chlorine at vacuum separation of spongy titanium were determined. Experimental check-up of impurity elements distribution by block volume of spongy titanium of up to 3.8 t mass was carried out. It was shown that the content of hydrogen in gas phase over melt and in the produced ingot can be controlled by changing melting parameters, inert gas flow rate, ingot drawing speed, chlorine content in spongy titanium and so on.

New technology of ingot melting from spongy titanium with higher (0.08–0.45 wt.%) chlorine content was developed for the first time. It includes the first remelting of spongy titanium in induction furnace with sectional crystallizer, as a result of this remelting redundant chlorine is removed, and the second remelting can be performed in vacuum-arc, electron-beam and plasma-arc furnaces to reduce hydrogen content in accordance with GOST 19807–91 requirements.

Spongy titanium of a new quality, obtained in high-capacity installations for reduction and separation, was remelted in vacuum-arc furnace VD-11. Ingots with the mass of 5 t and diameter of 780 mm were produced; they correspond to all required parameters of existing standards for alloys of VT1-0 grade.

In parallel with industrial development of ingots from new quality spongy titanium the experiments were carried out on manufacturing of shaped titanium ingots with applying of combined consumable electrode, that consists from two extruded and one cast blank in re-constructed cast skull furnaces with a crucible of a new design without water-cooling.

THESIS FOR A SCIENTIFIC DEGREE

V.V. Golovko (PWI) defended his thesis for Doctor's degree on March 29, 2006 on the subject «Interaction of Metal with Slag in Welding of Low-Alloyed Steels under Agglomerated Fluxes».

The thesis is dedicated to studies of thermodynamic and kinetic dependences of metal interaction with slag under agglomerated fluxes in welding of low-alloyed steels, construction on their basis of models that allow forecasting the structure and properties of weld metal.

The influence of oxygen potential variation of agglomerated fluxes on non-metallic inclusions formation was studied in a wide range. Based on the study results, integrated physical-chemical model of non-metallic inclusions formation in weld metal was created. The model describes the processes of growth and condensation of non-metallic phase in weld pool in the area of solid-liquid state of weld metal. Computer program was developed, calculations of content and quantity of non-metallic inclusions with the regard for thermodynamics and kinetics of metallurgical reactions running in the slag and metal phases were conducted, as well as changes of technological parameters of welding process.

Range of values of flux oxygen potential was determined, which lead to formation of non-metallic inclusions in the weld metal that are favorable for formation of certain structural components of weld metal.

It is shown that application of agglomerated fluxes allows performing directed alloying of the solid solution of weld metal, controlling its structure and properties.

Combinations of fluxes and wires were suggested that provide dosed alloying of the solid solution by titanium, aluminum and obtaining mechanical properties of weld metal on the level of base metal.

The evaluation of the main factors was done that determines the content of hydrogen in weld metal at welding under agglomerated fluxes. To obtain ultra low hydrogen content in low-alloyed steel weld metal (less than 3 cm^3 per 100 g) the methods of partial oxygen and hydrogen pressure regulation over molten slag and technology of manufacturing low hydrogen agglomerated fluxes were suggested.

Computer programs were created to forecast the content of agglomerated fluxes and mechanical properties of weld metal. The conducted theoretical and experimental studies of interaction processes between metal and slag served as scientific base for developing agglomerated fluxes ANK-57 and ANK-561 for welding constructions from low-alloyed steels. Flux contents are original and patented (Patents of Ukraine Nos. 5156, 5157).

The results of the work have found industrial application and were approved by Russian Sea Register, Det Norske Veritas and Lloyd's Register for manufacturing constructions of general shipbuilding.

THESIS FOR A SCIENTIFIC DEGREE

A.M. Zhernosekov (PWI) defended the Candidate's thesis on April 12, 2006 on the subject «System of Automatic Stabilization of Consumable Electrode Pulsed-Arc Welding Process».

The thesis is dedicated to creation and study of systems of automatic stabilization (SAS) of the process of consumable electrode pulsed-arc welding of materials with different thermo-physical properties under the conditions of disturbance action.

The quality of weld metal in consumable electrode pulsed-arc welding substantially depends on average values of arc voltage and welding current that are chosen as regulated values in designing systems for automatic stabilization of process parameters.

For welding materials with different thermo-physical properties, for example, carbon, low-alloyed steels or aluminum-manganese alloys under the conditions of disturbance action, promising is the application of suggested and implemented for the first time two-channel SAS of this process with application of feedback: for steels ---- stabilization channel of average voltage in the arc by means of action on the frequency of pulse sequence of arc power source and channel of stabilization of average value of welding current with action on the electrode wire feed speed; for aluminum-magnesium alloys ---- with application of stabilization channel of average value of welding current with action on the frequency of pulse sequence of power source, as well stabilization channel of average values of arc voltage with action on the welding wire feed rate.

The developed mathematical model of the system «arc power source ---- arc with consumable electrode ---- automatic stabilization system» taking into account nonlinearity of thermo-physical values adequately describes the electric and power parameters of welding process and allows determination of transfer functions of system elements and performing analysis of SAS stability. The suggested model permits designing blocks simulating the electric arc with consumable electrode in the mathematical package of computer programs.

The efficiency of two-channel SAS in consumable electrode pulsed-arc welding of steels St3sp, steel 25, 14G2, 09G2C or aluminum-magnesium alloys AMg6, AMg6M under the conditions of disturbance action by electrode wire extension, mains voltage, complex action of disturbing factors was experimentally determined. When welding carbon, low-alloyed steels SAS compensate arc voltage, caused by decrease of mains voltage, eliminate possible short circuits and, as the result, decrease metal spatter. Increase of extension is accompanied by appearance of hardening structural components on steels, and of porosity and macrostructural inhomogeneities on aluminum-magnesium alloys in the form of a central crystallite that impairs quality of welded joints. SAS application permits to obtain mechanical properties of the metal of welds made under disturbances action, on the level of properties without disturbance, also at consumable electrode pulsed-arc welding of critical constructions.

The systems of automatic stabilization as separate blocks and boards are perspective to be used with serial pulse sources for powering the arc and welding wire feed mechanisms, this expanding the functional capabilities of equipment for this welding process.

THESIS FOR A SCIENTIFIC DEGREE

V.A. Berezos (PWI) defended Candidate's thesis on April 12, 2006 on the subject «Development of Equipment and Technology to Obtain Hollow Ingots of Large Diameter from Titanium Alloys by Electron Beam Melting Method».

The thesis is dedicated to development of equipment and technology, as well as technological processes of manufacturing a new class of semi-finished products from titanium alloys ---- hollow ingots of a large diameter that in future can be used to obtain large-sized pipes. The requirement for such corrosion-resistant pipes has become more urgent during the last ten years in view of development of costal oil and gas production.

Mathematic model of heat transfer in ingots produced by electron beam melting with intermediate crucible (EBMIC) was optimized for the case of central mandrel availability. The dependence of the depth of liquid pool and two-phase zone on the melting process efficiency was determined. It was established that for hollow ingot of titanium alloy Ti–6A1–4V of ∅600 / 200 mm a critical melting efficiency of 150 kg / h is found, above which a deep (more than 20 mm) liquid metal pool forms. In accordance with the performed calculations optimal conditions were determined for crystallization of a hollow ingot of titanium alloy Ti–6Al–4V of ∅600 / 200 mm (power of uniform electron beam heating of free ingot surface is 120 kW, melting efficiency being 150 kg / h) that guarantee producing a homogeneous equiaxed structure in ingots.

Mathematical model of hydrogen removal process in EBMIC for hollow ingots was improved, taking into consideration the reduction of evaporation surface in the crystallizer. The dependence of refining efficiency on melting productivity was determined. It is established that in the broad range of melting productivity (from 50 to 250 kg / h), hydrogen and aluminum content in hollow ingots meets the standard requirements for titanium grade alloys.

The results of studying the technological features of producing hollow ingots allowed developing optimal technological conditions for manufacturing a large diameter (600 mm) hollow ingot from titanium alloys by EBMIC method. A large-sized hollow ingot with the mass of more than 2000 kg from titanium alloy VT6 (Ti–6A1–4V) was manufactured by the developed technology for the first time in the world with application of the process of EBMIC. The technology of obtaining hollow titanium ingots by EBMIC and application of electron beam melting of its surface allows considerably lowering the metal consumption and reducing the number of technological operations. For realization of the method of obtaining titanium pipes on the industrial scale, electron beam installation UE5810 was designed for melting titanium ingots with maximum diameter of 1200 mm and length of 6000 mm.

With the aim of further reduction of the number of technological operations and increase of the yield, a perspective new method of producing hollow ingots in electron beam installations with an intermediate crucible was suggested, that permits completely excluding the mandrel from the technological process of melting.

PATENTS IN THE FIELD OF WELDING PRODUCTION*

Universal mobile welding converter, characterized by that it is fitted with the module of welding current regulation in the form of two regulators with a common controller and switch for selection of welding current adjustment method, one of them being a current regulator by frequency, and another — current regulator by generator disturbance. The current regulator by frequency is further fitted with the block for setting and maintaining the welding current by acting on the regulator of the engine rotation frequency using an electric drive actuator. Patent for Usable Model 9944. P.S. Pikmanov, V.T. Pratasenya, A.V. Dabransky [10].

Device for recirculation of the automatic welding machine flux, characterized by that the flux feeding unit in its upper part is connected to the compressed air feed system and fitted with sleeve type dust catcher, detachably connected on the tube for air release from the flux feeding unit into the atmosphere, the flux suction tube being fastened in the upper part of the flux feeding unit and is made in the form of a flexible sleeve fitted with a bailer. Other features are also given. Patent for Usable Model 9727. K.G. Sherdits, D.A. Belyansky (OJSC «Glavny Spetsializirovanny KTI») [10].

Line for manufacturing compact materials in a metal sheath, characterized by that the forming rollers are made with the capability of axial and radial displacement and are connected using twin hinged couplings with electrically differential drives, which together with the winder assembly are connected to the frequency converter with program controller. Patent for Usable Model 9985. B.V. Gulenkov, V.V. Ivashina, V.V. Klimanchuk et al. (OJSC «Illyich Mariupol Metal Works») [10].

Machine for magnetically-impelled arc butt welding of pipes, characterized by that the upper arms of the two-arm loads of the compression mechanism are connected by crank-knee transmission with a nut connected to a screw fastened on the case of both the mobile and the stationary blocks. Patent 74192. S.I. Kuchuk-Yatsenko, V.G. Krivenko, V.S. Kachinsky et al. (IC for Pressure Welding of STC «The E.O. Paton Electric Welding Institute» of NASU) [11].

Nozzle for gas-oxygen cutter, characterized by that each nozzle of the internal contour has an additional channel connected to the circular groove for feeding the heating oxygen, the diameter of the channel connecting the inner contour nozzle to the circular groove for feeding the preheating gas, being greater than the diameter of the channel connecting this inner contour nozzle to the circular groove for feeding the preheating oxygen. Patent for Usable Model 10816. V.I. Skripchenko (OJSC «Glavny Spetsializirovanny KTI») [11].

Current-conducting tip for surfacing, characterized by that the casing wall encloses the external end face of the insert in the case around the circumference, the diameter of which is equal to 1.5 to 1.7 diameters of the through-thickness hole. Patent for Usable Model 10823. D.A. Zarechensky, E.T. Khorovets (Idem) [11].

Universal mobile welding converter, characterized by that the control block is fitted with a regulator-stabilizer, which consists of functionally electrically connected to each other voltage inverter, isolating transformer, rectifier, filter, assembly for comparing the voltage stabilizer and galvanic decoupling assembly, assembly for comparison of the circuit of current protection from overload and short-circuiting in the 110 / 220 V voltage circuit with the setter of the level of current protection of the generator and setter of the output voltage level, and electrically connected to the generator and storage battery. Patent for Usable Model 10527. P.S. Pikmakov, V.T. Pratasenya, A.A. Dabransky [11].

Method of fabrication of large-sized parts by pressure welding, characterized by that a layer of dispersed chemical substances is applied on the joining surface before assembly for welding, the layer is dried, which is followed by assembly for welding. Patent for Usable Model 10432. V.M. Semyonov, A.V. Zhartovsky, V.S. Krivun (Donbass Mechanical Engineering Academy) [11].

Method of manufacturing the flux-cored electrode, characterized by that a mixture is prepared from thermally-expanding vermicular graphite and layered joint of the thermal expansion with a low destruction temperature and low coefficient, this mixture is used to manufacture (stamp) a trough of the thickness of 1 / 8–1 / 6 of the metal trough diameter, which trough is placed into the metal trough, and then the trough is filled with the prepared powderlike mixture. Patent for Usable Model 10233. P.A. Gavrish, I.V. Serov, V.V. Chigarev (Idem) [11].

Method of manufacturing coated electrodes, characterized by that before electrode immersion into a tank with a galogenized multicomponent composition, an exothermal mixture in the amount of 35–50 wt.% of the weight of the homogenized mixture is added to it. Patent for Usable Model 10520. S.V. Bondarev, V.D. Kassov, S.V. Zharikov (Idem) [11].

Flux-cored wire composition, characterized by that the steel sheath composition has the following proportion of the components, wt.%: 0.02–0.08 of carbon, 0.06–040 of silicon, 0.50–1.80 of manganese; the balance being iron, the composition of the powder-like flux core is complemented by aluminium fluoride, calcium carbonate, and alumina-magnesium alloy with the following proportion of components, wt.% of the wire weight: 0.20–1.00 of titanium; 0.02–0.12 of boron; 3.00–6.00 of calcium fluoride; 1.00–3.00 of sodium fluoride; 0.50–1.50 of manganese; 0.30–0.50 of chromium; 0.20–0.50 of molybdenum; 1.00–3.00 of aluminium fluoride; 1.00–3.00 of calcium carbonate; 0.10–0.30 of alumina-magnesium alloy, and the ratio of titanium weight to boron weight is set in the range from 5 to 14. Patent 74469. A.M. Alimov, A.A. Rybakov, S.Yu. Bat et al. (OJSC «Arksel») [12].

Exothermal cutting tool, consisting of a case, which accommodates the technological exothermal mixture and igniting fuse, characterized by that a recess in the form of a paraboloid of revolution is made in the exothermal mixture, which accommodates the fuse and cutting element, fitted with an electrically driven combustible rod, located in the case along the longitudinal axis, a cutting element fitted with an electric power source. Patent for Usable Model 11021. E.A. Lyapin, G.L. Vajsberg, Yu.E. Lenkevich, D.V. Rimchuk (Subsidiary of the enterprise «Paramilitary emergency-rescue (gas rescue) unit LIKVO of oil and gas industry) [12].

Flux-cored wire for underwater welding of low-carbon and low-alloyed steels at greater depths, characterized by that the charge additionally contains cesium salt with the following proportion of the components, wt.%: 25–35 of rutile concentrate; 15–25 of hematite; 5–15 of ferromanganese; 5–15 of cesium salt; 0.7–1.3 of potassium bichromate; the balance is iron in the powder. Patent for Usable Model 10980. S.Yu. Maksimov, V.S. But, A.A. Radzievskaya et al. (Subsidiary of «Ukrtransgaz», the E.O. Paton Electric Welding Institute of NASU) [12].

*Data are given on Ukrainian patents published in the official bulletin in «Promyslova Vlastnist» for 2005 (Bulletin No. is given in brackets).